

# SEMICONDUCTOR SURFACE PHYSICS



ROBERT HILDRETH KINGSTON  
ELIAS BURSTEIN

# SEMICONDUCTOR SURFACE PHYSICS

*Proceedings of the Conference on the  
Physics of Semiconductor Surfaces  
held at Philadelphia, Pennsylvania,  
June 4-6, 1956*

SPONSORED BY  
THE OFFICE OF NAVAL RESEARCH,  
THE UNIVERSITY OF PENNSYLVANIA, AND THE  
LINCOLN LABORATORY OF THE  
MASSACHUSETTS INSTITUTE OF TECHNOLOGY



# SEMICONDUCTOR SURFACE PHYSICS

EDITED BY  
R. H. KINGSTON

WITH THE ASSISTANCE OF  
E. BURSTEIN, A. L. MCWHORTER, P. H. MILLER, JR.,  
D. T. STEVENSON, AND P. B. WEISZ



Philadelphia  
UNIVERSITY OF PENNSYLVANIA PRESS



© 1957 by the Trustees of the University of Pennsylvania

Published in Great Britain, India, and Pakistan  
by the Oxford University Press  
London, Bombay, and Karachi

Library of Congress Catalogue Card Number 56-13031

Reproduction in whole or in part permitted  
for any purpose of the United States Government

PRINTED IN THE UNITED STATES OF AMERICA

## FOREWORD

The Conference on the Physics of Semiconductor Surfaces was brought about through the efforts of the Office of Naval Research and it was the enthusiasm of Julius L. Jackson of that organization which led to the formation of the conference committee in the late summer of 1955. The committee consisted of:

J. L. JACKSON, Office of Naval Research, Arrangements and Invitations  
R. H. KINGSTON, Lincoln Laboratory, Program and Publications  
P. H. MILLER, JR., University of Pennsylvania, Local Arrangements and Publications  
J. BARDEEN, University of Illinois  
W. H. BRATTAIN, Bell Telephone Laboratories  
E. BURSTEIN, Naval Research Laboratory  
C. G. B. GARRETT, Bell Telephone Laboratories  
R. L. PETRITZ, Naval Ordnance Laboratory  
P. B. WEISZ, Socony Mobil Research Laboratory

In addition, the committee was benefited by the advice and encouragement of W. Gruner of the Office of Naval Research and H. Brooks of Harvard University.

The hosts for the conference, the University of Pennsylvania, supplied excellent facilities and the conference was particularly indebted to P. H. Miller and the University Physics Department for the smooth operation of the proceedings. Funds were also made available by the Lincoln Laboratory, which is supported jointly by the Army, Navy and Air Force under contract with the Massachusetts Institute of Technology. Through the support of these three sponsors it was possible to invite several participants from abroad and also underwrite the preparation of this volume.

The editors wish to acknowledge the facilities provided by the University of Pennsylvania and Lincoln Laboratory in the preparation of the final manuscript. Particularly helpful were Mrs. Wilma Hoff of the University, who handled the initial receipt and collation of the manuscripts, and Miss Nancy J. Loring of Lincoln Laboratory, who retyped much of the material and handled the editorial correspondence.

R. H. K.

*Lexington, Massachusetts  
July 23, 1956*



## INTRODUCTION

R. H. KINGSTON

*Lincoln Laboratory  
Massachusetts Institute of Technology  
Lexington, Massachusetts*

Without question the recent marked interest in the physics of semiconductor surfaces has arisen from the numerous problems encountered by the solid-state physicist in understanding those properties of semiconductor structures controlled by the surface treatment and ambient. One has only to consider the pronounced difference in sensitivity of a metal and a semiconductor to appreciate the importance of the surface boundary. Consider, for example, a layer of accumulated charge of  $10^{15}$  electrons per  $\text{cm}^2$  on the surface of a solid, or approximately one charge per lattice site. If the material is a metal, with the order of  $10^{22}$  free carriers per  $\text{cm}^3$ , then the charge may be neutralized by addition or depletion of carriers in a distance of  $10^{-7}$  cm, or the order of a lattice constant. In contrast, the average semiconductor, with a bulk carrier density of about  $10^{16}$  charges per  $\text{cm}^3$  would require a depletion or excess of carriers over a distance of about 1 cm! Actually, of course, this latter calculation is inaccurate since the change in potential energy across such a space charge region would be much greater than  $kT$  and the resultant changes in the Fermi factor would cause the carrier accumulation at the surface to approach the density of that in a metal. What one can say with certainty, however, is that the position of the Fermi level at the surface, with respect to the conduction and valence bands, would be completely determined by the charge density on the surface and *not* the bulk impurity density. In addition, one may also argue that densities of the order of  $10^{16}$  or less are sufficient to swing the surface potential over a range corresponding to the energy gap of the semiconducting material.

A complete understanding of the surface behavior involves a detailed study of the means by which such charge can accumulate

on the surface and a majority of the contributions to this volume are concerned with the sites for charge accumulation and the effects of the resultant shift in potential on such physical properties of the surface as the hole-electron recombination rate, contact potential and surface conductance. In addition to two sections on the physical problems, two are also devoted to phenomena of direct interest to the chemists. The first of these includes adsorption and catalysis, where it is apparent that the general behavior is determined by electron-transfer processes between the bulk semiconductor and the surface species. There is, in fact, ample evidence that adsorbed materials present one of the major sources for the accumulation of surface charge. The other section, on oxidation, is largely concerned with the structure and growth of oxide layers on semiconductors, since the oxide is not only a possible source for charge sites, but also has a profound moderating effect upon the action of ambient atmospheres.

From a historical point of view, it is interesting that surface states, or sites for charge storage, were first treated theoretically in the case of a "clean" surface, that is, an ideal crystal-vacuum interface. Yet until recently, the experimental realization of such a surface has been rare and fleeting. The recent advances in high-vacuum techniques have led to closer approaches to this ideal situation and as a result of work carried out in the past few years, the first session of the conference was devoted to the general question of clean surfaces. The proceedings were initiated with an excellent review by Herring of the ideas involved in the surface state theories of Tamm and Shockley based on an ideal lattice. In addition, he also discussed the effect of surface imperfections on the occurrence of localized states. Section I of the text includes two reports on the latest experimental work along these lines with particular reference to germanium. Schlier describes the general techniques for obtaining clean germanium surfaces by argon bombardment and annealing in a high vacuum, a method deduced from experiments on slow electron diffraction. In the companion paper, Handler reviews the results of electrical measurements on samples prepared by these techniques and suggests that the data indicate the occurrence of Tamm states. As will be apparent from the contributed discussion following these papers, the general interpretation of the results is somewhat controversial, the chief



difficulty being the establishment of a sound criteria for determining that a surface is, in the rigorous sense, truly clean.

Two sessions of the conference, making up Section II of the text, were devoted to real surfaces, or surfaces which have been prepared by etching or similar techniques and then exposed to the atmosphere or controlled gaseous ambients. In contrast to the clean surface studies, one can be quite certain that these surfaces have one, if not many, layers of oxide, as well as adsorbed foreign species. Schrieffer, in the initial paper, discusses the theoretical treatment of the mobility of carriers in an inversion layer, where the electron scattering is modified from its bulk behavior by the potential well at the surface. This calculation is of direct significance for most of the experimental measurements, since an interpretation of surface conductance data requires a theoretical prediction of the carrier mobility at the surface. The chief difficulty in the theory is the choice of scattering mechanism for the free surface, an isotropic law being the one here assumed. The remaining papers in the section are devoted to studies of the "slow" and "fast" states at a semiconductor surface. This categorization of states is based upon the observation that there are two distinct types of site for charge accumulation at the surface. The first type, the "fast" state, is believed to occur at the interface between the bulk semiconductor and the oxide and is chiefly involved in the recombination process. Measurements of the density and capture cross-section of these states are reported by Banbury, Many, Brown, Garrett and Statz. The techniques used are varied; change of conductance with applied field, surface recombination *vs.* applied field, and change in contact potential with illumination, to mention a few. The results reported are in surprisingly close agreement when one considers the difficulty of reproducing initial surface treatments in the various laboratories. The conclusion is that the "fast" states have a density of the order of  $10^{12}$  per  $\text{cm}^2$ , while the energy distribution is either discrete or continuous about the center of the gap, the latter information being somewhat ambiguous as of these reports. In addition to the measurements of the state distribution, Schultz, in a contributed discussion, points out some of the possible anomalies in lifetime measurements associated with storage of carriers in the "fast" states.

The "fast" states are characterized by capture cross-sections

of the order of  $10^{-16}$  cm<sup>2</sup>, leading to capture times less than a microsecond. In contrast, "slow" states have capture times from one millisecond to many hours, depending upon the surface treatment and ambient. In addition the density of these states, greater than  $10^{13}$  per cm<sup>2</sup>, is high enough to overwhelm the effects of the bulk impurities such that the conductivity type at the surface is almost completely controlled by the surface conditions. In this respect, it should be emphasized that, with a few minor exceptions, the "fast" states are insensitive to ambient, while the "slow" states seem to be intimately connected with the adsorption of foreign material from the gas phase, as was discussed earlier. The general behavior of the "slow" states was first studied in detail in experiments on "channels," or reverse-biased inversion layers on the base region of grown-junction transistors. Statz, in his contribution, reviews the work on "channels" and presents recent results on both "fast" and "slow" states on germanium and silicon, using this technique. At present the information in this paper and those to follow gives only the average energy of the states and their capture time. As yet, no detailed information on the state distribution is available, other than the observed shift in average energy with different ambients and etching techniques. Another problem which has been of especial importance to the semiconductor device field is the leakage current along the surface of a *p-n* junction in the presence of water vapor. Statz proposes that this current can be explained in some cases by hole conduction in the liquid at the immediate boundary between the solid and the liquid phases. In other words, he suggests that water or other liquids can be considered to have a forbidden gap and that a strong inversion at the surface can cause hole conduction in the valence band of the liquid. This suggestion is an alternative to previous theories which have associated the current with either carrier flow in the inversion layer or ion transport along the surface. In the succeeding three papers Morrison, Lasser and McWhorter present various ramifications of the "slow" state behavior. Morrison reviews the recent experimental data and discusses two possible explanations for the non-exponential decay characteristic of charge transfer into the states, as observed in the field-effect experiment. One theory attributes the effect to a change of capture time with charge flow, as a result of the change in barrier height as the charge accumu-



lates on the surface. The other theory attributes the character of the decay to a broad distribution of capture times in a given set of states. The conclusion seems to be that both effects are present, as the experimental data is not explainable using only one or the other model. The importance of the oxide layer is then emphasized by Lasser who describes field-effect measurements on germanium surfaces which have been purposely treated to have oxide layers much thicker than those observed under normal etching conditions. Since the capture times increase markedly in these experiments, he concludes that the "slow" states are most probably on the outer surface of the oxide layer, although there seems to be evidence that water vapor may penetrate the oxide and produce states in the interior regions. McWhorter applies the "slow" state capture time data to an explanation of excess or  $1/f$  noise in semiconductors. On the basis of the distributed time constant interpretation of the field-effect decay, he concludes that this type of noise can be associated with the random transitions of carriers between the states and the bulk material. Using the measured frequency spectrum obtained in the field-effect experiment, he is able to predict the amplitude and spectrum of the noise as observed in semiconductor filaments. The application of this theory to device structures is as yet quite difficult because of the complicated geometry and spurious leakage effects involved. In the last two papers in this section, Petritz and Scanlon discuss recent surface studies on a much more complicated semiconductor, lead sulfide. Petritz interprets the behavior of thin polycrystalline films in terms of "slow" and "fast" states at the surface of the crystallites, while Scanlon, in the companion paper proposes a method for the study of clean surfaces of single crystal lead sulfide by cleaving in an argon atmosphere. These two papers emphasize both the need and the possibility of carrying over to other semiconductors many of the techniques and concepts which have proved so valuable in the study of germanium and silicon.

In the section on adsorption and catalysis, the introductory paper by Weisz points out the common ground between the physicist and the chemist in connection with the electron exchange process in molecules and on surfaces. In the succeeding papers, Haufler and Schwab discuss, respectively, the theoretical and experimental aspects of catalysis on semiconductor surfaces. Of



most importance in these reactions is the free energy of electrons or the Fermi energy at the surface. Since this quantity can be measured independently by surface conductance and similar measurements, it would seem fruitful for experiments to be performed which establish a direct correlation between catalytic reaction rate and surface potential. In the final paper in the session, Pratt describes some interesting measurements of contact potential on both metals and semiconductors. He finds that changes in contact potential may be induced by application of transverse fields or by illumination. Although one might suspect that these changes are caused by induced adsorption-desorption of charged species, he concludes that the most likely explanation is an induced charge transfer between the bulk and "slow" states on the surface of the material.

Since the oxide layer has such a pronounced effect on the electrical behavior of semiconductors, the final session was devoted to this topic. In the first paper, Cabrera presents a review of oxidation theory for two different types of surface. In the first part, he considers a uniform surface and discusses the possible mechanisms which limit the growth process, mainly, electron transfer through the film. In the second part, he considers the more complicated case where the growth is controlled by nucleation centers such as the intersection of dislocations at the surface. The possible effect of such non-uniformities upon the surface behavior is certainly a subject worth pursuing further, since, as discussed in some of the preceding papers, an interpretation of the experimental measurements is complicated by the occurrence of such heterogeneity. The oxidation of germanium is considered by Green and Law, respectively, in the succeeding contributions. Green presents information on both the kinetics and the heats of adsorption as obtained on crushed powders at and below room temperature. The oxidation is logarithmic in this case and leads to at most two layers of oxide. This is to be contrasted with Law's results on vacuum-baked powders in the range of 500°C where a multi-layer process occurs and the mechanism is quite sensitive to the specific temperature. Additional information on the oxidation is supplied by Wolsky's preliminary data obtained with a quartz microbalance. Another oxidation process of great interest is yet to be described in detail. This is the formation and properties of

the layer produced in the etching process. As evidenced in some of the papers in Section II, this is also a multilayer phenomenon but there is little knowledge at present of the growth mechanism or the structure of the layer.

It is fair to say that this collection of papers is only a small contribution to a complete understanding of semiconductor surfaces. As pointed out by Bardeen in his concluding remarks to the conference, the energy and general behavior of the "slow" states is yet to be elucidated and the properties of clean surfaces are as yet not understood. In addition to these specific problems there are a myriad of semiconductors which have not been studied yet by the techniques used here for germanium and silicon. In fact, it should be emphasized that what success has been obtained so far is a result of the availability of excellent single crystal samples of these elements. The conference was also only a beginning in an attempt to closely relate the work of the catalysis expert with that of the physicist. As was pointed out above, it would be interesting to see some more direct connection between the reaction rate measurements and the electrical properties described in the earlier sections of the book. Still another area where the chemist and physicist may fruitfully cooperate is in a study of the detailed structure of the oxide layer and its connection with the electrical properties of the surface. Of particular interest is the effect of different etchants and trace impurities therein.

In summary, one may conclude that the study of surfaces in the past several years has led to a better understanding of the physics of the semiconductor surface as well as the chemistry, but that a direct relation between the two is still forthcoming. Hopefully, this book will point the right directions for such studies.



## CONTENTS

FOREWORD	v
INTRODUCTION. <i>R. H. Kingston</i>	vii
I. CLEAN SURFACES	
LOW ENERGY ELECTRON DIFFRACTION STUDIES OF CLEANED AND GAS-COVERED GERMANIUM (100) SURFACES. <i>R. E. Schlier and H. E. Farnsworth</i>	3
DISCUSSION. <i>H. E. Farnsworth</i>	20
ELECTRICAL PROPERTIES OF A CLEAN GERMANIUM SURFACE. <i>Paul Handler</i>	23
DISCUSSION. <i>H. E. Farnsworth, W. H. Kleiner, J. T. Law, C. G. B. Garrett, S. H. Autler, and A. L. McWhorter</i>	40
II. REAL SURFACES	
MOBILITY IN INVERSION LAYERS: THEORY AND EXPERIMENT. <i>J. R. Schrieffer</i>	55
FIELD EFFECT ON SURFACE CONDUCTANCE AND SURFACE RECOMBINATION. <i>P. C. Banbury, G. G. E. Low, and J. D. Nixon</i>	70
SURFACE RECOMBINATION PROCESSES IN GERMANIUM AND THEIR INVESTIGATION BY MEANS OF TRANSVERSE ELECTRIC FIELDS. <i>A. Many, E. Harnik, and Y. Margoninski</i>	85
DISCUSSION. <i>S. Wang, G. Wallis, and A. Many</i>	105
STORAGE OF INJECTED CARRIERS AT SURFACES OF GERMANIUM. <i>B. H. Schultz</i>	108
FIELD EFFECT AND PHOTO EFFECT EXPERIMENTS ON GERMANIUM SURFACES. 1. EQUILIBRIUM CONDITIONS WITHIN THE SEMICONDUCTOR. <i>W. L. Brown, W. H. Brattain, C. G. B. Garrett, and H. C. Montgomery</i>	111
FIELD EFFECT AND PHOTO EFFECT EXPERIMENTS ON GERMANIUM SURFACES. 2. NON-EQUILIBRIUM CONDITIONS WITHIN THE SEMICONDUCTOR. <i>C. G. B. Garrett, W. H. Brattain, W. L. Brown, and H. C. Montgomery</i>	126
MEASUREMENTS OF INVERSION LAYERS ON SILICON AND GERMANIUM AND THEIR INTERPRETATION. <i>H. Statz, G. A. deMars, L. Davis, Jr., and A. Adams, Jr.</i>	139
DISCUSSION. <i>C. G. B. Garrett and H. Statz</i>	167
SLOW RELAXATION PHENOMENA ON THE GERMANIUM SURFACE. <i>S. Roy Morrison</i>	169
DISCUSSION. <i>J. N. Zemel</i>	193



EFFECTS OF THICK OXIDES ON GERMANIUM SURFACE PROPERTIES. <i>M. Lasser, C. Wysocki, and B. Bernstein</i>	197
1. f NOISE AND GERMANIUM SURFACE PROPERTIES. <i>A. L. McWhorter</i>	207
DISCUSSION. <i>R. L. Petritz</i>	226
SURFACE STUDIES ON PHOTOCONDUCTIVE LEAD SULFIDE FILMS. <i>R. L. Petritz, F. L. Lummis, H. E. Sorrows, and J. F. Woods</i>	229
SURFACE STUDIES ON CLEAVED CRYSTALS OF LEAD SULFIDE. <i>W. W. Scanlon</i>	238
III. ADSORPTION AND CATALYSIS	
INTRODUCTORY REMARKS: BRIDGES OF PHYSICS AND CHEMISTRY ACROSS THE SEMICONDUCTOR SURFACE. <i>P. B. Weisz</i>	247
GAS REACTIONS ON SEMICONDUCTING SURFACES AND SPACE CHARGE BOUNDARY LAYERS. <i>Karl Hauße</i>	259
DISCUSSION. <i>C. G. B. Garrett</i>	281
EXPERIMENTS CONNECTING SEMICONDUCTOR PROPERTIES AND CATALYSIS. <i>George-Maria Schwab</i>	283
DISCUSSION. <i>W. H. Brattain</i>	295
LONG TIME WORK FUNCTION CHANGES INDUCED BY LIGHT AND ELECTROSTATIC FIELDS. <i>G. W. Pratt, Jr. and H. H. Kolm</i>	297
DISCUSSION. <i>C. G. B. Garrett, G. W. Pratt, Jr. and H. H. Kolm</i>	321
IV. OXIDATION	
THE OXIDATION OF METALS. <i>N. Cabrera</i>	327
THE INTERACTION OF OXYGEN WITH CLEAN GERMANIUM SURFACES: 1. EXPERIMENT. <i>M. Green, A. Kafalas, and P. H. Robinson</i>	349
THE INTERACTION OF OXYGEN WITH CLEAN GERMANIUM SURFACES: 2. THEORETICAL DISCUSSION. <i>Mino Green</i>	362
DISCUSSION. <i>G. A. Wolff, M. Green, C. G. B. Garrett, and J. T. Law</i>	377
THE HIGH TEMPERATURE OXIDATION OF GERMANIUM. <i>J. T. Law and P. S. Meigs</i>	385
VACUUM MICROBALANCE STUDIES ON SINGLE CRYSTAL GERMANIUM. <i>S. P. Wolsky and A. B. Fowler</i>	401
SUBJECT INDEX	407
AUTHOR INDEX	409

# LOW-ENERGY ELECTRON DIFFRACTION STUDIES OF CLEANED AND GAS-COVERED GERMANIUM (100) SURFACES\*

R. E. SCHLIER and H. E. FARNSWORTH

*Brown University  
Providence, Rhode Island*

## ABSTRACT

The low-energy electron diffraction technique, applied to the study of germanium surfaces, has furnished a great deal of information. It has been found that it is not possible to remove a stable layer of contaminant from (100) and (110) surfaces etched in CP-4 and carefully washed in distilled water, by outgassing alone. The proper use of the ion bombardment and annealing method of cleaning, however, results in a clean surface. The data are consistent with the hypothesis that the germanium atoms on a clean (100) surface are displaced from their normal lattice positions in a manner such that adjacent rows of atoms lying in [110] directions are moved in opposite directions, approximately along the surface, in the perpendicular [110] directions. Oxygen adsorbs on the surface in approximate germanium lattice positions and restores the germanium atoms to their normal sites. At room temperature, both oxygen and hydrogen adsorb approximately at an exponential rate up to a monolayer. The sticking probabilities for oxygen and hydrogen on the bare surface are about  $1.4 \times 10^{-3}$  and  $1 \times 10^{-4}$ , respectively.

## I. INTRODUCTION

The properties of clean surfaces are of considerable interest to investigators of surface phenomena. A better understanding of the properties of semiconductor surfaces can be gained through experimental work on clean and controllably contaminated surfaces. This requires a clean surface which remains stable for an appreciable time, so that it may be exposed to known contaminants under controlled conditions. Techniques of ultra-high vacuum production and measurement, such as those developed by Alpert,<sup>1</sup> make possible the necessary stability; the remaining problems are to prepare and to identify clean surfaces.

\* Supported by a Joint Services Contract with the Massachusetts Institute of Technology and a subcontract with Brown University.

### *1. General Considerations of Cleaning by Positive Ion Bombardment*

Although it is expected that cathode sputtering will remove surface contamination in the form of stable compounds, the resulting surface is not clean and the crystal lattice is damaged. During the discharge, positive ions are driven into the surface and trapped. Since sputtering is to some extent a momentum exchange process,<sup>2</sup> some of the atoms in the surface are driven from their equilibrium lattice positions, but not from the surface. Thus the ion-bombarded surface contains a large number of defects, and some occluded gas. Annealing at an elevated temperature is therefore essential to remove the occluded gas and the lattice imperfections.<sup>3</sup>

The process of ion bombardment and subsequent annealing, however, does not necessarily result in a clean surface. Contamination can occur by clean-up of non-desorbable gases during the bombardment, by diffusion from the bulk to the surface during annealing, and by adsorption from the ambient. In the absence of diffusion, the fractional impurity content in the interior is also found on the surface.

The amount of desorbable impurities can be reduced by thorough outgassing at the highest temperature possible, in the best vacuum obtainable. Some contaminants, however, have a vapor pressure which is too low to prevent accumulation at the surface by diffusion from the bulk at elevated temperatures. Such impurities can be removed from the surface by ion bombardment, but may recontaminate the surface during annealing if the rate of diffusion is high. In this case, a series of ion bombardments and annealings is required. The number of such cycles depends on the amount of impurity present and the rate of diffusion, as well as the equilibrium concentration of such impurities on the surface. It is seen that a series of cycles is more effective in removing impurities than a single cycle of the same total time. In practice the annealing portion of each cycle can be used to outgas by heating at a higher temperature for a longer time. The final annealing should be as little as possible, to keep the diffusion effects to a minimum.

At incident ion current densities of 100 microamperes per cm<sup>2</sup>,



from 0.1 to 1 monolayer of surface atoms is removed per second. At this rate of removal, partial pressures of between  $10^{-7}$  and  $10^{-6}$  mm Hg of active gas are required to produce contamination from the ambient. Clean-up of this active gas is negligible in comparison with its possible adsorption.

Active gas may be released into the vacuum system by sputtering from the surface. When the bombardment ceases, some of this gas may re-adsorb on the surface; it is therefore necessary to remove the active gas during the bombardment by gettering or pumping.

Contamination by adsorption, during exhaust of the inert gas and the subsequent annealing, can occur if the partial pressure of active gas is as high as  $10^{-10}$  mm Hg (approximately 0.1 monolayer can form at this pressure in 15 minutes, if a sticking coefficient of unity is assumed). Since this active gas pressure is orders of magnitude lower than that which could cause contamination during the bombardment, it is evident that the greatest probability of contamination exists during the exhaust and annealing.

The conditions under which the discharge is carried out are also important. To prevent contamination by foreign material that is sputtered onto the surface and by active gases liberated from other parts, the discharge should be confined to the surfaces being investigated. If this cannot be done, the geometry should be such that sputtered impurities cannot strike the portion of the surface that is of interest, and the gas pressure in the apparatus should be so low that the sputtered atoms travel in straight lines, without colliding with gas molecules. In practice this means that the gas pressure during the discharge should not be greater than about  $10^{-3}$  mm Hg.

## II. LOW-ENERGY ELECTRON DIFFRACTION

### 1. Introduction

It is apparent from the above discussion that a given amount of outgassing and ion bombardment followed by annealing may not always result in a clean surface. A method of determining the condition of the surface is therefore necessary, at least to the extent of finding the degree of effort required to clean surfaces of various



materials. One of the most direct methods is that of low-energy electron diffraction.

Historically, the first experiments utilizing the diffraction of low-energy electrons were carried out by Davisson and Germer.<sup>4</sup> In the course of their investigation, it was observed that the diffraction patterns were extremely sensitive to adsorbed gas. In fact, some of the diffraction effects were directly attributed to the presence of a two-dimensional crystalline lattice of adsorbed gas.

There has been relatively little use of low-energy electron diffraction, in spite of the obvious value of a technique that can detect a surface gas lattice. The method involves a rather difficult experimental technique and requires the use of single crystals. Because the penetration of the diffracted electrons is very small, the use of a step function for the inner potential is not always justified, and hence a complete interpretation of the data is not always possible. Nevertheless, the method is capable of detecting directly the presence of a small fraction of a monolayer of adsorbed gas on the surface, and of furnishing much information about its structure.

## *2. Apparatus*

The apparatus consists of an electron gun, a target, and an electron collector. The gun is constructed so that there is no direct path between the filament and the target.<sup>5</sup> The electron beam from the filament is electrostatically deflected into the collimating arrangement, which consists of two cylinders and a tube, all mounted along the same axis. The cylinders provide a means of altering the beam energy, and slits 1 by  $\frac{1}{4}$  mm at the ends of the tube define the beam. The target is a single crystal, and is placed so that the face is at the center of a cylindrical drum, which serves as an electrostatic shield and as a support for the collector. The collector is a triple box, each box insulated from the others. The outer box is in electrical contact with the drum, and contains a 1 by  $\frac{1}{4}$  mm slit in the side facing the crystal. Larger slits are cut in the sides of the inner boxes adjacent to the outer slit. The collector can be rotated so that the slit in the outer collector wall moves in an arc about the point of incidence of the beam on the target. A slot in the drum permits electrons to pass from the crystal to the collector. A scale is provided so that the angle between

the incident and the collected beam can be measured. The crystal (target) can also be rotated about the axis of the incident beam. By a combination of crystal and collector rotations, electrons scattered into the entire backward hemisphere about the crystal (except for a small cone about the incident beam) can be detected.

The target, drum, and collimator are all maintained at the same potential relative to the gun filament. This potential (except for corrections due to contact potentials and thermal energy) corresponds to the energy of the incident beam. The combined current to the drum and target is the total current of the incident beam, and is usually  $10^{-8}$  amperes. The inner box of the collector is grounded through the grid resistor of the dc amplifier used to measure the collector current. The middle box is grounded, and serves as shield to keep small fluctuations in drum potential from affecting the amplifier. A negative bias (with respect to ground) is placed on the filament so that only elastically-scattered electrons are measured.

### 3. Procedure

The usual procedure is to observe collector current as a function of collector angle, for a fixed beam current and energy, and a given crystal orientation or azimuth. The process is then repeated for other beam energies, and other azimuths. Since there are at least two different azimuths in which well-developed diffraction patterns are observed, and since many different beam energies must be used in order to obtain adequate data, a large number of data points is required by this procedure. These points are observed manually; hence the above procedure is both tedious and time consuming. Manual operation is necessary if the collector angle is to be changed after each reading, since the magnetic control used to alter the angle also affects the incident beam.

The method now in use allows the collector current to be recorded as a function of beam energy. In this case, the collector angle is kept fixed, and the beam energy is varied continuously by a precision potentiometer which is driven by the recorder chart drive. After each rotation of the potentiometer, a solenoid actuated mechanism moves the collector one-half degree. The beam current is kept constant with a galvanometer, photo-cell, and amplifier arrangement. With the new procedure, complete



data can be obtained, for one azimuth, over a range of energy from 35 to 235 electron volts, for collector angles from 70 to 11 degrees, in one-half degree steps, in 12 hours. No attention is required during that time, except for the initial setting. If a timer is provided, the apparatus can be operated at night. Twelve thousand data points would be required by the manual method in order to obtain comparable data. If one obtains one such point every 10 seconds, 33 hours of total effort would be required. Furthermore, complete data can be recorded before the surface is changed by adsorption from the ambient.

#### 4. *Interpretation of Data*

The low-energy electron diffraction maxima are sensitive to only the first few atomic layers of the surface. One of us<sup>6</sup> has found that for incident electron beam energies under 300 ev, 50 percent of the diffraction beam intensity is from the first layer of silver, and 90 percent is from the first two layers. At 50 ev, the first monolayer contributes more than 75 percent. The surface plane of atoms is therefore of primary importance, and the other layers act as modifiers of the diffraction effects from the first layer.

In most cases, the incident beam is normal to the surface of the crystal. If the surface is parallel to a principal crystallographic plane, there are several possible azimuthal orientations in which rows of surface atoms are perpendicular to the plane of the incident beam and the collector aperture. If the separation of the rows in one of the azimuths is  $d$ , then, by combining the plane grating formula

$$n\lambda = d \sin \theta, \quad (1)$$

and the expression for the wave length of the electron

$$\lambda = h/mv, \quad (2)$$

one obtains

$$V = 150 n^2/d^2 \sin^2 \theta, \quad (3)$$

where  $V$  is in volts and  $d$  is in Angstroms.

Eq. (3) is the surface grating condition. If only the first layer were present, diffraction maxima would be present whenever this condition is satisfied. The presence of the other layers modifies the intensities of the maxima found along the surface grating curve. If there were no effect analogous to an index of refraction, the positions of the strongest maxima, or beams, could be easily

calculated from the geometry of the crystal, and would be the same as the positions of the X-ray diffraction maxima for the same wave length.

There is an index of refraction, however, caused by the presence of an inner potential; electrons that enter the surface are accelerated in a direction perpendicular to the surface. Consequently the wave length inside the crystal is less than that in the vacuum.

The positions of the beams are easily calculated for the special case in which the inner potential can be represented by a step function having a value of  $\Phi$  inside the crystal, and zero outside. The maxima still follow Eq. (3), but the beams are found, not at the positions predicted by simple theory, but displaced along the surface grating curve by an amount corresponding to a decrease along the voltage axis of  $\Phi$ .

Unfortunately, the inner potential cannot be represented by a step function when low-energy electrons are used. The manner in which the inner potential varies in the region near the surface, as well as the magnitude of the inner potential, has a large effect on the position (in wave length or voltage) of the maximum intensities of the diffraction maxima. The surface grating condition, however, is unaffected by the inner potential, so that accurate data concerning the spacings and atomic arrangement of the surface monolayer can be obtained.

The surface grating condition is applicable only in the case where the surface monolayer of atoms is perpendicular to the incident beam. If there are regions of the surface which are not perpendicular to the beam, a different form of grating equation is required for these regions. Thus it is possible to determine if a significant portion of the surface is made up of other crystal faces, and these faces may be identified. Processes occurring on the desired plane only can be observed, since these processes affect only the diffraction beams from that plane.<sup>7</sup>

### III. INVESTIGATION OF GERMANIUM SURFACES

#### 1. *Vacuum System*

The vacuum system consists of the experimental tube, together with the necessary pumps, and contains provision for the admission of controlled amounts of gas. The experimental tube contains the electron diffraction apparatus, together with filaments for heating



the crystal by electron bombardment and for ionization of the inert gas during ion bombardment of the crystal.

Two single-stage mercury diffusion pumps in series are separated from the experimental tube by a dry ice cooled trap in series with a liquid nitrogen cooled trap. The tube is baked at 350–400°C for 8 to 16 hours, with the traps refrigerated by dry ice. After the tube reaches room temperature, the dry ice is replaced by liquid nitrogen. A molybdenum getter is then formed on the inner walls of a side tube by evaporation from a filament. A pressure of  $10^{-9}$  mm Hg or less can thus be obtained and maintained for several weeks without further effort.

In some cases the trap has been baked as well as the tube. There does not appear to be any gain by this procedure in the present system.

Because of the presence of the getter, the active gas pressure in the experimental tube is much less than the total pressure indicated by the gauge. Diffraction beams from the cleaned surface are stable for at least 48 hours, although detectable changes occur after an exposure to oxygen at  $10^{-8}$  mm Hg for 5 minutes. The active gas pressure in the tube is therefore less than  $2 \times 10^{-11}$  mm Hg, and is presumably due to oxygen.

## *2. Crystal Preparation*

The germanium crystal is cut so that the desired plane is parallel to the surface. The surface is then ground and lapped, and etched in CP-4<sup>8</sup> until a smooth surface is obtained. Just prior to insertion in the tube, the crystal is lightly etched and washed in distilled water. In the present procedure, the crystal is also rinsed in hydrofluoric acid before washing.

The crystal is clamped, by means of silica tubes, against a piece of pure graphite (previously outgassed) backed by molybdenum. Molybdenum springs attached to the tubes provide the necessary tension. Outgassing is accomplished by electron bombardment of the molybdenum backing, the crystal being heated by thermal conduction.

## *3. Surface Cleaning*

For best results, it is found necessary to outgas a germanium crystal, cut so that the (100) face is exposed, for about 60 hours at 700°C, or until the residual pressure in the apparatus, when

the crystal is hot, is below  $5 \times 10^{-9}$  mm Hg. The total ion bombardment required is from 10 to 20 cycles of 5 minutes' duration, using an argon ion current of 100  $\mu$ a and an energy of 400 ev. Satisfactory annealing requires 15 minutes at 500°C. Surfaces that have been subjected to positive ion bombardment, but not annealed, are so disturbed that no low-energy diffraction beams can be observed, even if the incident ion energies are as low as 150 ev.

Since the above requirements are to some extent dependent on the size of the crystal and the method of mounting, some more general conditions are useful. The outgassing should be continued until gas is no longer evolved when the crystal is hot. Gas should not be evolved when the crystal is heated from room temperature to 500°C, when no ion bombardment has taken place. The amount of cleaned-up argon evolved from the ion bombarded surface is quite large, perhaps as much as  $10^{-1}$  micron-liters, and the annealing should be continued until no more gas is evolved. At least 10 ion bombardments should be used, followed by heating for several hours after each bombardment, before the final ion bombardment and annealing.

The effect of outgassing alone has been investigated. A (111) surface, etched in CP-4 and rinsed in HF, can be partially cleaned by outgassing, but a two-fold improvement in the electron diffraction patterns is observed after one ion bombardment and annealing. (100) and (110) surfaces that are etched with CP-4 alone cannot be cleaned by outgassing for 24 hours at temperatures just under the melting point. From the weak diffraction patterns observed for the outgassed (100) and (110) surfaces it is concluded that the surface is covered with at least two atomic layers of amorphous or polycrystalline contamination. At present, it is not possible to state whether CP-4 etched (111), or HF treated (100) and (110) faces can be cleaned, at least partially, by outgassing.

It is also observed that oxygen adsorbed on a previously cleaned (100) surface can be removed by heating. In fact, some of the gas adsorbed by exposing a (100) surface to the atmosphere for a few months can be removed from the surface by outgassing.

#### 4. Diffraction Patterns

Thorough searches have been made for diffraction beams in the (001) and (011) azimuths of a crystal cut so that the (100) face

is exposed. Similar results were obtained for 12 and 28 ohm-cm crystals. The azimuths are defined as the crystallographic planes which are parallel to the incident and collected beams. The searches were made after cleaning and after exposure to gases.

Most of the data were taken by the automatic method and are consequently in the form of recorder traces. Some of these traces are shown in Fig. 1. Collector current is plotted against

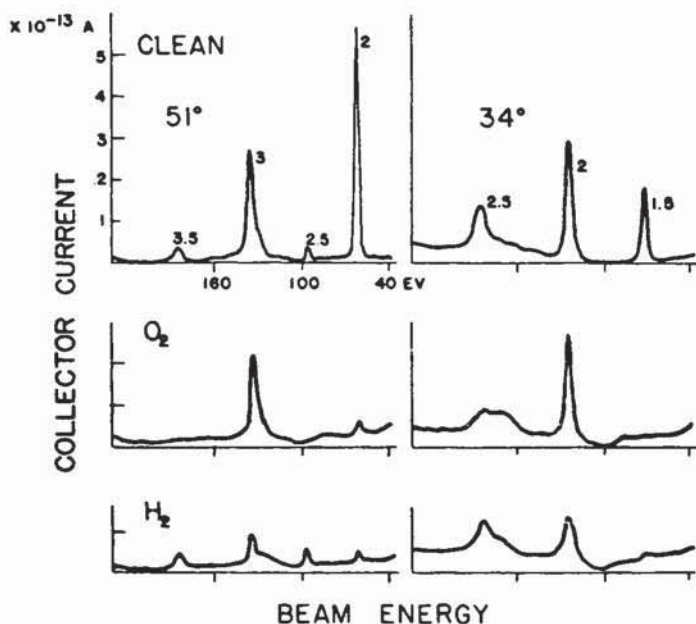


FIG. 1.—Diffraction maxima in the (011) azimuth. Representative curves obtained after cleaning, exposure to  $O_2$ , and exposure to  $H_2$ , for collector angles of 51 and 34 degrees. Numbers next to the peaks are the orders of reflection from the surface grating.

incident beam energy, for an incident current of  $10^{-8}$  amperes, and collector angles of 51 and 34 degrees. The curves observed after cleaning, and after exposure to oxygen and hydrogen, illustrate the sensitivity of the beams to adsorbed gas.

The energies corresponding to the maxima of curves such as those of Fig. 1 may be plotted against the collector (or colatitude) angle. All of the diffraction maxima that have been observed from



the (100) face, when plotted in this manner, lie on or close to surface grating curves of the form of Eq. (3). At least 95 percent of the surface is therefore the (100) plane. The intensities of the maxima corresponding to a given order of reflection from the surface grating vary as the angle and energy are changed. The values of angle and energy corresponding to the maximized intensities (the diffraction beams) are plotted in Fig. 2. The intersections of

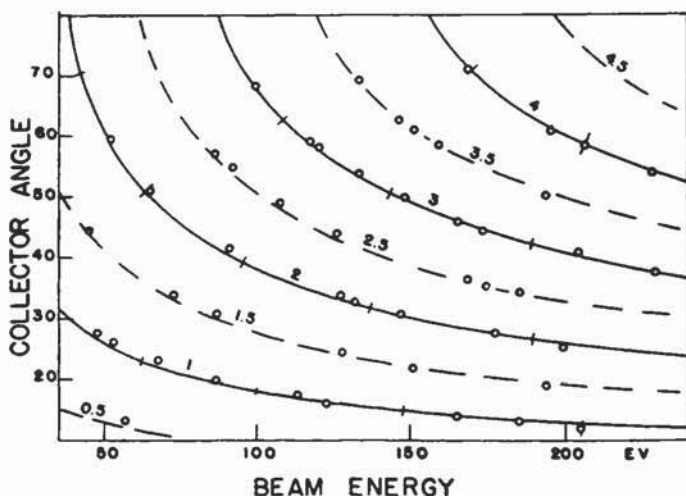


FIG. 2.—Positions of the diffraction beams in the (011) azimuth, for the cleaned surface. Numbered curves are integral and half-integral orders of the surface grating condition. Intersections of the short lines and the solid curves are theoretical positions.

the short lines and the solid curves are the theoretical positions of the strongest maxima, assuming unit refractive index. The strong maxima, or beams, do not coincide with these points, and many more are observed than are predicted.

Similar plots for other azimuths have the same general characteristics. Only those beams which follow integral or half-integral order surface grating curves are found. The observed diffraction beams, in all the azimuths that have been searched, fall into three classifications: (1) those beams which can be identified with the expected beams from the germanium lattice structure, by the assumption that the displacement from the predicted position



is due to an inner potential; (2) those which correspond to the same surface spacing as germanium, but not to the three-dimensional spacing; and (3) those which correspond to twice the surface spacing. The third class of beams, or half-order beams, can be found only in those azimuths for which the sum of the indices is even, such as the (011), (013), and (015) azimuths.

The searches for beams in the various azimuths have also been made after exposing the crystal to oxygen at room temperature. These observations were made after the tube had been re-evacuated, and hence the data are confined to non-reversible adsorption.

After exposure of the crystal to oxygen at  $10^{-7}$  mm Hg for 25 minutes, only those diffraction beams that can be identified with the three-dimensional germanium structure are readily observable. All of the extra beams (classes 2 and 3 above) are completely or very nearly extinguished.

The values of inner potential  $\Phi$  which must be assigned to the diffraction beams from the germanium structure are given in Table I, together with the observed and theoretical voltages, for both the cleaned and oxygen-covered surface.

The values of inner potential  $\Phi$  that are shown in Table I do not appear to be simply related to the incident beam energies. The inner potentials of corresponding beams, after cleaning and after adsorption, are not all the same.

Further exposure to oxygen causes a decrease in intensity of all beams, but they are still present immediately after an exposure of several hours at 1 mm Hg. When the crystal is allowed to stand in a vacuum of the order of  $10^{-7}$  mm Hg after the higher pressure exposure, the patterns revert after a few hours to those found after the 25 minute exposure. The effect observed after an exposure to oxygen at  $2.5 \times 10^{-7}$  mm Hg for 10 minutes is the same as that observed after an exposure at  $10^{-7}$  mm Hg for 25 minutes. The patterns are stable after evacuation following these exposures at lower pressure. The diffraction patterns characteristic of a cleaned surface can be restored by heating the oxygen-covered crystal to about  $500^{\circ}\text{C}$  for 30 to 60 minutes.

A change in the diffraction patterns is caused by exposure to hydrogen for 10 to 100 minutes at  $10^{-4}$  mm Hg. This change is stable with time for at least 48 hours. All three classes of beams

TABLE I  
DIFFRACTION BEAMS IDENTIFIABLE WITH GERMANIUM STRUCTURE,  
AND INNER POTENTIALS ASSOCIATED WITH THESE BEAMS

ORDER OF REFLECTION	THEOR. VOLT.	CLEAN		O <sub>1</sub> COVERED	
		Exp. Volt.	Φ	Exp. Volt.	Φ
(011) Azimuth:					
1	62	48	14	47	15
	100	87	13	86	14
	147	133	14	131	16
	205	185	20	196	9
2	63	52	11	52	11
	96	91	5	82	14
	137	127	10	130	7
		132	5		
	189	177	12	177	12
3	108	99	9		
	144	133	11	136	8
	189	173	16	172	17
	245	229	16		
(001) Azimuth:					
1	53	42	11	40	13
	127	119	8	119	8
	239	218	21	221	18
2	119	110	9	108	11
	208	200	8	200	8

are present after the exposure, but not in the same positions, and with different intensities. No half-integral order beams are present in the (001) azimuth. In this case the diffraction patterns characteristic of a cleaned surface are also restored by heating at 500°C.

#### IV. DISCUSSION AND CONCLUSIONS

##### 1. Structure of the Cleaned (100) Surface

The diffraction beams from the cleaned (100) face are found to include half-integral orders in only those azimuths for which the sum of the indices is even. This behavior indicates that the surface lattice of the germanium crystal, after cleaning, is as shown in Fig. 3A or 3B. In the figure, open circles represent surface atoms, and solid circles represent atoms immediately below the surface. In Fig. 3A, the surface layer is formed of rows of atoms lying along the surface in [110] directions; the atoms in the rows are separated by the same amount as the atoms in the rows below the surface,

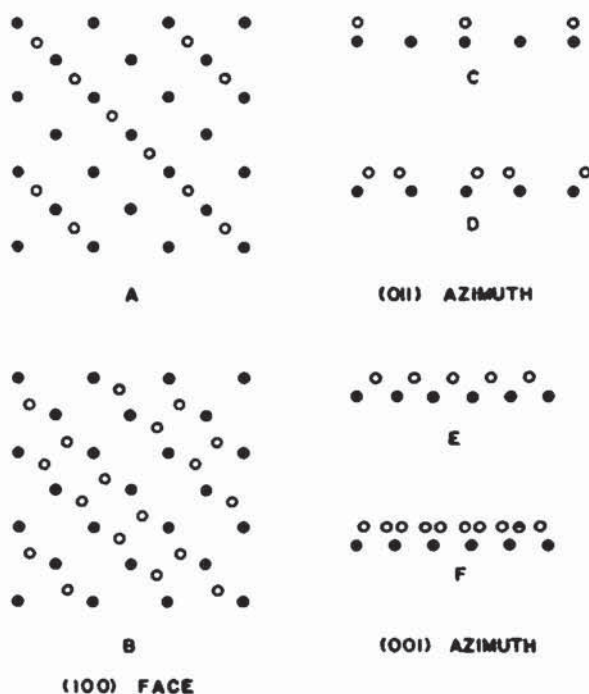


FIG. 3.—Possible arrangements of atoms on the cleaned surface. Open circles refer to surface atoms; solid circles refer to atoms in the layer below the surface. A, C, and E represent one possible arrangement; B, D, and F represent the other possible arrangement.

and the rows are separated by twice the distance between parallel rows below the surface. In Fig. 3B adjacent rows of surface atoms are displaced in opposite directions. Figures 3C and 3D are projections of the surface layers of atoms in the plane of the (011) azimuth. It can be seen that the separation of like surface configurations in both cases is twice the normal separation. Figures 3E and 3F show that the separation in the (001) azimuth is the same as the normal spacing. The relative positions of the surface layer with respect to the underlying layer, in both cases, are the most probable ones. In arrangement 3A, the atoms are placed in the normal germanium lattice positions; in arrangement 3B, the displacement is presumed to be caused by interaction between cut germanium bonds at the surface.



The results of the oxygen adsorption studies are of assistance in determining which of the two arrangements is correct. Only those beams which can be identified with the germanium crystal structure are observed after adsorption, and the intensities are not consistent with a structureless oxygen layer. Hence, it is apparent that the oxygen is adsorbed into approximately the germanium lattice positions in the next layer above the surface. If the arrangement in Fig. 3A exists, this observation requires that the surface layer is composed of oxygen atoms, since oxygen is not expected to extinguish all of the half-order beams if the resultant surface is composed of alternate rows of different kinds of atoms. If the arrangement in Fig. 3B exists, oxygen, which can form two covalent bonds, completes the bond structure of the surface and hence leaves no cause for a displacement. If it can be shown that the surface, after ion bombardment and annealing, is contaminated by substantially less than one-half monolayer, the arrangement in Fig. 3B must be correct; otherwise, an initial increase in the half-order diffraction beams would be observed when oxygen is adsorbed.

## 2. Evidence for the Clean Surface

In Sec. I-1 it is shown that, after sufficient treatment, any contamination of the crystal must occur during the exhaust of the ionizing gas and during the annealing, since the active gas pressure in the tube at other times is less than  $2 \times 10^{-11}$ . By exposing the crystal to the argon gas used for ion bombardment, and observing the effect on the diffraction beams, it is found that the partial pressure of oxygen in the argon is less than  $1 \times 10^{-8}$  mm Hg. At first glance, this upper limit might appear to be enough to contaminate the surface in a few minutes if the sticking probability is near unity. Since the total volume of the system is approximately two liters, the total number of oxygen atoms available for adsorption after closing the argon inlet leak is less than  $1.4 \times 10^{12}$ , a number which is entirely insufficient to form one-half a monolayer. Diffusion of oxygen from the interior to the surface of the crystal is also unlikely, since the number of ion bombardments used must have appreciably reduced any such effect. Further evidence for a clean surface is that it is possible to obtain essentially clean nickel<sup>9</sup> and titanium<sup>2</sup> surfaces by the

ion bombardment and annealing technique. The electron diffraction data, for these metals furnish conclusive evidence that they can be cleaned.

The above arguments assume that only one monolayer of oxygen can be adsorbed on the germanium at pressures of approximately  $10^{-7}$  mm Hg. Confirmation of this assumption can be found in the experiments of Green<sup>10, 11</sup> in which germanium is crushed in an oxygen atmosphere. The up-take of oxygen is reported to be rapid up to one adsorbed atom per surface germanium atom, and then very slow thereafter. This corresponds to the herein reported adsorption into a monolayer in 25 minutes at  $10^{-7}$ , and the further, reversible adsorption at higher pressures. Furthermore, it is not expected that an oxygen layer adsorbed on top of an existing layer would have a lattice structure. These considerations furnish strong evidence that the configuration of Fig. 3B is correct. Green's observation, and the fact that some diffraction beams (see Fig. 1) are greatly changed by the adsorption of oxygen, furnish additional evidence that this diffraction method is sensitive to a small fraction of an adsorbed monolayer.

### 3. *Structure of the Gas Layer*

Oxygen atoms, as mentioned above, are found to occupy approximately the positions that would be expected for germanium atoms in the layer above the surface. At the same time, any distortions in the surface layer of germanium, caused by the interaction between cut valence bonds at the surface, are removed. The structure of the hydrogen layer has not been determined, but the presence of half-integral order beams requires a configuration of the surface layer that has an effective double spacing in the [110] direction. One possibility is that two hydrogen atoms are attached to one germanium atom, but alternate rows of surface atoms are free of hydrogen.

### 4. *Rate of Adsorption*

Some of the electron diffraction beams are very nearly extinguished by the adsorption of oxygen and hydrogen. If the amplitude of such a beam is assumed to be proportional to the uncovered surface area, then the intensity should be given by

$$I = I_0(1 - \theta)^2, \quad (4)$$

where  $I$  is the intensity,  $I_0$  the intensity after cleaning, and  $\theta$  is the fractional coverage of the surface. If  $I$  is observed as a function of the exposure to gas, then the coverage with exposure can be deduced from Eq. (4). The calculations require assumptions

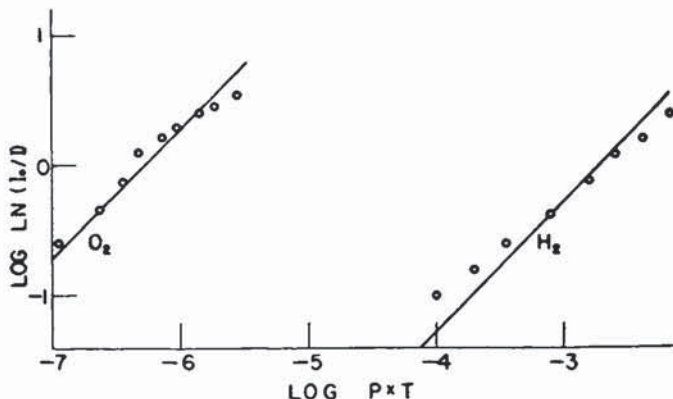


FIG. 4.—Rate of adsorption. Straight lines represent the predicted variation, for  $S = 1.4 \times 10^{-2}$  for  $O_2$  and  $S = 1 \times 10^{-2}$  for  $H_2$ .  $P \times t$  is in mm Hg-minutes.

concerning the number of adsorbed atoms in a monolayer, and the assumption that one monolayer has been adsorbed when the beams are extinguished.

The results of the calculations suggest that the coverage with exposure to oxygen and hydrogen is of the form

$$\theta = 1 - \exp(-\alpha S p t), \quad (5)$$

where  $\alpha$  is the number of atoms per site striking the surface in one second at a pressure of one mm Hg, and  $S$  is the probability that a molecule striking the bare surface is adsorbed. If Eqs. (4) and (5) are combined, then

$$\log \ln(I_0/I) = \log 2\alpha + \log S + \log p t. \quad (6)$$

If one assumes that one atom is adsorbed for each surface atom of germanium, then, at  $300^\circ\text{C}$ ,  $\alpha$  is  $6.83 \times 10^7$  for oxygen and  $2.83 \times 10^8$  for hydrogen, where  $p t$  is in mm Hg-minutes.

A plot of  $\log \ln(I_0/I)$  vs  $\log p t$  should therefore be a straight line with slope of unity. Such a plot is shown in Fig. 4. The circles



represent experimental points. The straight lines have a slope of unity and are drawn for the best fit. These lines represent values of  $S$  of  $1.4 \times 10^{-2}$  for oxygen and  $1 \times 10^{-6}$  for hydrogen. From the values of  $S$  an activation energy of 0.11 for oxygen, and 0.36 for hydrogen, in ev per molecule, can be deduced by assuming that only those molecules which have an incident energy greater than the activation energy can be adsorbed.

It is not implied that the activation energies are independent of surface coverage; rather, the data, within the large experimental error, are consistent with the assumptions of (1) a constant activation energy, and (2) a rate of adsorption which is proportional to the product of the sticking coefficient and the fraction of uncovered surface.

#### 5. Removal of Oxygen

Heating the oxygen covered crystal at 500°C for 30 minutes restored the diffraction patterns to their clean surface values. Clarke<sup>12</sup> has suggested that oxygen may diffuse into the surface during heating; Law<sup>13</sup> has reported that oxygen is pumped by heated germanium, and is possibly removed from the surface as volatile GeO. The diffraction observations are in agreement with either of these suggestions, since it is not probable that strongly bound oxygen can be desorbed as molecules at temperatures as low as 500°C.

The first electron diffraction data on the germanium crystals were taken by R. M. Burger.<sup>14</sup>

## DISCUSSION

(See also comments following paper of P. Handler)

H. E. FARNSWORTH (*Brown University*): In view of the interest which has been expressed in the method of obtaining a clean surface by ion bombardment and annealing, the following comments are made to avoid possible misunderstandings and incorrect interpretations in the application of this method to a variety of surface problems. As has been emphasized in the paper by Schlier and Farnsworth, this method of cleaning does not produce a surface which approximates an atomically clean one unless the procedures and precautions are followed as outlined. We have

emphasized that the low-energy electron diffraction method as now in use is not capable of detecting contaminations of less than about five percent coverage. Thus a cleaning treatment which produces a "clean" surface as determined by the diffraction method may not appear sufficiently clean for some other experiment. There is the possibility that not all of the argon imbedded in the solid during bombardment may have been removed during a short anneal. There is also the possibility that an appreciable number of lattice defects remain subsequent to a relatively short anneal of 15 minutes, and that these defects produce relatively large effects in some experiments even though they are not detected by electron diffraction. Such a surface even though clean in terms of the absence of contaminating material may nevertheless be highly objectionable because of the presence of lattice defects. This statement does not imply that the cleaning method is inadequate, but rather that a longer heating and annealing period subsequent to ion bombardment is required to reduce the number of lattice defects to a tolerable value. For example, Madden and Farnsworth<sup>15</sup> have observed that the minority-carrier lifetime in a germanium crystal with (100) surfaces continues to change with time of heating subsequent to ion bombardment for relatively long periods. A heating of 15 to 20 hours at 700° to 750°C followed by a slow anneal is required to obtain a stable value for the lifetime. On the other hand, Dillon<sup>16</sup> has observed that a 15 minute anneal is adequate to obtain stable values of work function.

Questions have been raised regarding the adequacy of the low-energy electron diffraction method to detect the presence of surface contamination in an amount of one atomic layer or less. After using this method for many years with a wide variety of crystals and several different faces, we believe that the probability of such a situation occurring in any particular case is negligible. Crystals of copper, silver, gold, nickel, titanium and germanium have been examined. The ion-bombardment cleaning technique has been successfully applied to the last three. In most cases the effect of contaminating gases or other material is so clear-cut that there is no ambiguity, because of the differences between the structures of the contamination and that of the supporting crystal. The only possible ambiguity appears to be a case in which the lattice structure of the surface gas is so nearly the same as that of the



supporting crystal that no distinction can be made between the gas and the supporting crystal. Because all experimental evidence to date is consistent with the view that effects of the first monolayer of contamination can be observed, we see no reason for considering this other alternative. There is no question about the diffraction method being capable of detecting a small fraction of one monolayer of surface gas, even in the case of hydrogen. Hydrogen has been observed to chemisorb on crystals of copper, nickel, titanium and germanium.

Finally, consideration should be given to the possibility that workers in other laboratories may not be duplicating the cleaning conditions we have specified, or may be introducing some other condition which is causing a spurious effect that produces a contaminated surface. Consideration should also be given to the possibility that a particular observation may be due not to the presence of contamination but to some other condition which has been overlooked.

#### REFERENCES

1. D. Alpert, *J. Appl. Phys.* **24**, 860 (1953).
2. G. K. Wehner, *Phys. Rev.* **102**, 690 (1956).
3. Farnsworth, Schlier, George, and Burger, *J. Appl. Phys.* **26**, 252 (1955).
4. C. Davisson and L. H. Germer, *Phys. Rev.* **30**, 707 (1927).
5. H. E. Farnsworth, *Rev. Sci. Instr.* **21**, 102 (1950).
6. H. E. Farnsworth, *Phys. Rev.* **49**, 605 (1936).
7. Using this method, one of us (H. E. F., *Phys. Rev.* **49**, 604 (1936)) has shown how a (110) silver crystal face is re-etched by thermal treatment.
8. An etch consisting of 15 cc acetic acid, 25 cc nitric acid, 15 cc 48 percent hydrofluoric acid, and 0.3 cc bromine.
9. R. E. Schlier and H. E. Farnsworth, unpublished data to be presented at the International Conference on Catalysis, Sept., 1956.
10. M. Green and J. A. Kafalas, *Phys. Rev.* **98**, 1566 (1955).
11. Green, Kafalas, and Robinson, this volume.
12. E. N. Clarke, *Ann. N. Y. Acad. Sci.* **58**, Art. 6, 937 (1954).
13. J. T. Law and E. E. Francois, *Ann. N. Y. Acad. Sci.* **58**, Art. 6, 925 (1954). See also J. T. Law and P. S. Meigs, this volume.
14. R. M. Burger, H. E. Farnsworth, and R. E. Schlier, *Phys. Rev.* **98**, 1179 (1955).
15. H. H. Madden and H. E. Farnsworth, *Bulletin Am. Phys. Soc.* **1**, 53 (1956).
16. J. A. Dillon, private communication.

# ELECTRICAL PROPERTIES OF A CLEAN GERMANIUM SURFACE \*

PAUL HANDLER

*Electrical Engineering Research Laboratory  
University of Illinois  
Urbana, Illinois*

## ABSTRACT

The recent measurements of the work function, photoconductance, surface conductance, and field effect of clean germanium surfaces are reviewed. The experimental data indicate that there is a large density of states localized at the surface. The density of states is estimated to be greater than  $1 \times 10^{13}$  per  $\text{cm}^2$  and possibly as great as  $4 \times 10^{14}$  per  $\text{cm}^2$  ev. These estimates indicate that the observed levels are most likely Tamm states. The conductivity of the clean surface is large, and chemisorption of oxygen decreases it by two orders of magnitude. The work function of the clean surface is found to change by tenths of electron volts with chemisorption of oxygen and hydrogen. A model is proposed in which the unfilled orbitals of the clean germanium surface are responsible for the observed electrical effects.

## I. INTRODUCTION

The existence of localized surface states in crystals was first suggested by Tamm <sup>1</sup> in 1932 on the basis of a study of a special one-dimensional model. A more general treatment of a one-dimensional model by Shockley <sup>2</sup> in 1939 showed that surface states can occur only if there is a separate potential trough at the surface or if the energy bands arising from separate atomic levels overlap. In generalizing his results, Shockley concluded that surface states should occur in the forbidden region between the highest filled band and the lowest vacant band of germanium, since this gap occurs as a result of the overlapping of an *s*-band and a *p*-band. These surface states should form a half-filled band at the surface, which in an ideal case should be conducting, and their number should be approximately equal to the number of surface atoms.

\* Work supported by the Office of Naval Research, Contract N6-ori-07140.

From another viewpoint, the surface states may be considered as the unfilled orbitals (dangling bonds) at the germanium surface. Since two electrons can occupy a free orbital, surface atoms may become negatively charged, thus acting as acceptor states. To demonstrate Tamm states experimentally, a clean surface would have to be obtained, which showed a density of states roughly equal to the density of surface atoms and which was strongly affected by surface effects such as chemisorption.

In recent years, ultra-high vacuum techniques which have been developed by Alpert and co-workers<sup>3,4,5,6</sup> have made it possible to achieve working pressures as low as  $10^{-10}$  mm Hg. At this pressure, a few hours will elapse before a monolayer of gas is formed and measurement of the properties of clean surfaces can be achieved.

The possibility of producing a clean germanium surface under ultra-high vacuum conditions was first demonstrated by Farnsworth and co-workers<sup>7</sup> at Brown University. Using low energy electron diffraction techniques, they showed that the diffraction maxima expected from the surface lattice of germanium could be observed after the crystal had been sputtered with argon and then annealed at 500°C.

Since then, many groups have been using this same technique to measure the work function<sup>8,9,10,17</sup> photoconductance<sup>11,12,13,14</sup> surface conductivity<sup>13,14,15</sup> and field effect<sup>11,13,15</sup> of the clean germanium surface. These investigations indicate that there is a large density of states localized at the surface. The density of surface states is estimated to be at least  $1 \times 10^{13}$  states per  $\text{cm}^2$  and as high as  $4 \times 10^{14}$  states per  $\text{cm}^2$  ev.<sup>15</sup>

The recent data<sup>11,12,13,14,15</sup> indicate that these surface states are the unfilled orbitals (dangling bonds) at the clean germanium surface, which act as acceptor type states by trapping bulk electrons and forming a *p*-type conducting layer. Also, the data suggest that the adsorption of gases which can bond covalently with these unfilled orbitals strongly affects the electrical properties of the clean germanium surface, since it has been observed that the chemisorption of oxygen changes the work function by tenths of electron volts<sup>10,17</sup> and the surface conductance by two orders of magnitude.<sup>15</sup> The experiments and data which have led to these conclusions will be discussed below.



## II. EXPERIMENTS AND RESULTS

All of the surfaces discussed below were cleaned by the argon sputtering techniques of Farnsworth et al.<sup>7</sup> The argon sputtering is estimated to remove anywhere from a few to as many as several hundred atom layers depending upon the length of time of sputtering. The surface is then annealed between 500 and 700°C and cooled slowly to room temperature. Recent experiments<sup>10,12,16</sup> indicate that the best results can be obtained if the sample is sputtered for approximately one hour and annealed close to 700°C for about ten hours. These temperatures and times of annealing are probably necessary to remove the last traces of argon trapped in the surface during sputtering. In general, it is found that surfaces produced in this manner are quite stable in vacua of  $10^{-9}$  mm Hg for periods of hours.

Allen<sup>8</sup> has measured the dependence of work function on crystal orientation, using the Kelvin contact potential difference method. The contact potential of six different faces of the same germanium crystal was measured, using the same (110) face of a nickel crystal for a reference electrode. The experiment had two important checks on the reliability of its results. First, the six faces were actually three pairs of identical faces, i.e., a pair each of (100) (110) and (111) faces. Secondly, after all six faces had been measured, the first one was remeasured to check against relative drift during the time of measurement. At pressures of  $10^{-9}$  mm Hg drifts in the contact potential with time were practically never seen. The average results for three different crystals are shown in the last column of Table I. Allen has also measured

TABLE I  
PHYSICAL PROPERTIES OF THREE GERMANIUM CRYSTAL FACES

FACE	DENSITY OF SURFACE ATOMS	NUMBER OF BONDS CUT/ATOM	BONDS CUT/CM <sup>2</sup>	RELATIVE NUMBER BONDS CUT/CM <sup>2</sup>	WORK FUNCTION RELATIVE TO (111) IN EV
(100)	$2/s^2 = 6.3 \times 10^{14}/\text{cm}^2$	2	$4/s^2$	1.73	.065
(110)	$2\sqrt{2}/s^2 = 8.92 \times 10^{14}/\text{cm}^2$	1	$2\sqrt{2}/s^2$	1.23	.013
(111)	$4/\sqrt{3}s^2 = 7.3 \times 10^{14}/\text{cm}^2$	1	$4/\sqrt{3}s^2$	1.0	.000

$s$  = cube edge for the f. c. c. lattices = 5.66 Å.



the change in work function with temperature up to 700°C. For the three samples studied, the range of doping should have provided a difference in work function of about 0.3 ev on the assumption that the energy levels run straight to the surface with no barrier. The observed values of the work function were actually equal within the experimental uncertainty of  $\pm 0.05$  ev. He concluded that the position of the energy bands at the surface remained essentially fixed with respect to the Fermi level, whose position in the bulk shifted by 0.3 ev in going from slightly *p*- to extremely *n*-type. Curvature of the bands in the space charge region near the surface must thus have changed enough to make up for this difference. He also concluded that a density of surface states of at least  $4 \times 10^{12}$  per  $\text{cm}^2$  would be required to explain his experimental results on temperature and doping effects if all the states were localized at the Fermi level, and up to one state per surface atom, as is expected for Tamm states, for less favorable distributions.

Dillon<sup>10</sup> and Farnsworth<sup>17</sup> have combined the Fowler photoelectric method and the Kelvin method to measure the work function of germanium. The work function of a gold-plated reference electrode was determined by the Fowler method, and the contact potential difference between this reference and the germanium crystal was measured by the Kelvin method. The results found for the clean surface of four crystals and the conditions of cleaning are shown in Table II. These values agree very well

TABLE II

## WORK FUNCTIONS OF GERMANIUM SINGLE CRYSTAL SAMPLES

After cumulative outgassing of at least 150 hours at 650°C in high vacuum and cumulative ion bombardment of 120 minutes

100 face (45 ohm-cm, 700 microsec, nearly intrinsic)	4.77 $\pm$ .02 ev
111 face (10 ohm-cm, 60 microsec, <i>n</i> type)	4.79 $\pm$ .02 ev
111 face (29 ohm-cm, <i>p</i> type) (somewhat disturbed)	4.85 $\pm$ .04 ev
110 face (42 ohm-cm, <i>n</i> type)	4.78 $\pm$ .02 ev

Conditions of ion bombardment plus annealing treatment

Argon * gas pressure	$1 \times 10^{-3}$ mm Hg
Ion current density	110 microamps/ $\text{cm}^2$
Voltage	500-600 volts
Annealing	500°C for about 15 minutes in vacuum

\* Argon passed through getter tube.

with those of Apker, Taft, and Dickey<sup>18</sup> who found a value of 4.80 ev for evaporated germanium films. Dillon<sup>10</sup> and Farnsworth<sup>17</sup> have also investigated the effect of various gases upon the work function of a nearly intrinsic crystal, and the results are shown in Fig. 1. On exposure to oxygen at a pressure of

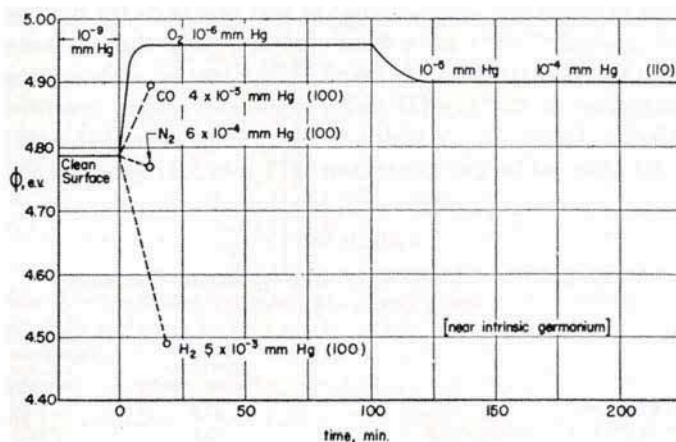


FIG. 1.—The change in work function due to the adsorption of  $O_2$ , N, CO, and  $H_2$ . (After Dillon<sup>10</sup> and Farnsworth<sup>17</sup>)

$10^{-6}$  mm Hg the work function increased, with equilibrium being reached in about seven minutes. When the pressure was increased to  $10^{-5}$  mm Hg, the work function decreased as is shown in Fig. 1, and no further changes occurred even with a maximum pressure of  $10^{-4}$  mm Hg. After the oxygen was removed, the work function value returned *slowly* to the maximum value, equilibrium being reached in about 1000 minutes. When the pressure was again raised to  $10^{-4}$  mm Hg, the same decrease was noted. This loosely bound oxygen may be associated with the formation of a second monolayer. Dillon<sup>10</sup> finds that after oxygen adsorption, the work function and photoelectric yield can be restored to their clean surface values by heating the crystal in vacuum for 15 minutes at  $500^\circ\text{C}$ . This same result has been observed by Schlier.<sup>16</sup>

With carbon monoxide and nitrogen, Dillon<sup>10</sup> and Farnsworth<sup>17</sup> have found that the work function increases 0.11 ev and

decreases 0.04 ev, respectively. There is no apparent desorption with pumping. With hydrogen the work function decreases 0.3 ev. Some of the hydrogen desorbs at room temperature because it was observed that the work function increased over its lowest value by 0.13 ev when the crystal was allowed to stand in an evacuated tube for 20 hours. Results for a ten ohm-cm sample were the same, except that no change was observed for hydrogen.

Four groups<sup>11,12,13,14</sup> have been investigating the surface recombination velocity of a germanium surface by measuring the photoresponse of the crystal under various vacuum conditions. The results found by Madden<sup>12</sup> for a well-annealed crystal, 705°C for over 20 hours, are shown in Table III. Madden found

TABLE III  
MEAN LIFETIME AND SURFACE RECOMBINATION VELOCITY  
FOR VARIOUS TREATMENTS

	MEAN LIFETIME (in microsec)	SURFACE RECOMBINATION VELOCITY (in cm/sec)
1. After CP-4 etch	475	50
2. After argon-ion bombardment	83	5,000
3. After heating an ion bombarded crystal at ~750°C for over 20 hours and annealing in vacuum	272	250
4. After heating and annealing a bombarded crystal in oxygen at 10 <sup>-6</sup> mm Hg	70	> 10 <sup>4</sup>
5. Changes due to oxygen adsorption on cleaned germanium surfaces at room tem- perature	< 3	< 7

that short anneals or lower temperatures were not sufficient to give the highest obtainable lifetimes. It has been observed by Wallis,<sup>11</sup> Autler,<sup>13</sup> and Law<sup>14</sup> that the room temperature adsorption of oxygen strongly increases the surface recombination velocity if the sample is annealed below 500°C. However, with annealing at higher temperatures, Wallis<sup>11</sup> has found results that are in substantial agreement with those of Madden, as shown in Table III. At present, the insensitivity of the photoconductance to adsorption of oxygen is not understood.

The surface conductance of clean germanium surfaces has been measured by Autler,<sup>13</sup> Law<sup>14</sup> and Handler.<sup>15</sup> Measurements of the field effect have been made by Wallis,<sup>11</sup> Autler,<sup>13</sup> and Handler.<sup>15</sup>



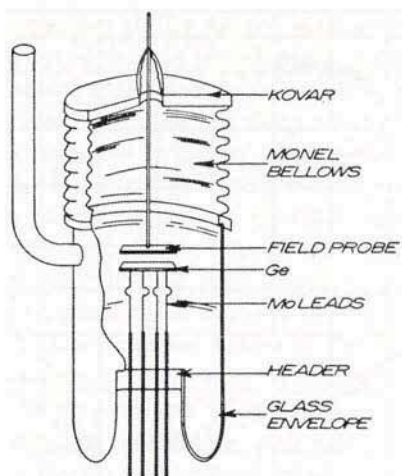


FIG. 2.—A schematic diagram of the experimental tube used for measurement of the surface conductance and the field effect mobility.

Figure 2 shows a schematic diagram of the experimental tube used by Handler<sup>15</sup> to measure the surface conductance and field effect. The conductance is measured by the standard four probe method, and the field effect is measured by observing the change in voltage across the sample with change of an electric field applied perpendicular to the surface.

Figure 3 shows the results of a typical experiment observed by Handler. In Fig. 3, the time and pressure have no real significance since the change in conductivity is really dependent upon the amount of oxygen adsorbed. At present, this quantity is unknown except that the surface is clean at the left and covered at the right. Recent work at Brown University<sup>10</sup> suggests that the conductivity decrease, after the initial rise, may be the commencement of a second monolayer of loosely bound oxygen or of a new mode of adsorption. The point at the far left shows the conductivity of the sample before cleaning. After cleaning by argon bombardment and annealing, the conductivity of the sample is greatly increased. The clean surface, as shown by these points, is very stable in a vacuum of  $10^{-8}$  mm Hg and, in one case, a sample was kept in a vacuum for 18 hours without significant change. This indicates that the partial pressure of



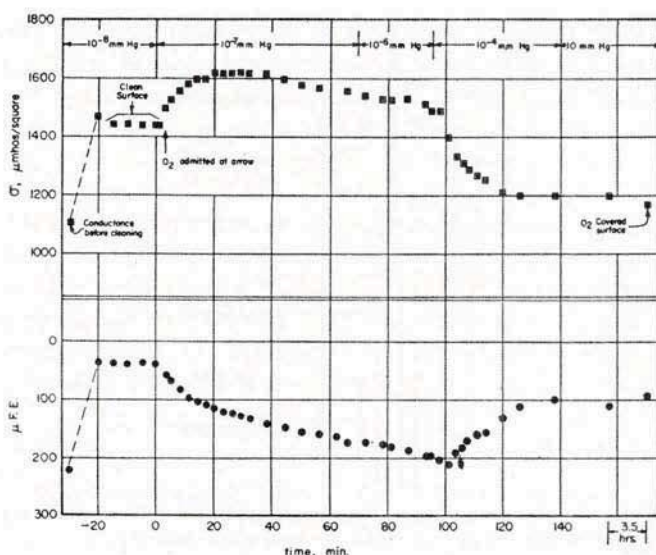


FIG. 3.—Experimental values of conductivity per square and of field effect mobility as a function of cleaning and oxygen adsorption.

adsorbable gases in the system was very low. In Fig. 3, the clean surface was observed for twenty minutes, and then oxygen at a pressure of  $10^{-7}$  mm Hg was admitted at the arrow. The conductivity began to increase immediately. It rose to a maximum, and, as the pressure was increased, the conductivity began to decrease to a value much below its clean surface value and close to the value before cleaning. The rate of oxygen admission was varied several times during the experiment. Similar changes in conductivity have been observed by Autler<sup>13</sup> and Law.<sup>14</sup> The maximum of conductivity probably corresponds to the increase in work function shown in Fig. 1 as observed by Dillon,<sup>10</sup> while the decrease in conductivity from the maximum corresponds to his observed decrease in work function. Also the maximum of conductivity probably corresponds to the first mode of adsorbed oxygen, as observed in the electron diffraction studies of Schlier.<sup>16</sup> The fact that the final value of the conductivity after complete oxygen adsorption is close to its value before cleaning indicates that there has been little or no change in the bulk properties of the sample. A second indication

that all the changes are at the surface is that the bulk resistivity of the oxygen covered sample is still near its original 40 ohm-cm value. The important quantities to notice in Fig. 3 are the differences in conductivity between the clean surface and the oxygen-covered surface, and the height of the maximum. The ratio of these two quantities for a clean surface is about 1.5.

The field effect mobility,  $\mu_{F.E.}$ , of the clean surface shows *p*-type conduction at the surface.<sup>13,15</sup> When oxygen is admitted at a pressure of  $10^{-7}$  mm Hg, the field effect mobility, as shown in Fig. 3, rises to a maximum and, as the oxygen pressure is increased, it then decreases. The observed values of the field effect mobility for the clean surface are not very reproducible and may vary from 20 to 50  $\text{cm}^2$  per volt sec.<sup>15</sup> The maximum of the field effect mobility is usually 5 to 6 times its clean surface value. The maximum of the mobility always occurs somewhat after the maximum in the conductivity. The field effect measurements were carried out at 100 cps. Autler<sup>13</sup> has observed field effect mobilities which are larger by a factor of 3, and also has measured the field effect mobility from 100 cps to 1000 cps and has found that it is essentially constant over this range. Wallis has also observed field effect mobilities as high as 350  $\text{cm}^2$  per volt sec for the clean surface. The large variations in the observed values of the field effect mobility observed by different groups is not well understood. The methods used for estimation of the capacitance may affect the results by as much as a factor of two, but they do not explain the observed differences which are as large as 10. The initial increase in conductivity with the adsorption of oxygen must increase the number of carriers at the surface, since it does not seem possible for the mobility to increase fast enough to compensate for a decrease in carriers.

Table IV shows the results<sup>15</sup> of sixteen oxygen admissions upon four different samples cut from the same near-intrinsic crystal. In the cases where the surface was only slightly etched, we see that just heating the samples gives changes in conductivity which are lower than those observed for the same samples which have been lightly etched and cleaned by argon bombardment. For the three samples which have been lightly etched and cleaned, there is a surprising reproducibility, indicating that the surfaces examined were very similar and, most probably, clean. Furthermore,

TABLE IV  
SUMMARY OF O<sub>2</sub> ADMISSIONS AT ROOM TEMPERATURES

SAMPLE	TREATMENT OF SURFACE	$\sigma_{\text{clean}} - \sigma_{\text{final}}$ ( $\mu\text{mhos/square}$ ) $\Delta\sigma_{\text{total}}$	$\sigma_{\text{max}} - \sigma_{\text{clean}}$ ( $\mu\text{mhos/square}$ ) $\Delta\sigma_{\text{max}}$	$\frac{\Delta\sigma_{\text{total}}}{\Delta\sigma_{\text{max}}}$
M-3	Very light CP-4 etch	{ Heated to 500°C for 20 hrs. }	75	
Mo-11		{ Heated to 550°C for 4 hrs. }	123	68
Mo-11			104	49
Mo-11			120	51
M-3		{ Argon bombardment and 550°C anneal }	123	93
M-3			141	84
Mo-10			134	—
Mo-10			149	—
Mo-11			149	104
Mo-10		{ Heated in vacuum to 550°C after admission of O <sub>2</sub> to Argon cleaned surface }	139	—
Mo-10			141	—
Mo-10			140	—
Mo-13	Heavy etch	{ Heated to 550°C for 4 hours }	29	No max observed
Mo-13		{ Argon bombardment and 550°C anneal }	28	
Mo-13			93	60
Mo-13			97	63

heating an argon-bombarded and annealed sample in vacuum after oxygen admission, as shown for sample Mo-10, gives the same results observed for the usual cleaning techniques. These results agree with the electron diffraction work of Schlier<sup>16</sup> and the work function experiments of Dillon.<sup>10</sup>

If the sample is heavily etched before introduction into the vacuum system and just heated, the observed change upon admission of oxygen is small and no maximum of conductance is observed. However, argon bombardment cleaning of such a sample gives the same character of results observed previously, except that the absolute value of the change in conductivity is smaller. The difference in results depending upon the amount of etch is probably due to the greater surface area of the lightly etched samples. The fact that the ratios of  $\Delta\sigma_{\text{tot}}/\Delta\sigma_{\text{max}}$  are about the same for the two treatments indicates that the same process was occurring on all the cleaned surfaces examined. A  $\Delta\sigma_{\text{tot}}$  close to the values tabulated here has been observed by Autler.<sup>13</sup>



The nature of the oxide on an etched surface seems to be different from the oxide formed by the adsorption of oxygen on a clean surface, since the etched surface must be sputtered to produce a clean surface, while in the latter case the surface has only to be heated. The etched surface is probably covered with several atom layers of germanium dioxide which are nonvolatile, while in the case of the chemisorbed oxide the surface is covered with a monolayer of oxygen which may volatilize as germanium monoxide. Observations to support this view are the following: The oxygen covered surface when heated in vacuum gives off very little gas, indicating that the oxygen does not leave the surface as  $O_2$ .<sup>15</sup> The results of Bernstein and Cubicciotti<sup>19</sup> and Law and Meigs<sup>20</sup> on the kinetics of the reaction of germanium and oxygen indicate that the oxidation rate above 500°C is controlled by the rate of evaporation of germanium monoxide from the surface. Above 600°C this rate of evaporation is in turn governed by both the extent to which the surface is covered by an impervious film of germanium dioxide and by the pressure of gas above the surface.<sup>19,20</sup> The observation that the germanium loses weight upon oxidation<sup>19</sup> also supports the evaporation mechanism. Therefore, it is reasonable to assume that in the high vacuum experiments the chemisorbed oxygen leaves the germanium surface as some volatile oxide and creates a new germanium surface.

There has been some question as to whether the surfaces observed here are really clean.<sup>14</sup> It has been suggested that perhaps a monolayer of chemisorbed gas is formed from impurities in the argon gas or in the first few minutes immediately after cooling. This layer would be tightly bound and stable under heat treatment, since the adsorption of oxygen on freshly cleaned surfaces has been shown to have a high heat of adsorption.<sup>21</sup> With this adsorbed layer present, the observed electrical effects are then believed to be the result of the adsorption of a loosely bound second monolayer.

To determine whether the partial pressure of adsorbable gases is large enough to form a monolayer in a few minutes, two experiments were performed:<sup>15</sup> a flash filament experiment and a rate of rise of pressure experiment. A tungsten filament was flashed at 1900°K in the same system in which the experiments had been performed. It was found that the surface had not been saturated

after 1000 minutes. The amount of gas leaving the filament after 100 minutes indicated that not more than a few percent of a monolayer had formed.

The rate of rise of pressure, as measured in the vacuum system used by Handler<sup>15</sup> agreed within a factor of three with the value calculated from the data of Rogers, Buritz, and Alpert<sup>22</sup> for the diffusion of helium through glass. This rate of rise of pressure experiment indicates that most of the residual gas in the system is helium and the flash filament experiment indicates that the partial pressure of adsorbable gases in the system is much less than  $10^{-10}$  mm Hg. This evidence may not be conclusive since the rate of adsorption for clean germanium and clean tungsten surfaces may differ greatly. However, the times for adsorption observed by Handler on the tungsten filament agree with the times for adsorption observed by Allen and Farnsworth for a clean germanium surface. Also Allen<sup>8</sup> has monitored the contact potential difference of a particular face continually as the germanium cooled, both from a high temperature (approximately 800°C) cleaning and from a medium temperature (approximately 500°C) annealing. In no case were any drastic changes in the work function of germanium observed.

A second source of contamination may be the impurity content of the argon. During a post-bombardment anneal of germanium, a pressure rise indicates that an appreciable fraction of a monolayer of gas has been driven into the surface. Allen<sup>8</sup> suggests that while the impurity content of the argon may be small, a large fraction of the impurity gas might nevertheless remain due to a high affinity for combination with germanium. This impurity gas could not be oxygen since it has been shown<sup>19,20</sup> that oxygen leaves the surface as a volatile oxide. However, if a fixed volume of argon is used for sputtering, there should be a purification of the argon as the many atom layers of germanium are removed, so that the final sputtering should be effected by very pure argon. Handler<sup>15</sup> has used both fixed volumes of argon and flow systems without noticing any observable differences. Perhaps the best evidence for the clean surface is that the clear electron diffraction patterns of the clean germanium surface, obtained by Farnsworth et al.,<sup>7,18</sup> remained for several hours in vacua of  $10^{-8}$  to  $10^{-9}$  mm Hg before adsorption effects from residual gases became observable.



## III. DISCUSSION

Reviewing the results, it can be seen that there is a strong similarity in behavior of the crystal surfaces examined in various laboratories and under diverse experimental conditions. Accordingly, the surfaces examined are most likely clean. Therefore, the observed experimental results can be used to support a model in which unfilled orbitals determine the electrical properties at the surface.

Allen's<sup>8</sup> results as tabulated in the last column of Table I show a strong correspondence between the relative number of bonds cut per  $\text{cm}^2$  and the work function for each of the crystal faces examined, and suggest that the unfilled orbitals at the germanium surface are responsible for a portion of the surface dipole. The work of Dillon<sup>10</sup> and Farnsworth,<sup>17</sup> as shown in Fig. 1, shows that the work function is strongly affected by interaction of these unfilled orbitals with chemisorbable gases. The effect of oxygen on the surface conductance<sup>15</sup> indicates that the energy band at the surface must first move up under pressures of  $10^{-7}$  mm Hg and then move down as the oxygen pressure is increased.

These results suggest the following model for the clean surface of germanium. Each germanium atom of the surface with its unfilled orbitals acts as an acceptor type surface state. A certain number of these states ionize by releasing their holes to the bulk. Or, conversely, a certain number of electrons leave the bulk and are trapped in the unfilled orbitals at the surface as is shown in Fig. 4. These trapped electrons give rise to the large *p*-type

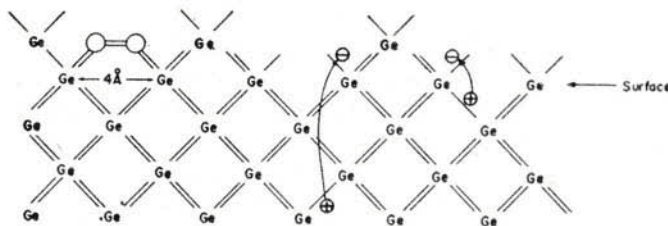


FIG. 4.—An atomic diagram of the clean (100) germanium surface, with every second atom in the (110) direction removed, showing electrons trapped in free orbitals and oxygen chemisorbed to the surface as a peroxide.



conducting layer observed in the surface conductance and field effect experiments.

A surface atom trapping an electron in the (111) plane is shown in Fig. 5a. To a first approximation, each surface germanium atom

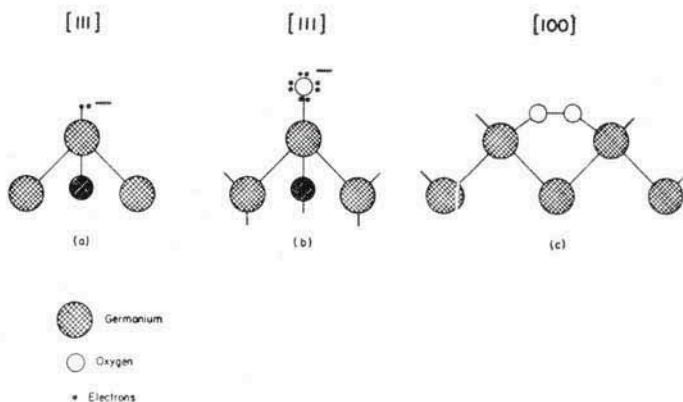


FIG. 5.—Possible modes of  $O_2$  adsorption

- (a) a pseudo-arsenic atom
- (b) oxygen chemisorbed as an  $O^-$  without the removal of a hole
- (c) oxygen chemisorbed as a peroxide with the removal of two free germanium orbitals.

can be considered as the termination of a large molecule, since its next nearest neighbor is  $4\text{\AA}$  distant. As Stranski and Suhrmann<sup>23</sup> have pointed out, the ratio of the distance between next-nearest neighbors to nearest (valence bond) neighbors for the diamond lattice 1.63 is much greater than the corresponding ratio for other metal lattices (1.1 to 1.4) so that, presumably, little account need be taken of next-nearest neighbors. Therefore, the most stable germanium surfaces should consist of either (111) or (110) planes where each surface atom is bonded to three germanium atoms below the surface and the (100) should be the least stable since the surface germanium atom is bonded to only two germanium atoms below the surface.

Allen<sup>8</sup> has looked for large steps in his surfaces using magnifications of  $250\times$  with glancing illumination. He observed no steps or facets and concludes that, if present, they are small compared to  $10^{-4}$  cm. Also, Allen upon examining one of his crystals with

an optical goniometer after removal from the vacuum system, found no light reflection from any plane other than that parallel to the sample face for each of six faces examined.

However, the possibility of steps of only a few atomic layers seems very probable. Schlier<sup>16</sup> has suggested that in the (100) plane every other atom in the (110) direction is removed as is shown in Fig. 4 to produce his observed half-order beams. Nevertheless, he rejects this model on the grounds that as the first oxygen is adsorbed, a germanium-like surface results and the relative scattering of oxygen and germanium would have to be very nearly identical. However, if the oxygen were chemisorbed as a peroxide as shown in Fig. 4, or as two O<sup>-</sup>'s, a germanium-like surface would result since the scattering for low energy electrons from two oxygens might be close to what would be observed for a germanium in that position. Also, the surface with every other atom removed in the (110) direction, as shown in Fig. 4, should be more stable than a normal (100) surface, since the number of free bonds is distributed over a greater number of surface atoms.

The valence bond picture suggests that a germanium atom bonded to three other germanium atoms is most likely to trap an electron. It may do this by using its *p*-orbitals to bond to the crystal and leaving its *s*-orbital free to hold two non-bonding electrons. Then an electron could leave the bulk and be trapped in this *s*-orbital with a gain in energy roughly equal to the difference between the 4*p* and 4*s* states. The germanium atom at the surface is then like a pseudo-arsenic atom, as shown in Fig. 5a, with five electrons in its outer shell. The hole formed by the formation of the pseudo-arsenic atom may be tightly bound to it. A certain fraction of these holes would ionize from the acceptor-like states to form the *p*-type conducting layer.

The adsorption of the first oxygen, which may adsorb as O<sup>-</sup>, as shown in Fig. 5b, may give acceptor states in which the hole is more weakly bound and therefore allow a larger fraction of holes to ionize from the surface. This type of adsorption could account for the initial rise in conductivity observed by Law<sup>14</sup> and Handler,<sup>15</sup> and the rise in work function observed by Dillon<sup>10</sup> and Allen.<sup>8</sup>

A second mode of oxygen adsorption, which might correspond to the final decrease in conductivity, is shown in Fig. 5c. In this

mode, the oxygen bonds to the germanium as a peroxide by filling the unfilled orbitals of two germanium atoms and, therefore, removing two surface states. With this mode of adsorption, the excess surface conductivity should disappear with full coverage of the surface. This type of adsorption would correspond to the decrease in conductivity observed by Autler,<sup>13</sup> Law,<sup>14</sup> and Handler<sup>15</sup> and to the decrease in work function observed by Dillon<sup>10</sup> for oxygen and for hydrogen. While the peroxide structure is a possible explanation for the second mode of adsorption, it is not a very stable configuration. The O-Ge-Ge angle is not strained very much but the O-O-Ge angle is very far from its preferred angle of 90°. The possibility of a single oxygen atom bonding to two surface germanium atoms 4Å apart is very small since the sum of the bond lengths is only 3.76Å.<sup>24</sup> At present, it is not understood why a pressure of greater than 10<sup>-6</sup> mm Hg is necessary to initiate the second mode of oxygen adsorption and also why its time for adsorption can be a matter of one minute, while its desorption as noted by Dillon<sup>10</sup> may be as long as 1000 minutes.

The observed values of the field effect mobility for the clean surface vary from 50 cm<sup>2</sup> per volt sec to 350 cm<sup>2</sup> per volt sec.<sup>11,13,15</sup> As oxygen is added, the bands at the surface are raised and the field effect mobility increases to from 200 to 700 cm<sup>2</sup> per volt sec. Schrieffer's theory of diffuse scattering<sup>25</sup> predicts that the true or effective mobility of holes at the surface should decrease with the raising of the bands. The increase in the observed field effect mobility must then be explained by a decrease in the amount of shielding by the surface states for the frequency range investigated. Accordingly, the true mobility of the clean surface must be at least the maximum observed value of the field effect mobility, since the conductivity data suggest that the energy well for the carriers is deeper for the observed maximum of the field effect mobility than it is for the clean surface.

Because of screening by surface states, the field effect mobility is probably considerably less than the mobility of the free holes in the surface barrier. The total induced charge,  $\delta Q/\text{cm}^2$ , is divided between the free holes,  $e\delta P/\text{cm}^2$ , and the charge in surface traps,  $-e\delta N_{\bar{T}}/\text{cm}^2$ :

$$\delta Q = e(\delta P - \delta N_{\bar{T}})$$



A surface conductivity,  $\Sigma$ , will be defined as the change in conductivity per square area of surface relative to the conductivity when the bands are flat all of the way to the surface, and the corresponding change in the total number of holes in the space charge layer relative to the flat band condition will be denoted by  $P$ . Then the field effect mobility is defined by

$$\mu_{F.E.} = \delta\Sigma/\delta Q,$$

while the effective mobility of the free holes is defined by

$$\mu_{eff} = \delta\Sigma/e\delta P,$$

or by

$$\mu_{eff} = \Sigma_{tot}/eP,$$

which is of the same order of magnitude. The shielding factor,  $f$ , is defined by

$$f = \mu_{F.E.}/\mu_{eff} = \delta P/(\delta P - \delta N_T^-)$$

Only rather broad limits can be set on the trap distribution and effective mobility from the present data. If it is assumed that  $f \sim 1$ , so that  $\mu_{eff} \sim 100$  cm<sup>2</sup>/volt sec, then  $P \sim 1 \times 10^{13}$ /cm<sup>2</sup> for  $\Delta\sigma_{tot} \sim 150$   $\mu$ mhos. This gives a lower limit on the surface state density, since electrical neutrality requires  $N_T^- = P$  and obviously  $N_T > N_T^-$ . If it is assumed that  $f \sim 0.1$  and  $\mu_{eff} \sim 1000$ , then  $P \sim 10^{12}$ /cm<sup>2</sup>. However, to get this much shielding requires  $N_T > P/f$ , so that  $N_T$  must be at least as large as for no shielding.

If the model of Tamm states is the correct one, the surface states have a density of the order of  $10^{15}$ /cm<sup>2</sup> and are probably spread out into a band which is half occupied for electrical neutrality. This band itself would contribute to surface conduction, but one would expect the mobility to be so much less than for the free carriers, that the latter would dominate. The effect of the transverse electric field is to cause a small shift of the Fermi level. If  $N(E)dE$  is the number of surface states in an energy range  $dE$  at the Fermi level,

$$\delta N_T^- = N(E) \delta E_F.$$

If the Fermi level crosses the valence band, there would be a corresponding expression for  $\delta P$ , and the shielding factor would

depend on the ratio of the density of states in energy for the two sets of states. If Boltzmann statistics applies to the holes,

$$\delta P \sim P(\delta E_F/kT).$$

To get  $f \sim 0.1$  would require

$$N(E) \sim 10 P/kT \sim 4 \times 10^{14}/\text{cm}^2 \text{ ev.}$$

The minimum number of surface traps for this model is obtained if it is assumed that all traps have energies equal to the Fermi energy.

This gives  $N_T \sim 4 P/f \sim 4 \times 10^{13}/\text{cm}^2$ ,

and  $N_T$  is independent of the value chosen for  $f$ .

Therefore, with no shielding by surface states the minimum number of states must be at least  $1 \times 10^{13}/\text{cm}^2$ . However, the increase in  $\mu_{F.E.}$  with the increase in conductivity indicates that shielding by the surface states is important. The least estimates for the number of surface states is then  $4 \times 10^{13}/\text{cm}^2$  for all the states at the Fermi energy and  $4 \times 10^{14}/\text{cm}^2 \text{ ev}$  for the states distributed evenly in the energy gap. These estimates are larger by a factor of ten than those estimated by Allen<sup>8</sup> for similar models. These estimates indicate very strongly that Tamm states do exist on a clean germanium surface.

Formation of the Tamm states requires taking approximately  $10^{15}$  states/ $\text{cm}^2$  from the valence band. This would, of course, have a very marked effect on the density of states and on the effective mobility of the free carriers. This makes any detailed theoretical analysis uncertain.

#### ACKNOWLEDGMENTS

I would like to thank Professor John Bardeen for many helpful discussions and for his guidance in the interpretation of this work. Also I would like to thank Dr. J. J. Ruddick, S.J., for help with some of the early measurements.

#### DISCUSSION

H. E. FARNSWORTH (*Brown University*): Handler states that a (100) germanium face with every other row of atoms removed

in the (110) direction is more stable than a normal (100) face and hence is more likely to exist under the experimental conditions in question. He further states that if the oxygen were chemisorbed as peroxide in the positions of the removed atoms, a germanium like surface would result. We should like to point out that, while the first of the above statements appears correct as a result of a comparison of the number of free bonds in the two cases, the surface with the alternate rows of atoms removed in the (110) direction probably does not exist because of the following evidence: (1) Schlier<sup>26</sup> has pointed out that if one makes the above assumptions, one should also expect oxygen to be adsorbed above the alternate rows of germanium atoms which are not removed. This follows since in these rows there are two free bonds available for each oxygen molecule and the orientation of these bonds with respect to the molecule are the same as they would be for Handler's postulated oxygen adsorption in the positions of the "removed" germanium atoms. However, this would still lead to a double surface spacing and hence half-integral order diffraction beams in the (110) azimuth after oxygen adsorption. Such half-integral order beams are *not* observed after oxygen adsorption. (2) On consideration of the above criterion of a minimum in the free bonds for stability, one should expect thermal etching parallel to (110) planes at the expense of the (100) planes rather than a simple removal of alternate rows. That this does not occur to any considerable extent is indicated by the fact that no (110) planes are observed by the low-energy electron diffraction. As has been pointed out previously, because of the exceedingly low penetration of the diffracted electrons, the surface monolayer determines the manner in which the diffraction beams grow and decay as the wave length is changed. If a surface becomes re-etched parallel to a different plane, the surface monolayer of atoms is changed and hence the growth and decay of the diffraction beams, with change in wave length, is altered so as to indicate clearly the presence of the etched planes. This method has been used by the writer (*Phys. Rev.* **49**, 604 (1936)) to show that a (110) chemically-etched, silver crystal face is re-etched by thermal treatment to form (100) and (111) surface planes. On the other hand, although the (111) planes of face-centered cubic metals such as copper and silver are more dense and hence presumably



somewhat more stable than (100) planes, it has been found possible to heat such crystals with a surface of (100) planes at temperatures where thermal etching can occur, with no apparent production of (111) surface planes. However, such thermal etching of a (100) face of copper to produce (111) surface planes has been observed subsequent to oxidation of the surface.

The question has been raised about the exact nature of a germanium crystal surface which has been etched parallel to a (100) set of planes. Such a surface must contain many steps and pits on an atomic scale even though it appears smooth in the range of visible wave lengths. One might expect that the sides of these steps and pits would be parallel to (111) and (110) planes which should be more stable than the (100) face. The evidence from low-energy electron diffraction shows that the surface area of such planes on a well-etched (100) surface is relatively small (less than five percent) and further that these planes do not develop at the expense of the (100) face during many hours of heating at 700° to 705°C, or during the ion bombardment and annealing process of cleaning. We believe these observations indicate that the plane parallel to the geometrical boundary is the favored orientation for existence as a result of the above treatment. In some cases (copper, silver, nickel), there is evidence that the sides of such steps and pits on a (100) face are also parallel to (100) planes.

W. H. KLEINER (*Lincoln Laboratory*): I would like to emphasize that care should be exercised in comparing results of measurements on surfaces cleaned in different ways and in comparing results of different types of measurements on the same surface.

It is important to know what fraction of the surface does not contribute coherently to the slow electron diffraction pattern, since some properties of the surface may be highly sensitive to sources of incoherent slow electron scattering. This information may be difficult to determine with accuracy from the diffraction pattern alone. Among the sources of incoherent slow electron scattering may be included surface regions where atoms are not regularly arranged, in analogy to 3-dimensional x-ray diffraction from liquid or glass, and regions with a regular lattice but containing randomly substituted impurities, in analogy to 3-dimensional x-ray diffraction from a crystal with substituted impurities or a

disordered alloy. In the latter case the intensity of coherent scattering is proportional to  $\langle f \rangle^2$ , the square of the average atomic scattering factor, and the intensity of incoherent scattering is proportional to  $\langle f^2 \rangle - \langle f \rangle^2$ , the mean square deviation of the atomic scattering factors. The ratio of the scattering factors of germanium and oxygen atoms for electrons<sup>27</sup> is close to 3 in the experimental range. If, for example, in a layer of germanium atoms arranged on a lattice a quarter of them are replaced randomly by oxygen atoms, the coherent electron scattering from the layer would decrease to  $\frac{3}{4}$  of its original value, and the incoherent intensity would increase to  $\frac{1}{4}$  of the value expected if all the atoms of the germanium layer scattered incoherently. It may be difficult to distinguish the two situations from the electron diffraction alone. It should be pointed out that the electron scattering analogue<sup>27</sup> of x-ray diffraction theory used above, although a fair approximation for fast electrons, gives at best rough qualitative information for slow electrons.

Clean surfaces obtained by crushing single crystals (see Green, Kafalas and Robinson, this volume) may be metastable, containing appreciable excess surface energy. Annealing may lead to better reproducibility of measurements and allow more valid comparison with ion-bombarded and annealed surfaces.

J. T. LAW and C. G. B. GARRETT (*Bell Telephone Laboratories*): We should like to caution against a too hasty acceptance of the belief that germanium surfaces prepared by the Farnsworth technique are clean. We too have made use of the ion bombardment techniques, and have studied changes in the surface conductivity and surface recombination velocity of germanium samples on cleaning and on subsequent admission of oxygen and other gases.<sup>28</sup> Our skepticism as to the cleanliness of the Farnsworth surface is based, however, not only on our own results, but also on those reported elsewhere, with which, to the extent that the experimental measurements overlap, there is good agreement. Our reasons are as follows:

(i) It was stated by Handler that a surface could be kept for 18 hours in a vacuum of  $10^{-8}$  mm without significant change in conductivity. Now data obtained by Hagstrum<sup>29</sup> on the adsorption of residual gases by a tungsten filament showed that even at total pressures as low as  $3 \times 10^{-10}$  mm, the monolayer formation time



was about 14 hours. This must mean either that the sticking coefficient of gases on a clean germanium surface is very low, or that the surface is already contaminated, since presumably the sticking coefficient would be expected to decrease with coverage, as has been found on tungsten.

(ii) There seems to be general agreement that oxygen which has been taken up by exposure of a cleaned germanium surface on that gas can be removed simply by heating the sample to a rather modest temperature. Handler reports that this process goes rapidly at 500°C. We have found that there is already some removal—perhaps 50 percent—at 200°C, that more and more comes off as the temperature is raised beyond that, and that the process is more or less complete at 400°C. In view of the high initial heat of adsorption of oxygen on crushed germanium surfaces, this cannot possibly be straight desorption of chemisorbed gas: while the low vapor pressure of germanium monoxide at these temperatures seems to rule out the mechanism  $\text{Ge} + \text{GeO}_2 \rightleftharpoons 2 \text{GeO}$ .

(iii) There are serious difficulties in the physics of the clean surface model proposed by Handler. He has attempted to account for the observed conductivity changes on exposure to oxygen and to hydrogen by reference to the changes in work function found by Dillon. Apart from the difficulty that the orders of magnitude of the changes in work function are wrong, it becomes impossible to reconcile the observed results as to the variation in surface recombination velocity. If the initial effect of oxygen is to raise the barrier (as one would guess from the increase in work function) and also to decrease the density of the effective Tamm states (as evidenced from the increase in the field effect mobility), why does the surface recombination velocity stay constant in this region, and why, at higher oxygen pressures, does it actually increase?

These considerations appear to us to shed doubt on the supposition that the surfaces prepared by the Farnsworth technique are atomically clean. On the other side, the only evidence for cleanliness is that provided by the electron diffraction patterns. But there are surely other possible reasons for the appearance of half-order diffraction maxima. For example, one can suppose that the surface is already covered, by the time that the initial



measurements are made, with half a layer of oxygen, bound interstitially in alternate surface lattice sites.<sup>30</sup> As more oxygen is admitted, coverage of the surface proceeds. However, the first set of oxygen atoms may now change places with the germanium atoms nearest to the surface, in the manner of oxide film formation discussed by Mott and Cabrera. The surface must now struggle to reach the structure corresponding to germanium dioxide rather than germanium, so that the transition region between germanium and film will be characterized by a considerable degree of disorder, and the half-order diffraction maxima will disappear. In this way, the lowest half-layer of oxygen atoms will always be more tightly bound than succeeding layers, and will stay behind on subsequent heating. Such a model would appear to account for the observed facts at least as well as that based on the assumption that the Farnsworth surface is clean. The need for further experiments—particularly aimed at understanding the easy removal of oxygen on subsequent heating—is obvious. Under the circumstances, it seems a little premature to erect an elaborate theory, based on the assumption of a clean surface, to account for a selected amount of experimental information as to the electrical properties of such a surface, before one even knows what is the nature of the system with which one has to deal.

H. E. FARNSWORTH: In the comments by Law and Garrett, reference is made to some of our early reports on electron diffraction from germanium contained in Lincoln Laboratory Quarterly Progress Reports. The statement is made that our tentative interpretation is similar to the picture of Law and Garrett in which they assume that the cleaned surface obtained is covered by one-half a monolayer of oxygen. We wish to point out that this is not the case. The postulated gas structure is that which resulted after an exposure of a few hours to the residual gas. In these early experiments the vacuum conditions were not as good as those obtained later after adding getter tubes. The effects of residual gas noted in the early Progress Reports were observable after short periods of a few hours. Subsequent to improvement in the conditions no effects of residual gas were detectable during 24 hours. It is also to be noted that the half-integral order beams were weak and few in number in the early experiments but became more intense and more numerous as the vacuum conditions were

improved, and were most fully developed under the best conditions. Also the early interpretation of the adsorbed gas structure later proved to be inadequate to account for more detailed observations.

The above explanation by Law and Garrett for the disappearance of the half-integral order beams when oxygen is adsorbed is not consistent with experimental observations. Their picture of the formation of germanium dioxide "so that the transition region between germanium and film will be characterized by a considerable degree of disorder" would also result in a very large decrease in intensity of all diffraction beams from the underlying germanium lattice. Such a decrease is not observed while all half-integral order beams and all "additional" integral order beams not associated with a Bragg reflection from the germanium lattice decrease to a negligible value.

The regeneration of the clean surface condition by heating at a few hundred degrees subsequent to chemisorption of oxygen was reported by Dillon (*Bul. Am. Phys. Soc.* **30**, 17 (1955): II, 1, 53 (1956) and by Schlier (*Bul. Am. Phys. Soc.* II, 1, 53 (1956)). The experiments on crushed germanium surfaces at Lincoln Laboratory indicate a high heat of adsorption of oxygen for the first monolayer varying "from 250 Kcal/mol of  $O_2$ , at zero coverage, to approximately 150 Kcal/mol at monolayer coverage" (Robinson, Rosenberg, and Gatos, *J. App. Phys.*, in Press). Hence the argument which Law and Garrett use for the stability of the first half monolayer should also apply to the second half monolayer.

It should be pointed out that the high initial heat of adsorption of oxygen on a clean germanium surface combined with the removal of the gas by heating at relatively low temperatures is not a unique characteristic of germanium. For example, it has been observed by Russell and Bacon (*J. Am. Chem. Soc.* **54**, 54 (1932)) that, although large thermal effects are involved when oxygen adsorbs on nickel at  $0^\circ C$ , the surface can be reactivated by heating at  $300^\circ$  to  $400^\circ C$ . They also observed that no oxygen can be pumped from the surface at these temperatures. Since the removal of nickel oxide is not appreciable at these temperatures, it follows that the adsorbed oxygen diffuses into the interior of the nickel. Recently we have observed a similar phenomenon for



nickel, using low-energy electron diffraction (unpublished results). After obtaining a clean (100) nickel surface by the ion-bombardment and annealing technique, oxygen adsorbs in a double-spaced, face-centered lattice. This adsorbed monolayer is removed by heating at only 150° to 200°C for 30 minutes and hence must diffuse into the nickel.

Although the sticking coefficients for oxygen on molybdenum and tungsten are very high, we have observed low coefficients for oxygen on clean titanium, nickel and germanium.

The statements in the first paragraph of (iii) of the comments have no bearing on the question relating to a clean surface. These statements apply equally well to a clean or contaminated surface. Sources of the difference other than contamination must be sought.

S. H. AUTLER and A. L. MCWHORTER (*Lincoln Laboratory*): We would like to take this opportunity to summarize what we consider to be the main arguments for and against the proposition that the surfaces obtained by Professor Farnsworth's technique are really clean. Most of these arguments have already been presented by others during or after the relevant papers, or in private conversations during the conference, but we feel it would be useful to have them all collected in one place.

*Pro:* The surfaces are clean because the electron diffraction measurements give reproducible patterns which can very plausibly be interpreted as arising from 100 germanium surfaces.

*Con:* The fact that reproducible diffraction patterns are obtained is not proof of a clean surface, for a regularly contaminated surface might also give such diffraction patterns.

*Pro:* But it seems unlikely that reproducible results would be obtained if the surface were not clean. In the case of the electrical measurements the results obtained by different workers have been in essential agreement, although there is no reason to expect the degree of contamination to be the same in each case.

*Con:* There are several reasons why it is actually not so hard to believe that different workers would end up with the same degree of contamination after the anneal. First, the sticking coefficient for the contaminating gas might decrease rather sharply after a certain degree of coverage, so that the contamination would tend to settle at this level. Second, and even more likely, is the



possibility that during the anneal all loosely bound gas is driven off, leaving a residue of tightly bound atoms which would be the same whatever the initial degree of contamination. The data of Robinson<sup>31</sup> on the heat of adsorption of oxygen on germanium shows a fairly rapid decrease in binding energy with coverage, and would tend to support this.

The fact that these measurements indicate such large binding energies for low coverage makes it hard to reconcile another observation with the existence of a clean surface. This is the fact that after oxygen has been admitted to a surface, one can restore the diffraction and electrical properties of the "clean" surface by simply heating the sample. The temperatures required for this are much too low to permit evaporation of oxygen atoms from a clean surface, which indicates that the original surface was already partly contaminated.

*Pro:* Here are two mechanisms which would remove oxygen from a clean surface at relatively low temperatures:

1. The oxygen is removed as some volatile compound such as GeO.
2. The oxygen on the surface may diffuse into the bulk upon heating, which would restore a clean surface.

*Con:* In answer to (1), there is data<sup>32</sup> which shows that the rate of removal of GeO is negligibly small at temperatures of 200°C, while the conductivity changes measurably upon heating to this temperature after exposing the surface to oxygen. Also experiments on crushed powders<sup>33</sup> indicate that heating to as high as 500°C does not renew more than 10 percent of the surface, as determined by the amount of oxygen reabsorbed after heating. This also indicates that diffusion of oxygen into the bulk does not renew the surface.

*Pro:* With regard to rate of removal of GeO from surface, the following should be noted:

None of the data on the rate of uptake of oxygen has been obtained on bombarded 100 surfaces and is, therefore, not applicable to the case of interest. In addition, the fact that there is a partial restoration of conductivity at 200°C might be explained by assuming that a relatively small amount of loosely bound oxygen in a second or third layer is removed. Also, if the data of Law and Meigs<sup>32</sup> on the rate of removal of GeO were applicable

to the bombarded surfaces, it would seem to indicate that the removal should go at a rapid rate above 500°C and therefore heating might reclean the surfaces.

The crushed-powder experiments<sup>33</sup> do not help settle the question of whether a clean surface can be restored by heating because they were done under conditions where the powders were so tightly packed that the speed at which volatile gases could be pumped away was very low. Also, if the gas tended to come off the surface at a pressure of less than  $10^{-6}$  mm, it would be removed from the bombarded surfaces, but would not come off at all in the relatively poor vacuum used in the crushed-powder experiments. The latter work would also seem to indicate that surface oxygen does not diffuse into the bulk, but here again conditions are different. The surface-to-volume ratio is vastly greater in the case of the powders than for bombarded samples. A monolayer of oxygen would give a bulk concentration of about  $10^{16}$ /cc in the latter case but  $10^{19}$ /cc in the former, which might well inhibit diffusion from the surface into the bulk.

It seems to us that no argument or combination of arguments presented this far is capable of settling the question at hand. The fact is that there is too little good data, and the need is for more experiments rather than more debate. A few fairly obvious experiments are:

1. Determine the amount of contaminating gas present in the bombarding tube by using a tungsten filament which is kept hot (and therefore clean) until the moment at which it is desired to look for condensable gases. (The most critical time is probably just at the end of the bombardment.) Later the tungsten filament can be flashed and any gases which come off identified by the mass spectrometer.

2. Repeat the crushed-powder experiments<sup>33</sup> on the renewal of surfaces by heating, using less tightly packed powder and possibly lower surface-to-volume ratio. Also repeat the experiments on bombarded surfaces with samples having a higher surface-to-volume ratio, and go through oxygen-anneal cycle many times in attempt to saturate the bulk. This should give two tests of the ability of surface oxygen to diffuse into the bulk upon heating.

3. Measure the electrical and diffraction properties of bombarded surfaces with orientations different from the (100).



## REFERENCES

1. I. Tamm, *Physik. Z. Sowjetunion* **1**, 733 (1932).
2. W. Shockley, *Phys. Rev.* **56**, 317 (1939).
3. D. Alpert, *J. Appl. Phys.* **24**, 860 (1953).
4. R. T. Bayard and D. Alpert, *Rev. Sci. Instr.* **21**, 571 (1950).
5. Alpert, Matland, and McCoubrey, *Rev. Sci. Instr.* **22**, 370 (1951).
6. D. Alpert, *Rev. Sci. Instr.* **22**, 536 (1951).
7. Farnsworth, Schlier, George, and Burger, *J. Appl. Phys.* **26**, 252 (1955).
8. F. Allen, *Tech. Rep.* 236, Cruft Laboratory, Harvard University, Cambridge, Mass., December 1955 (unpublished).
9. F. Allen, *Tech. Rep.* 237, Cruft Laboratory, Harvard University, Cambridge, Mass., December 1955 (unpublished).
10. J. A. Dillon, *Bull. Amer. Phys. Soc.* **1**, 53 (1956), J. A. Dillon and H. E. Farnsworth, *Phys. Rev.* **99**, 1643 (1955), and private communication.
11. G. Wallis and S. Wang, *Bull. Amer. Phys. Soc.* **1**, 52 (1956).
12. H. H. Madden and H. E. Farnsworth, *Bull. Amer. Phys. Soc.* **1**, 53 (1956).
13. S. H. Autler, A. L. McWhorter, H. A. Gebbie, *Bull. Amer. Phys. Soc.* **1**, 145 (1956).
14. J. T. Law and C. G. B. Garrett, *J. Appl. Phys.* **27**, 656 (1956).
15. P. Handler, *Bull. Amer. Phys. Soc.* **1**, 144 (1956).
16. R. E. Schlier, *Bull. Amer. Phys. Soc.* **1**, 53 (1956), R. E. Schlier and H. E. Farnsworth, *Phys. Rev.* **98**, 250 (1955), and Burger, Farnsworth and Schlier, *Phys. Rev.* **98**, 1179 (1955). See also R. E. Schlier and H. E. Farnsworth, this volume.
17. H. E. Farnsworth, unpublished reports, Lincoln Laboratory, Mass. Inst. of Technology.
18. Apker, Taft, and Dickey, *Phys. Rev.* **74**, 1462 (1948).
19. R. B. Bernstein and D. Cubicciotti, *J. Amer. Chem. Soc.* **73**, 4112 (1951).
20. J. T. Law and P. S. Meigs, this volume.
21. Green, Kafalas, and Robinson, this volume.
22. W. A. Rogers, R. S. Buritz, and D. Alpert, *J. Appl. Phys.* **25**, 686 (1954).
23. I. N. Stranski and R. Suhrmann, *F.I.A.T. Report No. 1030* (13.1, 47).
24. L. Pauling, *Nature of the Chemical Bond* (Cornell University Press, Ithaca, New York), Sec. Ed., p. 164.
25. J. R. Schrieffer, *Phys. Rev.* **97**, 646 (1955).
26. R. E. Schlier, private communication.
27. P. Gombas, *Die Statistische Theorie des Atomes und ihre Anwendung* (Springer-Verlag, 1949), Sec. 29.
28. J. T. Law and C. G. B. Garrett, *J. Appl. Phys.* **27**, 656 (1956).



29. H. D. Hagstrum, *Rev. Sci. Instr.* **24**, 1122 (1953).
30. As a matter of fact, this picture appears to be quite close to that originally proposed by Farnsworth himself, in the discussion of his early experiments. (Lincoln Laboratory Quarterly Progress Reports, unpublished).
31. P. H. Robinson, to be published. See also Green, Kafalas and Robinson, this volume.
32. J. T. Law and P. S. Meigs, this volume.
33. Rosenberg, Robinson, and Gatos, to be published.



# MOBILITY IN INVERSION LAYERS: THEORY AND EXPERIMENT

J. R. SCHRIEFFER

*Department of Physics  
University of Illinois  
Urbana, Illinois*

## ABSTRACT

A brief review of the theory of conduction in a space-charge layer with boundary scattering is given. The theoretical work of Ham and Mattis on the anisotropy of surface conductivity is discussed and contrasted to the scalar mass theory. Recent experimental work on the field effect and the channel effect is compared with the effective mobility theory and evidence is found to support the random surface scattering hypothesis. Conduction in narrow channels where quantization effects may be important is considered and it is concluded that surface scattering most likely broadens the discrete levels into a continuum and the simple theory should be adequate to describe the mobility in this limit.

## I. INTRODUCTION

In considering the flow of carriers in a macroscopic semiconductor specimen, one usually takes the normal bulk scattering mechanism into account and neglects the collisions of the carriers with the surface. Such a procedure is in general valid only when one is not specifically interested in the flow of carriers near the surface. In recent years, many problems have arisen in which the behavior of the carriers near the surface plays a dominant role, for example the channel effect<sup>1-5</sup> and the field effect<sup>6-9</sup>. The analysis of the experimental data on these effects depends rather critically upon the mobility of the carriers near the surface. Since an experimental determination of the surface mobility has not been made up to the present time, a theoretical estimate appears to be of value.

The detailed calculation of the surface mobility is based upon several assumptions, the validity of which is still somewhat uncertain. Rather indirect experimental support of these assumptions is now available. However, we shall defer the discussion of



these experiments until the later part of this paper, following the discussion of general theory.

There is good evidence that a space-charge layer exists at the free surface of a semiconductor and extends of the order of  $10^{-4}$  cm into the bulk of intrinsic germanium.<sup>10</sup> Carriers which are located in the potential well formed by the space-charge layer will frequently collide with the surface and one would expect a reduction of the mobility of these carriers relative to their bulk mobility.

Figure 1 shows an  $n$ -type layer existing at the free surface of a

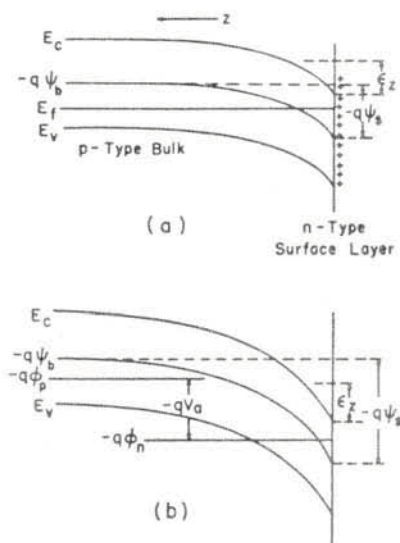


FIG. 1.—(a) Energy level diagram of an  $n$ -type inversion layer existing at the free surface of a  $p$ -type material.

(b) A voltage  $V_a$  applied across the surface shown in (a).

$p$ -type bulk specimen. The space-charge layer contains a net negative charge which just counterbalances the positive charge on the surface. We define  $\psi_s$  as the electrostatic potential at the surface relative to the potential deep within the bulk. If an oxide layer exists on the semiconductor,  $\psi_s$  is the potential at the semiconductor-oxide interface.

The surface conductivity,  $\Sigma$ , is defined as the change in conductance per square area of surface relative to the conductance

when the bands are flat all of the way to the surface, that is  $\psi_s = 0$ . We define the effective mobility as <sup>11</sup>

$$\Sigma = q(\mu_{\text{eff}} N + \mu_{\text{eff}} P) \quad (1)$$

where  $N$  and  $P$  are the changes in the total number of electrons and holes in the space-charge layer relative to the flat band condition.

The discussion shall deal primarily with  $\mu_{\text{eff}}$  however similar considerations apply to  $\mu_{\text{eff}}$ .

## II. MOBILITY IN A LINEAR POTENTIAL WELL

We begin by considering the idealized potential well in which  $\psi$  is a linear function of the distance from the surface as shown in Fig. 2 and limit the analysis to electrons. A crude estimate of  $\mu_{\text{eff}}$  can be obtained in the following manner. An electron will

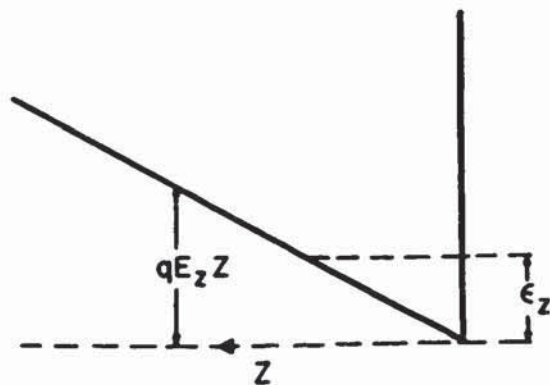


FIG. 2.—Idealized potential well.

hit the surface on the average  $\bar{v}/2w$  times per second where  $\bar{v}$  is the average thermal velocity and  $w$  is an effective width given by the position at which the component of velocity normal to the surface goes to zero. If the collisions with the surface are more frequent than the normal bulk scattering in the well, then the assumption that the carrier loses all of its drift velocity upon collision with the surface leads to

$$\begin{aligned} \mu_{\text{eff}}' \mu_b &= \tau_{\text{eff}}/\tau_b \simeq 2w/\tau_b \bar{v} \simeq (kT/\tau_b qE_z)/\sqrt{kT/m} \\ &\simeq \sqrt{kTm}/q\tau_b E_z \equiv \sqrt{2}\alpha \end{aligned} \quad (2)$$

where  $E_z$  is the electric field normal to the surface and the subscript b means the quantity is evaluated in the bulk. Thus when  $\alpha \leq 1$  we expect to get appreciable surface scattering. In the limit  $\alpha \ll 1$ , detailed calculation gives

$$\mu_{\text{eff}}/\mu_b = 2\alpha/\sqrt{\pi} \quad (3)$$

Inserting typical values for germanium we see that at room temperature the surface scattering will become important when  $E \geq 10^3$  volts/cm, a condition which is often satisfied experimentally.

### III. GENERAL THEORY

We consider a volume extending inward from a unit surface area subjected to an electric field  $E_x$  parallel to the surface and a space-charge field  $E_z$ , along the inward normal. Under steady state conditions, the distribution function of the carriers is determined by the Boltzmann equation<sup>12</sup>

$$\vec{v} \cdot \text{grad}_r f + (2\pi q \vec{E}/h) \cdot \text{grad}_k f = -(f - f_0)/\tau_b \quad (4)$$

where  $\tau_b$  is the relaxation time for bulk scattering and  $f_0 = C \exp(-\epsilon/kT)$  is the distribution function in the absence of  $E_x$ . Ham and Mattis<sup>13</sup> have introduced a transformation which changes the scale of the wave vector and the spatial coordinates in such a manner that if the energy surfaces in  $k$  space are ellipsoids of revolution, then Eq. (4) is transformed into the Boltzmann equation with spherical energy surfaces in the new space. The conductivity tensor can then be calculated in a straightforward manner and the result transformed back to physical space. Because of the complexity of the resulting expressions, we shall only consider the problem in which the energy surface is spherical in real space and quote results from the more general treatment.

Under the assumptions of a scalar effective mass and an energy dependent relaxation time, Eq. (4) can be transformed into an ordinary differential equation by introducing a new variable,

$$\epsilon_z = mv_z^2/2 + q[\psi(z) - \psi_0] \quad (5)$$

Thus

$$(qE_z/m) \partial f_1 / \partial v_z + f_1 / \tau_b = qv_x E_x f_0 \quad (6)$$



where  $f = f_0 + f_1(\epsilon_z, v_z)$  and we have neglected the product of  $E_x$  and  $f_1$ , which is a second order term in  $E_x$ .

The critical assumption is now made that each carrier approaching the surface has an equal probability of being scattered into any solid angle in the bulk. The justification of this assumption rests upon experimental verification of the resultant mobility and as we shall see, there is some justification at the present time. It is very difficult to deduce the scattering law from first principles because of our lack of detailed knowledge of the surface. By imposing the random scattering boundary condition, we are led to a general expression for the surface current density.<sup>11</sup>

$$I_x = [2\pi q^2 E_x C k T \tau_b^2 / m^3] \exp(-q\psi_s / kT) \int_0^\infty d\epsilon_z \exp(-\epsilon_z / kT) [\exp 2K(\epsilon_z) - 2K(\epsilon_z) - 1] \quad (7)$$

where

$$K(\epsilon_z) = (m/q) \int_0^{\sqrt{2\epsilon_z/m}} dv_z / \tau_b E_s(\epsilon_z, v_z)$$

and  $E_x$  must be expressed as a function of  $\epsilon_z$  and  $v_z$  through Eq. (5).

If the space-charge field can be approximated by a constant field, then  $I_x$  can be expressed in closed form. Defining the effective mobility by

$$I_x = Nq\mu_{\text{eff}}E_x \quad (8)$$

where  $N$  is the total number of carriers in the well, Eq. (7) reduces to

$$\mu_{\text{eff}}/\mu_b = 1 - (\exp \alpha^2)(1 - \text{erf } \alpha) \simeq 2\alpha/\sqrt{\pi} \text{ for } \alpha \ll 1 \quad (9)$$

and  $\alpha$  is given by Eq. (2). For small fields the effective mobility reduces to the bulk mobility as expected.

Ham and Mattis introduce the variables

$$\begin{aligned} w_i &= \alpha_i^{1/2} k_i \\ y_i &= \alpha_i^{-1/2} x_i \\ u_i &= \alpha_i^{-1/2} v_i \\ \mathcal{E}_i &= \alpha_i^{1/2} E_i \end{aligned}$$

which transforms the ellipsoidal energy surfaces in  $k$ -space to spherical surfaces in  $w$ -space. The  $\alpha_i$  are the components of the reciprocal effective mass tensor in diagonal form and  $i = 1, 2, 3$  refer to the principal axes of the ellipsoid. The problem is some-

what complicated by the fact that the electric field along the channel is in general no longer parallel to the surface in the transformed space.

They express the conductivity tensor per ellipsoid in their transformed space as

$$\lambda' = \begin{pmatrix} S_1^c & 0 & 0 \\ 0 & S_1^c & 0 \\ 0 & 0 & S_3^c \end{pmatrix} \quad (10)$$

and the matrix elements are given by

$$S_1^c = \Lambda S_1 = \Lambda [1 - (\exp \xi^2)(1 - \operatorname{erf} \xi)]$$

$$S_3^c = \Lambda S_3 = \Lambda [1 - (\exp \xi^2)(1 - \operatorname{erf} \xi)(1 - 2\xi) - 2\xi/\sqrt{\pi}]$$

$$\Lambda = N(\xi) q^2 \tau_b / m_e \sqrt{\alpha_s \alpha_p}$$

$$\xi = \sqrt{2m_e kT} / q \mathcal{E}_c \tau_b$$

$$\mathcal{E}_c = E_s (\alpha_s \sin^2 \theta + \alpha_p \cos^2 \theta)^{1/2}$$

Here  $\alpha_s$  and  $\alpha_p$  are the reciprocal effective mass components,  $1/m_{11} = 1/m_{22} = \alpha_s$ ,  $1/m_{33} = \alpha_p$  and  $\theta$  is the angle between the normal to the surface and the  $p$  axis of the ellipsoid in physical space. The functions  $S_1$  and  $S_3$  along with  $\mu_{\text{eff}}/\mu_b$  are shown in Fig. 3. We note that even for fairly thick channels, the conduc-

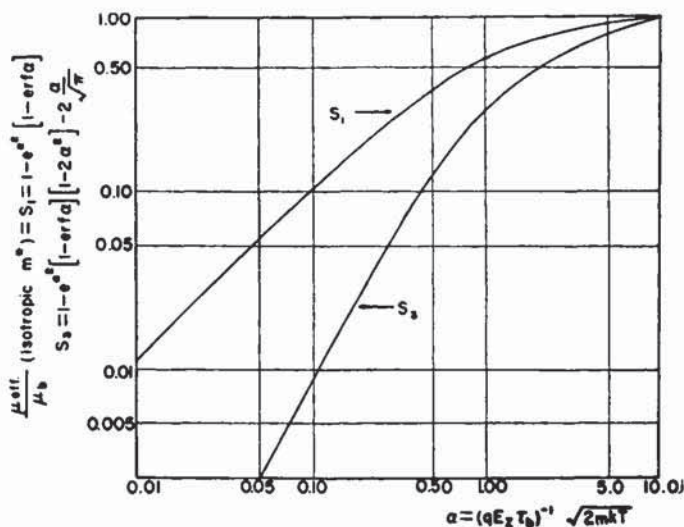


FIG. 3.—Conductivity tensor components.

tivity tensor deviates from a multiple of the unit tensor and thus one would expect some anisotropic effects to be important.

There are certain crystallographic orientations for which the conductivity is independent of direction in the plane of the surface. For example, in germanium, if the [100] or the [110] direction lies along the normal, then the surface conductivity is isotropic. The reader is referred to the paper by Ham and Mattis for explicit expressions of the conductivity tensor for various crystallographic orientations.

The calculations thus far have been carried out for a constant relaxation time; however, if one assumes a constant mean free path the results change but slightly and it should be sufficient in most cases to assume  $\tau_b$  is a constant. For thin channels, Ham and Mattis find that if the mean free path,  $l$ , is assumed constant, then  $\tau_b$  should be replaced by

$$\tau'_b = (4l/3\sqrt{\pi})(m/2kT)^{\frac{1}{2}} \quad (11)$$

For thicker channels,  $(1 - S_1)$  and  $(1 - S_3)$  should be reduced by  $9\pi/32$ , again replacing  $\tau_b$  by  $\tau'_b$ .

The application of the general theory to the case where  $\psi(z)$  is given by a solution of Poisson's equation for a biased space-charge layer has been carried out by the author. In this analysis it is assumed that the energy surfaces can be represented by an expression with a scalar effective mass and  $\tau_b$  and the quasi Fermi level are taken constant, as shown in Fig. 1b. An energy dependent  $\tau_b$  complicates the calculation somewhat and because of the relative insensitivity of the linear potential theory to the exact form of  $\tau_b$ , it is likely that a more general assumption about  $\tau_b$  would be of little importance. The anisotropy of the effective mass, on the other hand, is rather important as pointed out in the linear potential theory and should be taken into account. Ham and Mattis were able to estimate the effect of an ellipsoidal energy surface on the surface conductivity from their work on the linear potential case and give curves of the two independent components of the conductivity tensor in their transformed space. The total surface conductivity tensor in real space reduces to a manageable form for certain crystallographic orientations and for this reason it is suggested that experimental work be carried out on oriented



crystals, particularly since the conductivity is isotropic in the plane of the surface for these orientations.

The effective mobility can not be expressed in analytic form for the general space-charge potential and numerical integrations have been carried out as a function of two physical parameters. The parameters which come into the space-charge potential theory are

$$\beta = [m\kappa/8n_s]^{1/2}/q\tau_b \quad B = \frac{N_s}{n_s} [q\psi_s/kT] \quad (12)$$

where  $n_s$  is the concentration of carriers in the well or channel at the surface and  $N_s$  is the uniform bulk impurity concentration. The ratio  $\mu_{\text{eff}}/\mu_b$  for the scalar mass theory and the components of the conductivity tensor in the transformed space,  $S_1$  and  $S_3$ , are shown in Fig. 4. The expressions for  $\mu_{\text{eff}}/\mu_b$  and  $S_1$  turn out

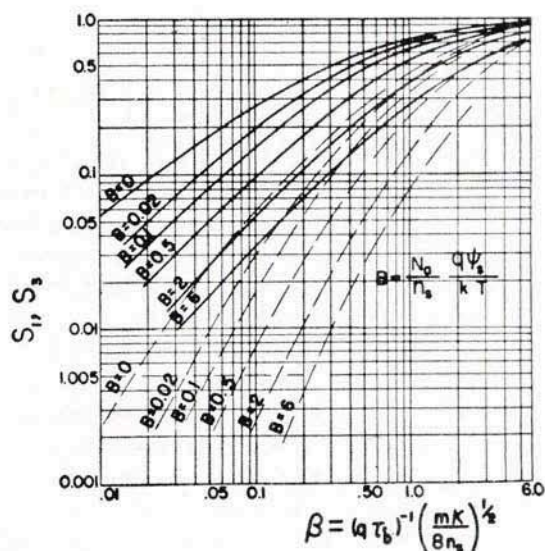


FIG. 4.— $S_1$  and  $S_3$  for constant  $\tau$ , a space charge potential which satisfies Poisson's equation and various values of  $B$  as a function of  $\beta$ .

to be identical, however the parameter  $\beta$  in the anisotropic theory involves an orientation dependent factor. We note that even for high resistivity material with zero bias ( $B = 0$ ), the an-

isotropy should be considered for  $\beta \leq 5$  or for intrinsic germanium  $n_s \geq 5 \times 10^{14}$ .

In order to gain a feeling for the order of magnitude of the effective mobility in practical cases, the ratio  $\mu_{\text{eff}}/\mu_b$  is plotted as a function of surface potential for a free surface in Fig. 5 for

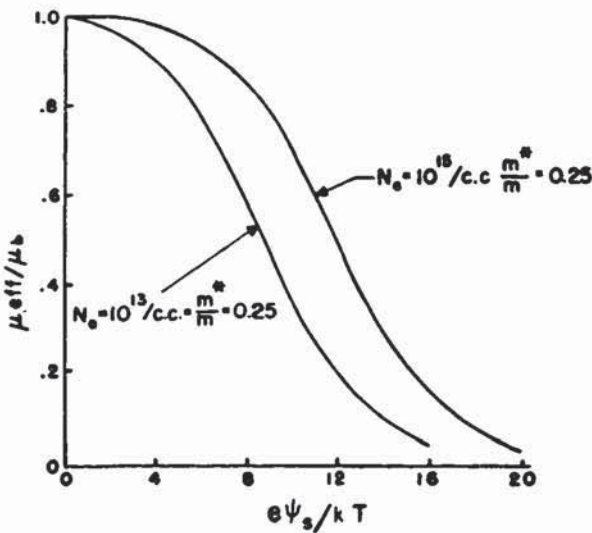


FIG. 5.— $\mu_{\text{eff}}/\mu_b$  as a function of surface potential.

germanium. We have assumed a scalar effective mass equal to  $0.25 m_e$ . Thus at room temperature, for a surface potential of 0.25 volts, the mobility is reduced by a factor of about two.

For simplicity one would like to use the approximate theory of the linear potential well in practical applications. Comparison of the mobility based upon the two theories is shown in Fig. 6 for an 8 ohm-cm *n*-type germanium sample with a *p*-type inversion layer and  $\phi_s = 0.14$  volts, where  $\phi_s$  is the position of the Fermi level at the surface with respect to the mid-band energy. The field for the linear potential approximation was chosen to be the field at the surface and the resulting mobility is somewhat lower than that given by the space-charge theory since the effective well width is smaller for high energies with this constant field. By making other assumptions about the magnitude of the constant

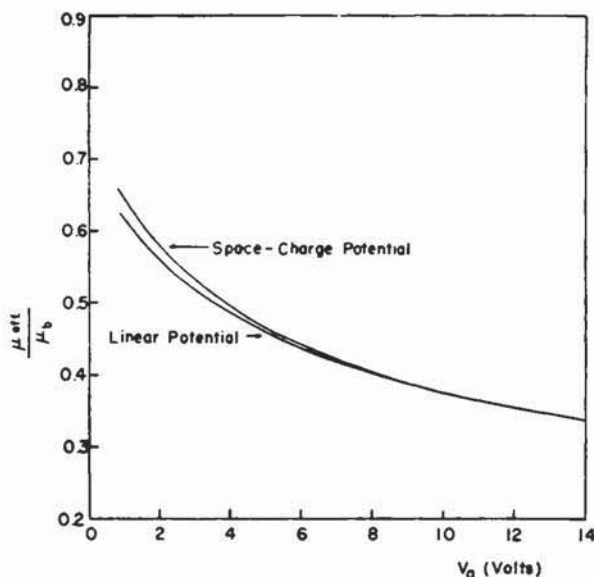


FIG. 6.— $\mu_{eff}/\mu_b$  for an 8 ohm-cm *n*-type germanium sample with a *p*-type inversion layer ( $\phi_s = 0.14$  volts) assuming a linear potential and the space charge potential.

field, a better approximation can be obtained, however even this simple assumption is in error less than 5 percent for biases over 2 volts and the curves virtually coincide for biases above 8 volts. One should investigate the approximation for low biases or a light inversion layer on a free surface, however.

#### IV. APPLICATIONS TO EXPERIMENT

In some early measurements, Kingston<sup>14</sup> found that the *n*-type channel conductance on germanium varied roughly inversely with bias. He attributed this to the fact that if the quasi Fermi level is quenched at the surface then the number of carriers in the channel vary approximately as  $1/\sqrt{V_a}$  and as we have seen, the effective mobility varies roughly as  $1/\sqrt{V_a}$  for large bias. Further measurements have been carried out by Statz, deMars



and Davis<sup>5</sup> and by Sirrine<sup>13</sup> on *p*-type inversion layers and they find a somewhat similar behavior.

However, if one analyzes the data more critically, it appears that the quasi Fermi level can not be rigidly fixed at the surface. As the bias is increased the Fermi level moves closer to mid-band and the rate of change of  $\phi_s$  with bias depends upon the specific assumptions made about the nature of the surface scattering. Figure 7 shows  $\phi_s$  versus the field at the surface for a set of data

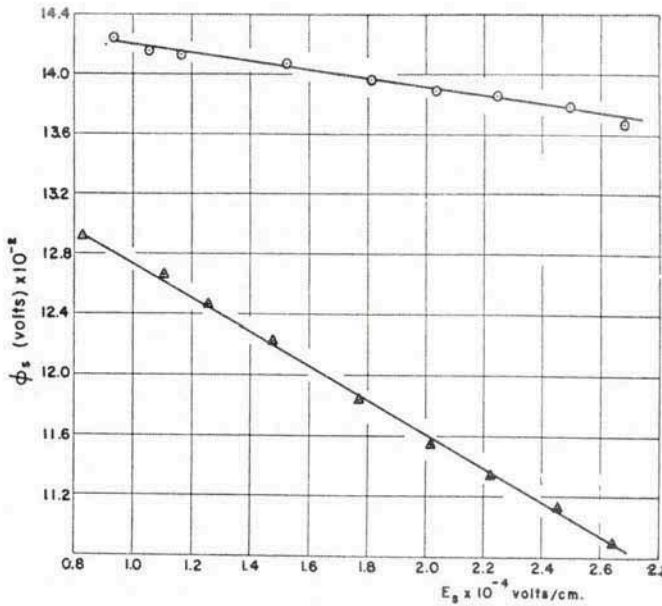


FIG. 7.— $\phi_s$  vs field at the surface on a *p*-type channel on germanium. (After Sirrine.<sup>13</sup>)

taken by Sirrine<sup>13</sup> on a *p*-type channel on germanium. The curve with smaller slope was calculated using the random scattering boundary condition while the other was obtained by assuming no reduction from the bulk mobility. The bias ranged from 1 to 14 volts for these data and the scatter in the values of  $\phi_s$  is about 1 percent. We notice a linear relation between  $\phi_s$  and  $E_s$  fit the data in either case. Such a relation is to be expected if

it is assumed that  $\phi_s$  is rigidly fixed relative to the external states and an oxide layer of finite thickness separates these states from the channel. Using an idealized model which treats the oxide as a homogeneous dielectric with dielectric constant one-quarter the bulk germanium value, the thickness of the oxide turns out to be 7 Å and 30 Å for the effective mobility and the bulk mobility theories respectively. The former appears to be somewhat more reasonable for a typical oxide thickness for the surface treatment used; however, no direct conclusion can be drawn. If the density of external states is not extremely large, then part of this apparent thickness will be due to a shift in  $\phi_s$  relative to these external states. Statz et al.<sup>6</sup> obtain results very similar to those of Sirrine with the exception of an initial rise of  $\phi_s$  with  $E_s$  and then the linear decrease. The slope of  $\phi_s$  versus  $E_s$  is approximately the same as observed by Sirrine.

It would be desirable to make measurements of surface conductance as a function of temperature since the temperature dependence of the bulk mobility is quite different from that of the effective mobility with random surface scattering. If the effective mass and dielectric constant are assumed temperature independent, then in the limit of large bias, that is  $\alpha \ll 1$ , the effective mobility is proportional to the square root of temperature. Care should be taken to insure equilibrium between the bulk and the external states in such measurements since deviations from equilibrium result in an increase of the apparent oxide thickness.

Another indication of the validity of the random scattering theory comes from the field effect work done on germanium,<sup>9</sup> that is the change in surface conductance with an external field applied transverse to the free surface. The field effect mobility is defined as the negative ratio of the change in surface conductivity to the charge induced by the external field. The ratio  $\mu_{F.E.}/\mu_{nb}$  is shown in Fig. 8 for typical runs on near intrinsic germanium samples along with the theoretical curve for no internal surface states, that is no fast states at the germanium-oxide interface, based on the random scattering theory. If surface scattering effects were not taken into account, the theoretical curve would be asymptotic to one and  $\mu_{pb}/\mu_{nb}$  for large positive and negative  $\psi_s$  respectively. There is a clear indication that the experimental curves begin to decrease in the vicinity predicted by the random scattering

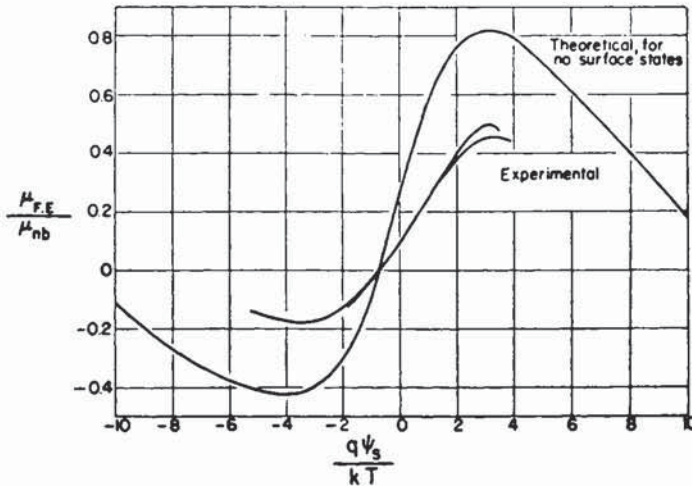


FIG. 8.—Experimental and theoretical values of the field effect mobility as a function surface potential for near intrinsic germanium.

theory for both *p*- and *n*-type layers. Unfortunately, the experiments did not allow investigation of the field effect mobility for large surface potential since the measurements were carried out by swinging the bands with gaseous ambients. Again, no clear-cut evidence can be gained for random scattering, however it is interesting to note that the density of internal states determined from these field effect measurements agree fairly well with the measurements of Statz et al.<sup>5</sup> on the channel effect.

Montgomery<sup>15</sup> has carried out field effect measurements on both *p*- and *n*-type germanium with inversion layers at a frequency of 1 mc. He finds a field effect mobility of about 3000 cm<sup>2</sup>/volt-sec for the *p*-type sample exposed to wet air and about 5000 cm<sup>2</sup>/volt-sec for the *n*-type sample exposed to dry oxygen. The surface potential for the *p*-type material was presumed to be about 0.15 volts. It is his belief that the high frequency conduction involves majority carriers from the interior of the specimen and minority carriers supplied from the interface states and feels that it is unlikely that these carriers would be constrained to flow in the inversion layer as would minority carriers at low frequencies. Thus, it appears that Montgomery's experiments are not in conflict with the random scattering hypothesis.



## V. CONDUCTION IN A HIGH FIELD SPACE-CHARGE LAYER

Thus far it has been assumed that the carriers can be described in terms of a band picture with an appropriate effective mass tensor. This is strictly valid only for a small space-charge field where the carriers are not held to a region very near the surface. If the space-charge field becomes large due to either a large bias or a large surface charge on a free surface, then the carriers may well be held within a region such that a discrete set of levels arises due to quantization in this well. The larger the field the greater is the separation between these quantized levels. For fields of practical interest, the effective mass approximation is still valid.

If it is assumed that the surface is perfectly smooth then the levels may be labeled by  $k_x$ ,  $k_y$  and  $n_z$ , and for an isotropic effective mass

$$E = (\hbar^2/8\pi^2m^*)(k_x^2 + k_y^2) + \epsilon(n_z) \quad (13)$$

It follows from the previous discussion however that the scattering at the surface may well be random and therefore the levels will be broadened. It can be shown quite generally that a wave packet made up from a set of adjacent states will oscillate in the well with a frequency  $\sim \Delta\epsilon/\hbar$  where  $\Delta\epsilon$  is the level separation near the energy of interest. The lifetime of the state will be of the order of the reciprocal of the frequency of oscillation and it follows from the uncertainty principle that the levels will be broadened by  $\sim \Delta\epsilon$ . On the basis of this crude estimate it appears that the quantization effects get washed out by the surface scattering mechanism and a continuum of levels again results. The electron-lattice interaction may be effected somewhat by this new distribution of states however it is to be expected that the surface scattering mechanism would dominate in the region in which a modification of the bulk relaxation time is required. Thus, it is most likely sufficient to use the bulk relaxation time in a detailed calculation of the surface mobility. A simple phase space argument shows that the total number of electrons in the well is independent of whether the levels are quantized or a free electron approximation is used and thus the general theory of Section III is expected to be valid for fairly high fields, as long as breakdown does not occur.

It should be pointed out that the effective mobility theory in

its present form does not apply in detail to conduction in space-charge layers in which the band structure is appreciably perturbed, for example, to the clean surface experiments of Handler.<sup>16</sup> It is believed that a number of states are removed from the top of the valence band near the surface and form bound hole states with the occupied dangling bonds of the germanium surface atoms. Since the remaining band structure may have a rather complicated form, the mobility theory will need revision but the general line of argument given in Section II should still apply.

#### ACKNOWLEDGMENTS

The author would like to express his appreciation to Prof. J. Bardeen, Mr. D. Mattis and Mr. R. Serrine for many helpful discussions. He is also indebted to Dr. H. Statz et al., Dr. H. C. Montgomery and Dr. F. S. Ham and Mr. D. Mattis for the results of their work prior to publication.

#### REFERENCES

1. W. L. Brown, *Phys. Rev.* **91**, 518 (1953).
2. R. H. Kingston, *Phys. Rev.* **93**, 346 (1954).
3. deMars, Statz and Davis, *Phys. Rev.* **98**, 539 (1955).
4. R. H. Kingston, *Phys. Rev.* **98**, 1766 (1955).
5. Statz, deMars, Davis, and Adams, *Phys. Rev.* **101**, 1272 (1956).
6. W. Shockley and G. L. Pearson, *Phys. Rev.* **74**, 232 (1948).
7. J. Bardeen and S. R. Morrison, *Physica* **20**, 873 (1954).
8. G. G. E. Low, *Proc. Roy. Soc. (London)* **B68**, 10 (1955).
9. Bardeen, Coover, Morrison, Schrieffer, and Sun, *Phys. Rev.* (to be published).
10. W. H. Brattain and J. Bardeen, *Bell System Tech., J.* **32**, 1 (1953).
11. J. R. Schrieffer, *Phys. Rev.* **97**, 641 (1955).
12. See A. H. Wilson, *The Theory of Metals* (Cambridge University Press, London, 1953), Chap. VIII.
13. F. S. Ham and D. Mattis, *Phys. Rev.* (to be published).
14. R. Serrine, private communication.
15. H. C. Montgomery, private communication.
16. P. Handler, *Bull. Am. Phys. Soc.*, **1**, No. 3, 144 (1956).

# FIELD EFFECT ON SURFACE CONDUCTANCE AND SURFACE RECOMBINATION

P. C. BANBURY, G. G. E. LOW, and J. D. NIXON,

*Physics Department  
University of Reading  
Reading, England*

## ABSTRACT

The influence of steady capacitively applied fields on surface conductance in single crystal germanium specimens is discussed, with particular reference to the effects occurring within the first few hundred microseconds. Procedures for varying and determining the surface barrier height are described with the object of evaluating surface state densities and cross sections. Measurements of the effect of fields on the surface recombination velocity are also discussed, together with some results.

## I. INTRODUCTION

The measurements to be described in this paper concern the effect of capacitively applied electric fields on surface conductance and surface recombination in germanium crystals. Observations of the field effect on conductance were first reported by Shockley and Pearson<sup>1</sup> using evaporated films, and subsequently a number of investigations have been carried out on single crystal specimens using alternating fields.<sup>2,3</sup>

The work on surfaces in this laboratory has been primarily concerned with measurements obtained using short voltage pulses or switched dc voltages. The general form of the conductance effect under these conditions and its qualitative interpretation have been discussed by Low.<sup>4</sup> The character of the results from the two types of measurement may be represented schematically as illustrated in Fig. 1, and interpreted as follows. The discussion will apply throughout to a specimen sufficiently far removed from the intrinsic condition for minority carriers to be disregarded in the bulk conduction process. The sudden application of a potential



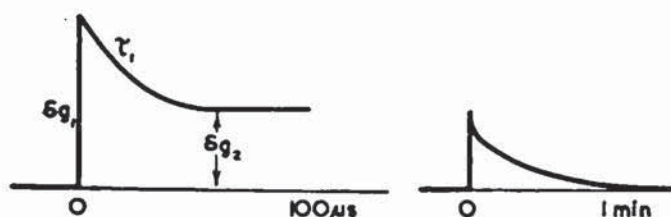


FIG. 1.—Diagrams showing the short and long term time dependence of the field effect on surface conductance.

difference between the specimen and a neighboring electrode gives rise to a field penetrating the semiconductor and causing a flow predominantly of majority carriers towards or away from the surface. A change in the barrier allows the induced charge to be accommodated on the impurities or in the majority carrier band near the surface. The conditions corresponding to the initial conductance change  $\delta g_1$  are thus established, in a time normally limited by the constants of the circuit used to apply the field.

Disequilibrium now exists, in a region near the surface where the space charge resides, between the occupancy of the majority carrier band and other allowed electron states. The subsequent changes in conductance are attributed to changes in the operative mobility of the induced charge as a thermal equilibrium distribution is restored. A change with a time constant related to the time of relaxation between the valence and conduction bands must be expected even in the absence of additional states at the surface; if there are surface states through which recombination occurs, the amplitude and detailed time dependence of this relaxation will be modified. This type of relaxation may be identified with the decay  $\tau_1$  in Fig. 1, leaving the quasi-stable part of the conductance change  $\delta g_2$ . Any bound states associated with this relaxation will here be called fast surface states. The presence of significant numbers of other surface states of lower cross-section is postulated to account for the changes associated with long time constants and for the long term stability of the surface potential. Such states are here referred to as slow surface states.

For more detailed discussion it is necessary to distinguish between various types of barrier. Following Bardeen, the term accumulation layer is used to indicate a barrier in which the

majority carrier concentration increases as the surface is approached, while barriers in which a decrease occurs are termed inversion or exhaustion layer barriers according as to whether or not the minority carrier is predominant near the surface.

## II. THE INITIAL CONDUCTANCE CHANGE

If a known charge density  $\sigma$  is induced on the surface of the specimen, the initial conductance change may be written

$$\delta g_1 = \sigma \mu_1$$

where for a low barrier  $\mu_1$  is approximately the bulk mobility of the majority carrier. Exact agreement is not expected for the following reasons:

(a) In the case of an accumulation barrier, the mobility is expected to be reduced by the restriction of the carriers to a surface channel.

(b) In the case of an exhaustion or inversion layer barrier, the changes of minority carrier mobility in the channel may be significant. They operate in a direction tending to increase the amplitude of  $\delta g_1$  and hence the apparent mobility of the induced charge.

(c) Even in the case of extrinsic material, for an inversion type barrier the assumption that minority carriers do not contribute to the initial charge flow may break down. Minority carriers are not expected to flow out of the specimen but for one direction of applied field they may enter the bulk material and there be neutralized by added majority carriers. Their mobilities will then be uninfluenced by the surface conditions.

(d) The existence of surface irregularities will reduce the mobility of the induced charge to an unknown extent dependent on the barrier thickness.

## III. THE QUASI-STABLE CONDUCTANCE CHANGE

In the condition reached some hundred microseconds after application of the field, when the initial fast change of conductance is completed, equilibrium may be assumed to exist in the carrier

distribution between the valence and conduction bands in the barrier. The normal relations between barrier height and barrier space charge as discussed in detail by Kingston and Neustadter,<sup>5</sup> and the conductance calculations of Schrieffer,<sup>6</sup> may then be applied. For example, it is possible to determine the minimum conductance condition, and then evaluate subsequent variations of barrier height  $V_s$  from the measured conductance using Schrieffer's calculations. Knowing the total induced charge and the charge now remaining in the barrier as deduced from the known value of  $V_s$ , the charge in the fast surface states may then be obtained as a function of the surface potential, giving information as to the numbers and energies of any fast surface states which may be present. This procedure has been used in this laboratory as reported below. Results have been published by Brown<sup>7</sup> using a similar method.

#### IV. THE SHORT RELAXATION TIME

With a knowledge of the distribution of fast surface states, information as to their cross-sections for the capture process may then be obtained from measurements of the time constant  $\tau_1$ . If no fast surface states are present, it could still be envisaged that the relaxation might be a surface phenomenon, attributable to direct transitions between the bands at the surface. An exponential decay with a single time constant for the relaxation may then be expected. If, however, surface states are involved, different trapping times for majority and minority carriers must be envisaged. In this case, unless the surface states are close to the edge of the minority carrier band, effects associated with this band should be negligible when measurements are made on barriers in the accumulation layer condition. The relaxation time should then yield a cross-section for the trapping of majority carriers in surface states. Some measurements of this type have been reported,<sup>8</sup> and are now being extended to other surfaces.

It is hoped in the future to relate these to measurements of the field effect on surface recombination, which are being made by one of us (J. D. N.). Some aspects of these two experimental methods will be discussed here, together with some results.



## V. EXPERIMENTAL PROCEDURES

(a) *Method of Varying the Barrier Height*

In order to make the measurements, a method is required for the controlled variation of the surface potential just inside the semiconductor. It has been shown that this can be achieved by varying the ambient gas at the surface of the specimen, but the possibility exists in principle that this causes a significant alteration in the states at the surface. For the experiments reported here, the mean value of  $V_s$  has been controlled by the application of electric fields.

The method used in the surface conductance experiments<sup>8</sup> may be explained as follows. From the existence of the long time constant effects, it can be inferred that if pulses are applied whose repetition period is shorter than the time taken to return to final equilibrium, the surface will develop a bias owing to charging of states with long relaxation times. For example, consider the case when a positive potential is applied to a metal electrode near the face of a  $p$ -type crystal. The surface potential of the crystal is raised, and the slow surface states tend to take up the negative charge induced on the surface. The subsequent removal of the pulse leaves these states negatively charged, and so the surface potential is temporarily lowered with respect to its equilibrium condition. This effect may be used to provide a means of varying the barrier height in a controlled manner. Consider a system subjected to two alternating series of pulses, as illustrated in Fig. 2.

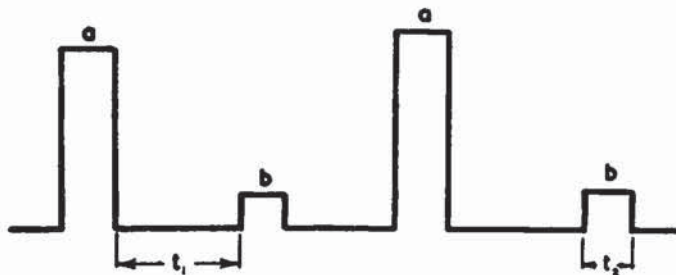


FIG. 2.—Schematic diagram showing the form of the voltage used in the double pulse experiments.

A constant delay  $t_1$  is maintained between the two series, this delay being long compared with the fast decay constant  $\tau_1$ . A dynamic equilibrium is then reached in which the charge gained by the slow states during pulses equals that lost in the intervals. The series of pulses (a) of variable amplitude may thus be used to vary the surface potential and the small pulses (b) then employed to study the field effect as a function of this potential. In order that the surface potential may be regarded as constant during the measurement, it is of course necessary that  $t_2 \ll t_1$  (Fig. 2.). In order that a linear theory may be applied in interpretation, the amplitude of the measuring pulse is now limited to give an excursion of surface potential  $\delta V_s$  small compared with  $kT/q$ , as evidenced by the linearity of the readings as a function of this amplitude.

It must be noted, however, that this procedure is useful only for lowering the surface potential on *p*-type material or raising that on *n*-type. The reason for this may be seen as follows. Consider the case of an *n*-type specimen. If a biasing pulse is applied of such polarity as to induce positive charge on the surface, this charge is provided initially by the repulsion of electrons and the resultant exposure of ionized donors. Large initial changes of surface potential may arise, limited perhaps only by Zener breakdown in the barrier. The barrier relaxes to a relatively small height in a time determined by the short time constant  $\tau_1$ , but appreciable charge may leave the slow surface states during this time in the presence of such large disturbances, and so, on removal of the applied pulse, a large positive bias may be obtained on the surface. It appears that in this way the potential of the surface may readily be raised to a value corresponding to a close approach of the conduction band at the surface to the Fermi energy during the time when the measuring pulse is applied.

When the opposite polarity of biasing pulse is applied, however, the induced negative charge in the initial condition can be left in the conduction band at the surface as it approaches the Fermi level. Thus the change in surface potential is restricted to fractions of a volt, the rate of charging of the slow surface states is low, and when the biasing pulse is removed the negative bias on the surface is small. A similar argument applies to *p*-type material.

In order to obtain excursions opposite in sign to those given

by the above method, the procedure adopted in these experiments has been to superimpose the small measuring pulse on a switched dc field, and make measurements as the surface potential relaxes, owing to the charging of the slow surface states, towards its original value.

(b) *Evaluation of the Barrier Height*

The interpretation of the type of measurement discussed here depends on a knowledge of the barrier height  $V_b$ . The procedure for evaluating  $V_b$  has usually been based on Schrieffer's analysis.<sup>6</sup>

One possibility is to find the minimum conductance condition to determine an origin and then deduce  $V_b$  from subsequent measurements of the quasi-stable conductance. This method has been employed in the surface recombination measurements with switched dc fields reported in Section VI.

In the case of the double pulse measurements one of the experimental quantities obtained using the small measuring pulse is in effect a value of  $dg_2/d\sigma_{\text{tot}}$  where  $\sigma_{\text{tot}}$  is the total surface charge density. This may be related to Schrieffer's predictions only when effective surface state densities are already known for this value of  $V_b$ ; the observation of the minimum conductance condition  $dg_2/d\sigma = 0$  is not sufficient to determine other values of  $V_b$  unless dc conductance measurements are also made. Since the biasing system depends on dynamic equilibrium being reached in the slow surface states, it would therefore be necessary to compare dc conductances measured at times separated by minutes with consequent stability problems.

An alternative method depends on the measurement of the initial conductance changes  $\delta g_1$ , and the evaluation of an effective mobility. The situation was discussed in Section II, and the influence of factors (a) and (b) may be calculated again from Schrieffer's analysis.

The accumulation layer barrier of interest in the present experiments offers the most favorable condition for the use of this method, since factors (b) and (c) may be neglected, and (a) is having its maximum effect. The results obtained, however, were not always self-consistent. This was attributed to the effect of surface irregularities, whose importance is increased by the narrowness of this type of barrier. The method served to give a



rough estimate of  $V_s$ , and allowed conclusions to be drawn as to the disposition of fast surface states. This enabled  $V_s$  to be re-determined by a method which will be described later. It must be borne in mind, however, that the presence of surface irregularities as evidenced above will tend to reduce the quantitative significance of the numerical results obtained.

(c) *Evaluation of Fast Surface State Distribution*

One method of obtaining the densities and energies of these states has been outlined in Section III. In connection with the measurements on surface recombination, results have been obtained on CP-4 etched *n*-type germanium surfaces closely similar to those given by Brown,<sup>7</sup> corresponding to densities of a few times  $10^{10}$  per energy interval  $kT$ . These results were obtained using steady fields and insulating spacers, by a method to be described later. The evaluation of surface state density depends on the assumption that negligible charge is transferred to the surface of the insulator in a time of about ten milliseconds.

For the case of measurements on extrinsic material in the absence of a barrier or with an accumulation layer present, the presence of minority carriers may be neglected. The trapping of majority carriers only is important, and this simplification has been made use of in the following way.<sup>8</sup> For the small excursions measured, it follows immediately that  $(\delta g_1 - \delta g_2)/\delta g_2$  gives the ratio of majority carriers trapped to those remaining free in quasi-equilibrium. A simple calculation shows that this may be related to the surface state densities by the expression,

$$q \sum N_i f_{pi} f_{ni} = -(1/\beta)(d\sigma_b/dV_s)(\delta g_1 - \delta g_2)/\delta g_2 \quad (1)$$

where  $N_i$  are the surface densities of traps with probabilities of occupancy  $f_{ni}$ ,  $f_{pi} = 1 - f_{ni}$ ,  $\sigma_b$  is the charge of majority carriers in the barrier per unit area, and  $\beta = q/kT$ ;  $d\sigma_b/dV_s$  may be calculated. Because of the restriction to low barriers or accumulation layers, however, this expression can be used to evaluate  $N_i$  only for traps nearer in energy to the majority than the minority carrier band. For traps outside this range, the Fermi functions,  $f$ , reduce to Boltzmann factors in the range of measurements permitted, and so  $N$  and the relevant Boltzmann term cannot be evaluated separately.

These conductance experiments have been carried out so far on surfaces prepared by an etch in CP-4 or hydrogen peroxide (20 vols; 30 mins; 65°C). In the first place the initial mobility of the induced charge was used to determine  $V_s$ , as described in Section V(b). On these surfaces measurements on both  $n$ - and  $p$ -type specimens could be explained by the presence of fast surface states in the middle region of the forbidden gap, with a negligible density near the majority carrier band. The evaluation of  $N_1$  by this method is therefore not possible for the reason given above. The form of trapping seen over the permissible range of measurements on each type of material was such as could qualitatively be accounted for by the presence of the minority band, but, assuming the validity of the values of  $V_s$  derived as described above, was found quantitatively to imply too high a density of states.

(d) *Evaluation of Fast Surface State Cross-Sections*

As it appeared in the latter results given above that the surface states were far removed from the Fermi level in the accumulation layer condition, it was possible to deduce values of the cross-sections for majority carrier capture in the following way. A detailed analysis is being published elsewhere;<sup>9</sup> an outline will be given here.

The time constant  $\tau_1$  will depend on the density and cross-section of the fast states. The density may be eliminated by the use of Eq. (1), giving the relation (quoted for  $p$ -type material)

$$4/Av = \tau(\delta g_1/\delta g_2)(p_b/f_p) \exp(-\beta V_s) \quad (2)$$

where  $A$  is the trap cross-section,  $v$ , the thermal velocity of holes, and  $p_b$  the equilibrium concentration of holes in the bulk of the specimen. In view of the energy of the traps,  $f_p$  may be taken as unity, and  $A$  is calculable if  $V_s$  is known.

As the values of  $V_s$  previously obtained were not entirely self-consistent, a redetermination was made as follows, on the same assumption of a single trapping level near the center of the band. The method depends on the fact that as the barrier height passes through zero from the exhaustion to the accumulation condition, the rate of change of barrier space charge with barrier height undergoes a rapid increase. With the knowledge already available that the traps are distant from the Fermi level by an energy large compared with  $kT$ ,  $V_s$  may be deduced by, in effect, observing

this increase.  $d\sigma_b/dV_s$  may be introduced into Eq. (2) from Eq. (1) giving

$$4/AvN = -q\tau_1[\delta g_1/(\delta g_1 - \delta g_2)]p_b f_n \beta (dV_s/d\sigma_b) \exp(-\beta V_s)$$

Setting  $f_n = \exp \beta(V_s + V)$  where  $V$  is a constant, it follows that

$$\tau_1[\delta g_1/(\delta g_1 - \delta g_2)] = [4/(AvN)][\exp(-\beta V)/(q\beta p_b)]d\sigma_b/dV_s$$

Here the left-hand side contains measured quantities only, while the right-hand side depends on  $V_s$  only through  $d\sigma_b/dV_s$ . This quantity may be calculated as a function of  $V_s$ , the calculation being simplified again by the fact that the minority carrier can be neglected. In this range one obtains the relationship

$$d\sigma_b/dV_s = - (q/2)(\epsilon_0 p_b / 2\pi kT)^{\frac{1}{2}} \left[ |\exp(-\beta V_s) - 1| / (\exp(-\beta V_s) - 1 + \beta V_s)^{\frac{1}{2}} \right]$$

The form of this expression as a function of  $V_s$  is illustrated in Fig. 3.

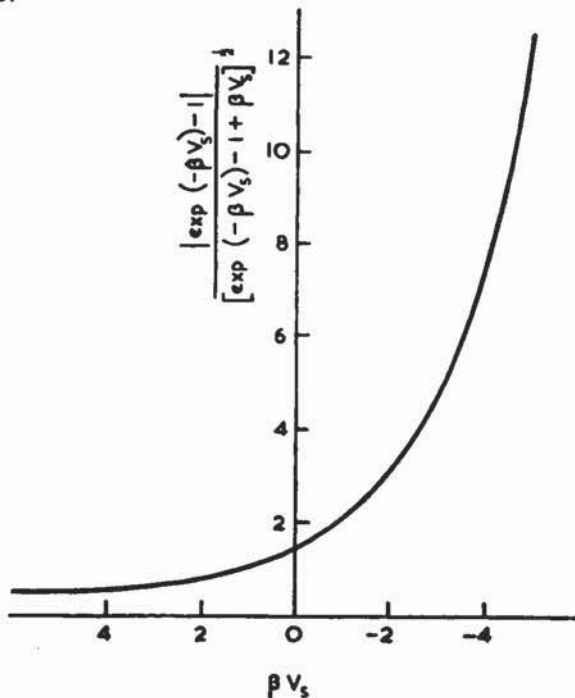


FIG. 3.—Plot showing the dependence of  $d\sigma_b/dV_s$  on barrier height.



For large positive values of  $V_s$ , it is comparatively constant, varying in fact as  $(\beta V_s)^{-\frac{1}{2}}$ , while for negative values it varies as  $\exp [(-\beta V_s)/2]$ . As  $V_s$  is swept through zero from positive to negative values the quantity  $\tau_1[\delta g_1/(\delta g_1 - \delta g_2)]$  should behave in the same manner. Actual results are given in Fig. 4, where this quantity has been plotted in the progressive order of the readings, which were in fact taken at approximately equal increments of initial conductance change  $\delta g_1$ . It may now be deduced, for example, that when the experimental quantity plotted has increased by a factor of three,  $V_s$  is approximately zero. The cross-section  $A$  may now be calculated, and checked by new evaluations using values of  $V_s$  deduced from other regions in Fig. 4.

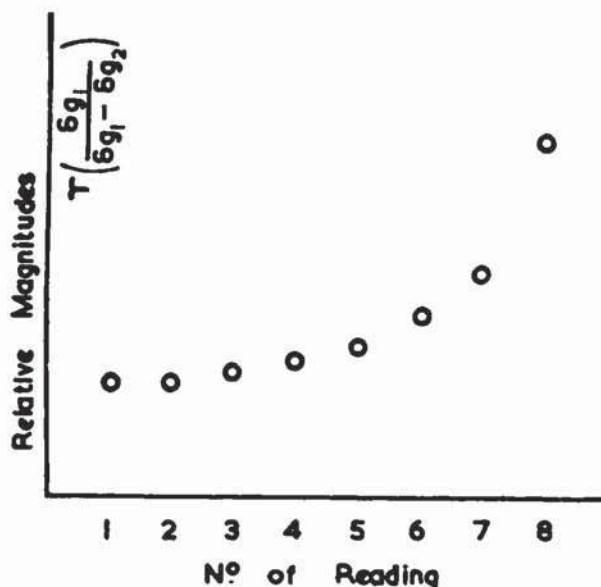


FIG. 4.—Graph showing a set of experimental results plotted for redetermination of the barrier height (see text).

By this method, on the surfaces referred to earlier, the cross sections for majority carrier capture on both  $n$ - and  $p$ -type material were found to lie between  $10^{-17}$  and  $10^{-16}$  cm<sup>2</sup>. If it is assumed that the same set of states is involved in the two cases, a value for the state density can be obtained which, when combined with

these cross-sections, gives a reasonable value for the surface recombination velocity.

## VI. FIELD EFFECT ON SURFACE RECOMBINATION

Lifetime measurements in the presence of applied fields have been reported by Henisch and Reynolds,<sup>10</sup> who found a field dependence of the surface recombination velocity  $s$ , and recently by Thomas and Rediker.<sup>11</sup> In observations of the dc photoconductance of illuminated specimens in the presence of applied fields, Nixon and Banbury<sup>12</sup> found a field dependence of  $s$  which relaxed to near zero with a period similar to that of the slow decay observed in measurements of surface conductance. Similar observations have been made and related by means of conductance measurements to the barrier height, by Many.<sup>13</sup>

In the recent experiments in this laboratory<sup>14</sup> the quasi-equilibrium conductance and added carrier lifetime are being simultaneously observed after the application of a surface field. For this purpose a bridge of the type described by Many<sup>15</sup> for lifetime measurements is used, in which the specimen is subjected to pulses of current through a slightly injecting end contact. The changing voltage across the specimen throughout the duration of the pulse is compensated by the adjustment of an RC network whose time constant is then equal to the filament lifetime. This balance condition is set in the absence of the field, and departures from balance on application of a field are displayed on an oscilloscope and photographed. Records of the type illustrated in



FIG. 5.—Form of the oscillograph display obtained in the surface recombination measurements.

Fig. 5 show the changes resulting within milliseconds of the application of the field. The trace subsequently reverts to the balanced condition in a total time of the order of minutes owing to the action of the slow surface states.

It is found that within the range of injection levels suitable for the measurement of lifetime by the Many method the changes of specimen resistance arising from the field effect on surface conductance are comparable with those associated with the injection, and consequently both may be deduced from one observation of the type illustrated. The procedure may be summarized as follows. The filament lifetime in the absence of an applied field is obtained from the balance condition, and the total number of added carriers in the specimen in dynamic equilibrium with the injecting current pulse applied is evaluated. Upon application of a surface field,  $\Delta_1$  then gives a measure of the quasi-stable conductance change before any injection has taken place, while  $\Delta_1 - \Delta_2$  gives the change in carriers added by injection in dynamic equilibrium. Assuming constancy of the injection ratio, the change in lifetime and hence in  $s$  is calculable.

The surface state densities mentioned in Section V(c) were deduced from measurements of this kind. A set of results showing the dependence of  $s$  on barrier height as deduced again from the conductance measurements is given in Fig. 6 for the case of a CP-4 etched face of roughly (100) orientation on an  $n$ -type specimen of resistivity 13 ohm-cm.

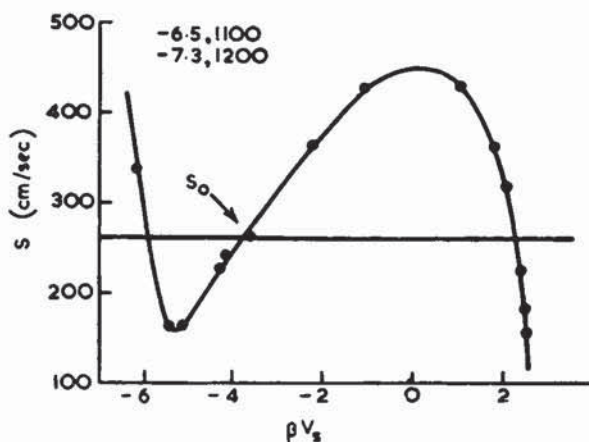


FIG. 6.—Results of measurements of surface recombination velocity versus barrier height. Two further readings not plotted, corresponding to higher  $s$  values, are given numerically.



## VII. CONCLUSION

The experimental methods described give means of determining fast surface state distributions and cross-sections for majority carrier trapping in these states, and, independently, surface state distributions again and the dependence of surface recombination velocity on barrier height. Such determinations can be made on the same surface consecutively, and the deductions of surface state distributions compared for consistency. It would then appear that measurements on a surface in various conditions offering a range of  $s$  values would give information as to the relationship between  $s$  and surface state density. Whether this can be done depends on the existence of surfaces of higher  $s$  values without large surface irregularities. Investigations of the type discussed here require ideally a perfectly plane surface of uniform barrier height. The first of these conditions is subject to experimental control, and attention to it should increase the significance of the measurements. As irregularities on an atomic scale are inevitably present, the ultimate value of such measurements may depend on whether these produce significant local variations in the barrier height.

## ACKNOWLEDGMENTS

We wish to thank Professor R. W. Ditchburn for his interest and for the provision of research facilities, and the Admiralty for permission to publish this paper and for funds in connection with a part of this work. One of us (G.G.E.L.) is indebted to the New Zealand Defence Research Organisation for financial support.

## REFERENCES

1. W. Shockley and G. L. Pearson, *Phys. Rev.* **74**, 232 (1948).
2. J. Bardeen and S. R. Morrison, *Physica* **20**, 873 (1954).
3. A. L. McWhorter, Sc.D. thesis, Dept. of Elect. Eng., M.I.T., May, 1955.
4. G. G. E. Low, *Proc. Phys. Soc. (London)* **B 68**, 10 (1955) and *Proc. Phys. Soc. (London)* **B 68**, 1154 (1955).
5. R. H. Kingston and S. F. Neustadter, *J. Appl. Phys.* **26**, 718 (1955).
6. J. R. Schrieffer, *Phys. Rev.* **97**, 641 (1955).

7. W. L. Brown, *Phys. Rev.* **100**, 590 (1955).
8. G. G. E. Low, *Proceedings of the Spring Meeting on Semiconductors of the Physical Society (London)*, 1956 (in publication).
9. G. G. E. Low (to be published).
10. H. K. Henisch and W. N. Reynolds, *Proc. Phys. Soc. (London)* **B 68**, 353 (1955).
11. J. E. Thomas, Jr., and R. H. Rediker, *Phys. Rev.* **101**, 984 (1956).
12. J. D. Nixon and P. C. Banbury, *Proc. Phys. Soc. (London)* (in publication).
13. A. Many (private communication).
14. J. D. Nixon and P. C. Banbury (to be published).
15. A. Many, *Proc. Phys. Soc. (London)* **B 67**, 9 (1954).

# SURFACE RECOMBINATION PROCESSES IN GERMANIUM AND THEIR INVESTIGATION BY MEANS OF TRANSVERSE ELECTRIC FIELDS

A. MANY, E. HARNIK and Y. MARGONINSKI

*Department of Physics  
The Hebrew University  
Jerusalem, Israel*

## ABSTRACT

A brief review of work on surface recombination is given. Present theories are outlined and the comparison with experimental data is discussed. Recent measurements made at this laboratory on the variation of surface recombination velocity with barrier height, employing transverse electric fields, are described. The results indicate that in some samples the simple theoretical model assuming the presence of one type of significant recombination centers at the surface is adequate. Other surfaces studied exhibit a more complex structure involving two types of significant centers. On the whole, the basic assumptions of the theory are found to be sound.

An analysis of the experimental data gives the activation energies of the dominant recombination centers, as well as the ratios of their capture cross-sections for holes and electrons. In almost all samples examined, of both *n*- and *p*-type material, the dominant centers lie above the energy gap center, and are characterized by a larger cross-section for holes than for electrons. Preliminary results indicate that the ambient gas surrounding the surface may affect directly the characteristics of the recombination centers.

## I. INTRODUCTION

It is well known that the equilibrium between holes and electrons in a semiconductor can be displaced by various external stimuli, e.g. by illumination or by contact injection of minority carriers. After the cessation of the external stimulus, the equilibrium relations are restored by processes which are in many cases exponential and can be described in terms of a single decay constant. The effective lifetime so determined is made up of two contributions which arise from bulk and surface recombination. If the bulk lifetime is known and not too small, measurement of the effective lifetime of the minority carriers in the filament can be used to



evaluate the rate of decay at the surface.<sup>1</sup> This can be expressed in terms of the surface recombination velocity,  $s$ , as defined by Shockley.<sup>1</sup>

The rates of recombination of excess carriers in the bulk and at a free surface of germanium crystals have been found to be extremely structure sensitive properties. This suggests that the recombination processes take place through intermediate energy levels in the forbidden gap arising from imperfections of some sort in the bulk and at the surface of the crystal. Using a model which assumes the presence of such recombination centers, Shockley and Read<sup>2</sup> analyzed the statistics of recombination in the bulk of a semiconductor. A similar analysis was carried out by Brattain and Bardeen<sup>3</sup> for surface recombination. It is well established that a potential barrier exists at the free germanium surface, which can be ascribed to the presence of charged surface states as discussed in detail by Bardeen.<sup>4</sup> It is to be expected that the surface recombination velocity would depend on the characteristics of this barrier. Indeed, Stevenson and Keyes<sup>5</sup> obtained, on the basis of the Shockley-Read and Brattain-Bardeen theories, an explicit expression for  $s$  involving both the barrier height and the characteristics of the recombination centers.

Measurement of the dependence of  $s$  on barrier height would thus seem to be a most promising tool in the study of surface recombination processes. This can be done by correlating measurements of  $s$  with those of other surface properties which also depend on barrier height, in particular surface conductance. The work to be described subsequently was carried out along these lines. The barrier height was varied by the application of transverse electric fields and the corresponding values of  $s$  and surface conductance measured simultaneously. The results indicate that Stevenson and Keyes' theory is valid on the whole. Accordingly such properties as the energy level of the significant recombination centers and their capture probabilities could be determined. These results combined with data obtained from other measurements<sup>6,7,8</sup> may lead to a further elucidation of the electronic structure of the surface under various conditions. The next two sections will be devoted to a brief review of the present status of the work on surface recombination, while the remaining sections will deal with some recent results obtained in this laboratory.

## II. PRESENT THEORIES OF SURFACE RECOMBINATION

In this section a resumé of surface recombination theories, based on references 2, 3 and 5, will be presented. Figure 1 represents the

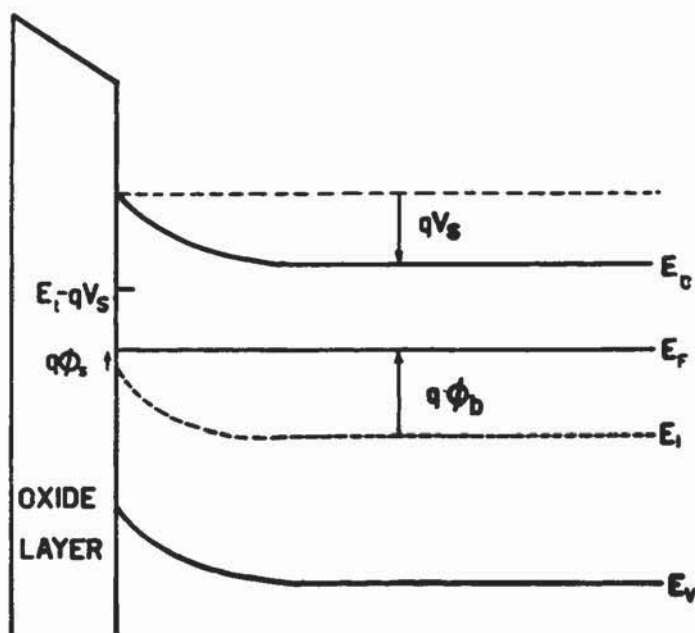


FIG. 1.—Energy level diagram at a germanium surface.

equilibrium situation at the free surface of a semiconductor.  $E_c$  and  $E_v$  are the energies at the bottom of the conduction band and at the top of the valence band.  $E_F$  is the Fermi level, while  $E_i$  is the value of  $E_F$  in an intrinsic sample. The presence of surface states in the forbidden gap (such as  $E_t$ ) gives rise to a space charge layer near the surface.<sup>4</sup> A potential barrier is established such that the excess charge in the surface states is balanced by that of the ionized impurities and the mobile carriers in the space charge layer. The barrier height is denoted by  $V_s$  corresponding to a potential energy  $-qV_s$  of an electron. The hole and electron densities at

any point of the semiconductor can be conveniently expressed in terms of the quantity  $q\phi = E_F - E_i$ ,

$$p = n_i \exp(-q\phi/kT), \quad n = n_i \exp(q\phi/kT) \quad (1)$$

where  $n_i$  is the electron or hole density in an intrinsic sample. In this notation positive values of  $\phi$  correspond to  $n$ -type conduction while negative values, to  $p$ -type conduction. The values of  $\phi$  in the bulk and at the surface are denoted in Fig. 1 by  $\phi_b$  and  $\phi_s$  respectively.  $\phi_b$  is determined by the bulk impurity density, while  $\phi_s$  depends on the barrier height as well and is given by  $q\phi_s = E_F - E_i + qV_s$ .

It is assumed that the surface contains a uniform density,  $N_t$ , of centers per unit area which contribute to the recombination processes and which are all at one discrete energy level  $E_t$ . These recombination centers are characterized by their capture cross-sections for holes and electrons. The rate of recombination is determined by the magnitude of these cross-sections and by the availability of holes and electrons at the surface to enter the centers. An analysis of the statistics of the recombination processes for the case in which the hole and electron distributions are non-degenerate yields for the rate of recombination per unit area

$$U = N_t c_p c_n (p_b + n_b) \Delta p / [c_p (p_s + p_{s1}) + c_n (n_s + n_{s1})] \quad (2)$$

where:  $c_p$  and  $c_n$  are the capture probabilities per center per unit time for holes and electrons when the centers are filled and empty respectively, and are given by the product of the corresponding capture cross-section with the thermal velocity;  $p_s$  and  $n_s$  are the free carrier densities at the surface;  $p_{s1}$  and  $n_{s1}$  are the surface densities if the Fermi level passes through the centers;  $p_b$  and  $n_b$  are the bulk equilibrium carrier densities; and  $\Delta p$  is the excess minority carrier density at the surface just inside the space charge layer, where  $\phi = \phi_b$ . If it is further assumed, as was done by Brattain and Bardeen,<sup>3</sup> that the densities  $p_s$  and  $n_s$  at the surface are in equilibrium with the densities in the interior, then, from Eq. (2), the surface recombination velocity is given by

$$s \equiv U' \Delta p = N_t c_p c_n (p_b + n_b) \div n_i [c_n \exp \{(E_t - E_i)/kT\} + c_p \exp \{(E_i - E_t)/kT\} + c_n \exp (q\phi_s/kT) + c_p \exp (-q\phi_s/kT)]. \quad (3)$$



Stevenson and Keyes<sup>5</sup> assumed that  $c_p = c_n$ , in which case Eq. (3) represents a symmetrical curve around  $\phi_s = 0$ , as shown, for example, by the dashed curve in Fig. 5. As will be described subsequently, all available data indicates that this assumption is not valid as a rule. We shall therefore treat the more general case in which  $c_p \neq c_n$ . This possibility has also been considered by Kingston.<sup>9</sup> It would be convenient to introduce an energy level defined by

$$q\phi_0 = (kT/2) \ln (c_p/c_n) \quad (4)$$

Then, Eq. (3) can be rewritten in the form

$$s = N_t c_p (p_b + n_b) \div 2n_i \exp(q\phi_0/kT) [\cosh\{(E_t - E_i - q\phi_0)/kT\} + \cosh\{q(\phi_s - \phi_0)/kT\}] \quad (5)$$

The recombination velocity is seen to be symmetrical around  $\phi_s = \phi_0$ . The value of  $\phi_0$  is a measure of the inequality between the center's cross-sections for holes and electrons. It is positive or negative according as  $c_p$  is larger or smaller than  $c_n$ . In the region about  $\phi_s = \phi_0$ ,  $s$  is constant but falls off rapidly for large  $|\phi_s - \phi_0|$ , as the second term in the denominator of Eq. (5) becomes predominant.

For subsequent use, some of the features of Eq. (5) will be examined. For a given  $s$  curve and temperature, two possible values of  $E_t - E_i$  can be deduced. If  $|E_t - E_i - q\phi_0| > kT$ , these can be conveniently expressed in terms of the two values,  $\phi_s^+(\frac{1}{2})$  and  $\phi_s^-(\frac{1}{2})$ , on the two sides of  $\phi_0$ , at which  $s$  equals half its maximum value  $s_M$ :

$$\begin{aligned} E_t^{(1)} - E_i &= q\phi_s^+(\tfrac{1}{2}) \\ E_t^{(2)} - E_i &= 2q\phi_0 - q\phi_s^+(\tfrac{1}{2}) = q\phi_s^-(\tfrac{1}{2}) \end{aligned} \quad (6)$$

Thus,  $E_t - E_i$  cannot be determined uniquely from the given  $s$  curve. However, as  $q\phi_0$  depends on temperature (Eq. (4)), it follows that only one of the two values in Eq. (6) can be temperature independent. This constant value gives, therefore, the actual level of the recombination centers, while the other has no physical significance. To determine the former, additional information is needed. This can be supplied by another  $s$  curve, taken at a different temperature, or alternatively, from the temperature

dependence of  $s_M$ . As  $q\phi_s^+(\frac{1}{2}) - q\phi_s^-(\frac{1}{2}) = 2|E_t - E_i - q\phi_0| > kT$ , it follows from Eq. (5) that

$$s_M = \text{const. } (c_p/n_i) \exp \{-q\phi_s^+(\frac{1}{2})/kT\} \quad (5a)$$

If it is assumed that  $c_p$  and  $c_n$  are temperature dependent only through the thermal velocity which contains a  $T^{\frac{1}{2}}$  factor, then, for the case in which  $\phi_s^+(\frac{1}{2})$  is temperature independent

$$s_M T = \text{const. } \exp \{(E_c - E_t^{(1)})/kT\}, \quad (7a)$$

while for the case in which  $\phi_s^-(\frac{1}{2})$  is temperature independent

$$s_M T = \text{const. } \exp \{(E_t^{(2)} - E_v)/kT\}. \quad (7b)$$

Thus the actual level of the recombination centers is given by  $q\phi_s^+(\frac{1}{2})$  or by  $q\phi_s^-(\frac{1}{2})$  according as Eq. (7a) or Eq. (7b) holds, respectively.

Lastly, it can easily be shown that the slopes of the  $s/s_M$  function at  $s/s_M = \frac{1}{2}$  are  $\pm 0.25(kT)^{-1}$ , for all values of  $E_t$  and  $\phi_0$ .

### III. REVIEW OF PREVIOUS WORK

There are various electrical properties, such as contact potential, surface recombination and surface conductance which are intimately connected with the presence of a potential barrier at the free surface of germanium crystals. The investigation of these properties constitutes the basis for the study of the electronic structure of the surface. It was found that by changing the ambient gas or by applying electric fields normal to the surface, the barrier height could be varied within appreciable limits and the changes in surface properties followed. One of the first studies along these lines was carried out by Brattain and Bardeen.<sup>3</sup> These authors measured contact potential, change of contact potential with light and surface recombination while the ambient surrounding the filament was cycled through ozone, dry oxygen and wet oxygen. It was later shown that direct information on the barrier height could be obtained by surface conductance measurements. These are based on the fact that the conductance per unit area of the space charge layer,  $\Delta\sigma$ , is a unique function of barrier height, for a given resistivity material and temperature. This function has been calculated by Schrieffer,<sup>10</sup> Kingston and Neustadter<sup>11</sup> and

Garrett and Brattain.<sup>12</sup> Schrieffer took into account as well the reduction of mobility due to surface scattering. Such a  $\Delta\sigma$  curve versus  $\phi_s$  is illustrated in Fig. 5.

Brattain and Bardeen<sup>3</sup> found that the surface recombination velocity for the specimens studied was independent of the ambients used. Measurements by Stevenson and Keyes,<sup>5</sup> however, indicated that  $s$  may change appreciably in the Brattain and Bardeen cycle, in qualitative agreement with the predictions of the theory. Experiments in which  $s$  and surface conductance were measured simultaneously and could thus lead to quantitative information were later reported by Noyce<sup>13</sup> and Stevenson.<sup>14</sup> The results were not in complete agreement with those obtained for a simple model (Eq. (5)), but could be explained by a reasonable distribution in energy of active recombination centers. The energy levels of the centers could not be determined from the available

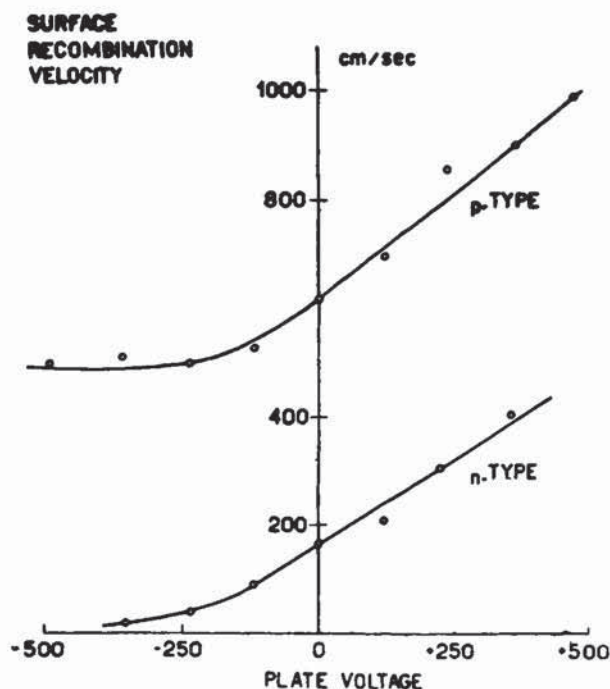


FIG. 2.—Effect of electric fields on surface recombination (Henisch and Reynolds).



data. Other attempts to determine the energy of the centers by measuring the temperature dependence of  $s$ <sup>5,15,16</sup> have not been too successful, since the variation of  $\phi_s$  with temperature complicates the interpretation of the data.

In order to draw definite conclusions from the variation of  $s$  with ambients for comparison with a theoretical model, one has to assume that the density and characteristics of the recombination centers are not affected by these ambients. As will be described subsequently, there are indications that this assumption may not always be valid. The study of surface recombination by the application of electric fields, on the other hand, seems to avoid this difficulty. Such measurements were first reported by Henisch, Reynolds and Tipple.<sup>17,18</sup> The dc fields were applied normal to the surface under test. As a result the free barrier shifts so as to accommodate the extra charge induced by the field. In cases where surface trapping is not appreciable, large variations in  $\phi_s$  can be obtained in this manner. Typical results for the effect of fields on  $s$ , taken from these authors, are shown in Fig. 2.

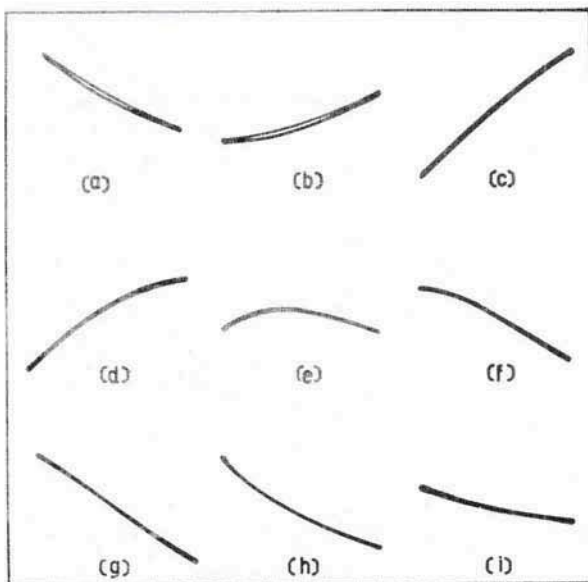


FIG. 3.—Effect of electric field on surface recombination velocity (Thomas and Rediker).

Thomas and Rediker<sup>19</sup> investigated the effect of alternating fields on surface recombination. Changes in  $s$  were deduced from the variation in inverse current in a junction diode alloyed near the surface under test. A series of oscillograms representing  $s$  versus applied field for various ambients is shown in Fig. 3. In these experiments the stationary values of  $\phi_s$  are determined by the ambients while the excursions around these values are effected by the ac field. The photographs may be fitted together to make a smooth  $s$  curve exhibiting a maximum and falling off for strong  $n$ - and  $p$ -type surfaces. As, however, the  $\phi_s$  values corresponding to the different ambients and fields were not determined, the results could only serve as a qualitative confirmation of Eq. (5).

Employing dc fields and measuring both  $s$  and changes in surface conductance,  $\Delta\sigma$ , simultaneously, results of a more quantitative nature have been obtained by the present authors.<sup>20,21</sup> The technique of measurement was complicated by relaxation effects exhibited by  $s$  and  $\Delta\sigma$ . A strong field was suddenly applied

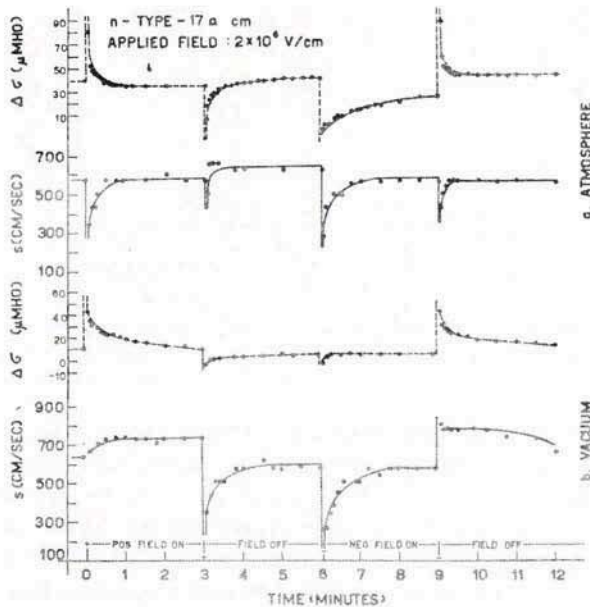


FIG. 4.—Typical field cycles of surface recombination velocity for short (a) and long (b) relaxation times (Many et al.).

(or switched off) and the filament lifetime and conductance were measured during the subsequent relaxation. The results obtained from such a field cycle are illustrated in Fig. 4. By the analysis of measurements of this type the experimental dependence of  $s$  on  $\phi_s$  could be evaluated, using the appropriate Schrieffer curve of  $\Delta\sigma$  versus  $\phi_s$ . The results for an  $n$ -type sample, together with Stevenson and Keyes' theoretical curve,<sup>5</sup> corresponding to  $c_p = c_n$  in Eq. (5), are shown in Fig. 5.<sup>22</sup> It is seen that the experimental

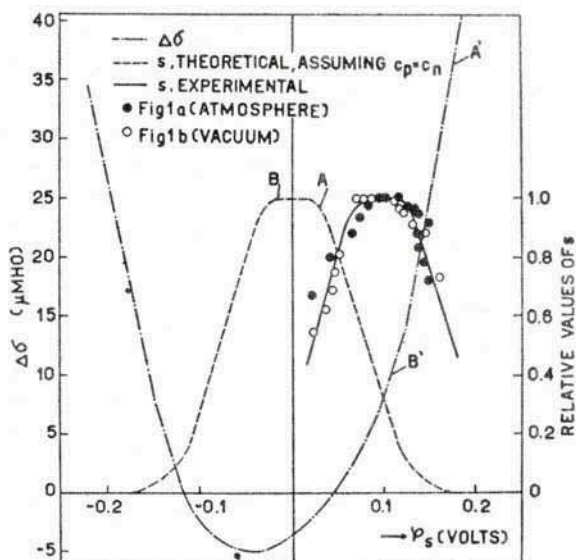


FIG. 5.—Theoretical curves of  $\Delta\sigma$  and  $s$  (assuming  $c_p = c_n$ ) and experimental results for  $s$  versus  $\phi_s$  (Harnik et al.).

$s$  curve is displaced by about 0.1 volt from  $\phi_s = 0$  but is in good agreement, within the margin of error, with Eq. (5) for  $\phi_0 = 0.1$  volt.

These results were of a preliminary nature. With improved technique and accuracy further work along these lines was carried out on a considerable number of samples. The experimental method and results obtained will be described in the following sections.



## IV. EXPERIMENTAL METHOD

The filaments investigated were about 2 cm long, 0.3 cm wide and 0.05 cm thick. They were mounted on small brass rods, etched in CP-4 and placed between two mica sheets of about 0.001 cm thickness, as shown in Fig. 6. The outer faces of the mica

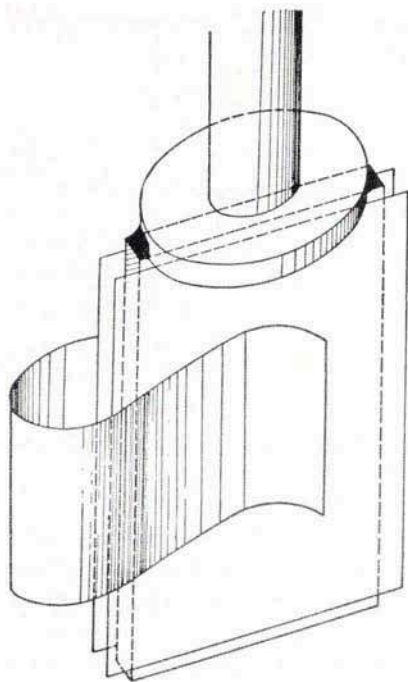


FIG. 6.—Experimental arrangement. The filament is placed between two silver painted mica sheets.

were coated with silver paint to serve as electrodes in the application of the transverse fields. The sheets were held in place by a metal spring which could be connected to a dc voltage supply. This assembly was then inserted into a cryostat in which the ambient gas could be altered and the temperature varied from liquid air to room temperature.

The quantities actually measured were filament lifetime  $\tau$  and filament resistance  $R_f$ . The two were measured simultaneously by

means of the double bridge shown in Fig. 7. The lifetime bridge<sup>23</sup> and a simple Wheatstone bridge were connected in such a manner that the arm containing the filament was common to both. By manipulating only the resistors in the outer arms, the two bridges could work without mutual interference.

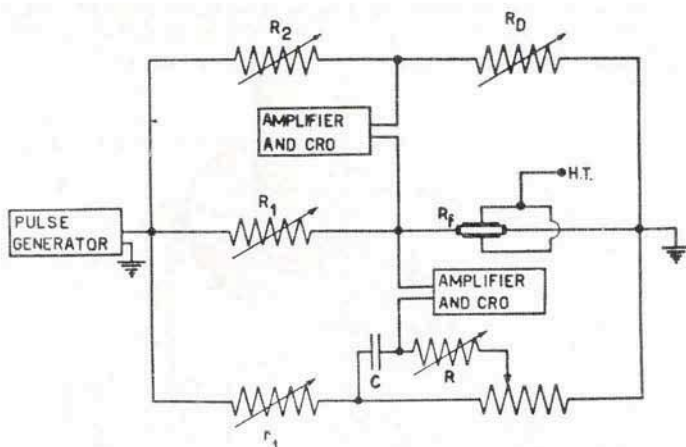


FIG. 7.—Double bridge circuit for the simultaneous measurement of lifetime and surface conductivity.

Electric fields were applied between the electrodes and the specimen, and the filament resistance and lifetime measured by means of the decade resistance  $R_D$  and the series combination  $RC$ , respectively, the two CRO's serving as null indicators. The actual procedure in each case depended on the speed of the relaxation effects. If these were slow, the electric field was gradually increased from zero to about  $\pm 3.10^6$  volt/cm, while corresponding values of  $R_f$  and  $\tau$  were taken at suitable intervals. When the relaxation times were fast this procedure could not be employed as the relaxation counteracted the slow change in field. It was, however, possible to use the relaxation itself to aid in the measurements.  $R_D$  was pre-set to a certain value and an electric field of such magnitude was applied that it caused the filament resistance to overshoot its pre-set value. While the relaxation was returning the resistance towards its pre-set value,  $\tau$  was continually followed and was measured at the very instant of bridge balance. As will

be discussed subsequently, the maximum value of filament resistance,  $R_{\max}$ , is of utmost importance for the interpretation of results. It was therefore determined as accurately as possible and checked repeatedly throughout the measurements. This introduced some difficulty as a drift in temperature of  $0.2^{\circ}\text{C}$  was often sufficient to introduce an error into  $R_{\max}$  greater than that permissible. To overcome this difficulty each group of measured  $(R_i, \tau)$  pairs was correlated to that value of  $R_{\max}$  just previously determined.

To determine the temperature dependence of  $s_M$ , the minimum value of  $\tau$  was measured at each temperature. This could readily be done by gradually increasing the electric field until  $\tau$  assumed its constant minimum value, as indicated by changes in  $R_i$  no longer being accompanied by corresponding changes in  $\tau$ .

The values for the  $(R_i, \tau)$  pairs obtained from repeated measurements on each filament were plotted on graph paper and the mean values, obtained from the smooth curve, were taken for the evaluation of  $s$  as a function of  $\phi_s$ . In the calculation of  $s$  from  $\tau$ <sup>1</sup> a small correction had to be applied due to the fact that the two filament surfaces parallel to the field were not affected by it. The changes in surface conductance relative to that at  $R_i = R_{\max}$  were evaluated and transformed into the respective  $\Delta\sigma$  values used in Schrieffer's curve corresponding to the resistivity material and temperature under consideration. This transformation is based on the fact that the value of  $\phi_s$  at the minimum of  $\Delta\sigma$ , and therefore at  $R = R_{\max}$ , is theoretically known. Thus the  $\phi_s$  values corresponding to the measured  $R_i$  values can be determined, and the  $s$  versus  $\phi_s$  curve drawn.

The accuracy of each  $s$  value ranges from 3 to 10 percent, depending on several factors such as the properties of the injecting contact,<sup>23</sup> the magnitude of the lifetime measured and the speed with which the reading had to be carried out (due to the relaxation effects). A more serious source of error is introduced in the evaluation of  $\phi_s$  in the region about  $\Delta\sigma$  minimum. As can be seen, for instance, from the Schrieffer curve shown in Fig. 5, an error in  $\Delta\sigma$  of  $0.5 \mu\text{mho}$  near the minimum, corresponding roughly to an error of 1 ohm in a typical filament of 2000 ohm resistance, may introduce an error of about  $1 kT$  in  $q\phi_s$ . Fortunately, however, in most cases examined only a relatively small portion of the  $s$  curve falls in this region.



## V. EXPERIMENTAL RESULTS

The behavior of the different filaments after etching varied considerably. The surfaces of most of them exhibited a steady decrease in recombination velocity with time, becoming stable only after an hour or so. Accordingly the filaments were put between the mica sheets and inserted into the vacuum cryostat after this period. Henceforth their characteristics remained almost unaltered. All measurements (except where otherwise stated) were taken in vacuum (better than  $0.1 \mu$  Hg).

The initial value of  $\phi_s$ , before the application of the field, was usually found to be near the  $\Delta\sigma$  minimum, i.e. negative for  $n$ -type and positive for  $p$ -type samples. With the maximum field used, a swing of  $\phi_s$  from about  $-8kT$  to  $+8kT$  could usually be effected. In surfaces exhibiting a simple structure, this was sufficient to cover most of the  $s$  curve. In some filaments, especially after a long exposure to air, screening of the external field by surface trapping<sup>6,7</sup> was so appreciable that only a negligible swing in  $\phi_s$  could be obtained, and therefore such filaments had to be discarded. On the whole screening effects were not appreciable except for large  $|\phi_s|$  values. In these ranges the relaxation times became much faster, too.

The temperature range used was 240–320°K. The lower limit was imposed by the lifetime usually becoming too low to be accurately measured, and the higher, by the relaxation becoming too fast. It was invariably found that the speed of relaxation is very temperature dependent.

An interesting feature observed at some surfaces, especially at low temperatures, was an effect of "surface fatigue." After several repeated cycles of applied field a hysteresis could be noted in the sense that the recombination velocity depended on the previous direction of the field. This effect disappeared if the field was switched off for 10 or 20 minutes.

In Fig. 8 the results for an  $n$ -type filament are shown.  $s/s_M$ , where  $s_M$  is the maximum value of  $s$ , is plotted as a function of  $q\phi_s/kT_0$ ,  $T_0$  being the temperature at which the measurements were carried out. The experimental curve, except for large values of  $|\phi_s|$ , is in good agreement with Eq. (5) for  $q\phi_0/kT_0 = 1.7$ , i.e., from Eq. (4), for  $c_p/c_n = 30$ . In particular, the slope at

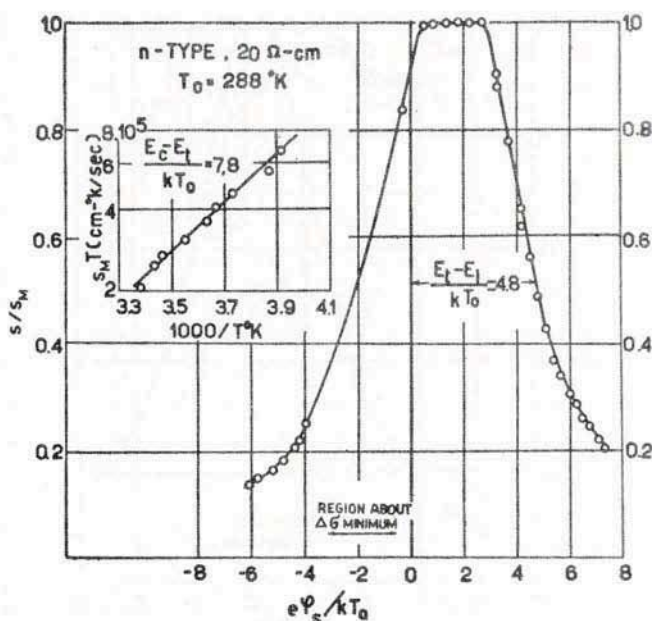


FIG. 8.—Experimental curves of  $s/s_M$  versus  $q\phi_s/kT_0$  and the temperature dependence of  $s_M T$ , for an  $n$ -type sample.

$s/s_M = \frac{1}{2}$  is  $0.23 (kT_0)^{-1}$ , compared with the theoretical value of  $0.25 (kT_0)^{-1}$ . For large  $|\phi_s - \phi_0|$ ,  $s$  is larger and varies slower than predicted by theory. Also shown in Fig. 8 is a plot of the logarithm of  $s_M T$  versus  $1/T$ . The slope of the straight line passing through the experimental points gives for the activation energy of the recombination centers  $7.8 kT_0$ . This indicates that of the two possible values of  $E_t - E_i$  deduced from the  $s/s_M$  curve,  $q\phi_s^+(\frac{1}{2}) = 4.8 kT_0$  and  $q\phi_s^-(\frac{1}{2}) = -1.4 kT_0$ , the former is the actual level of the centers.

A similar curve of  $s/s_M$  for a  $p$ -type sample is shown in Fig. 9. In this case the region of maximum  $s$  coincides with the minimum of the  $\Delta\sigma$  curve, and hence the accuracy in this range is poor. This coincidence, however, makes it possible to determine accurately both branches of the  $s/s_M$  curve. The results can be fitted with Eq. (5) for  $c_p/c_n = 30$  and  $E_t - E_i = 4.5 kT_0$ , but the deviations from the theoretical curve are larger here than those

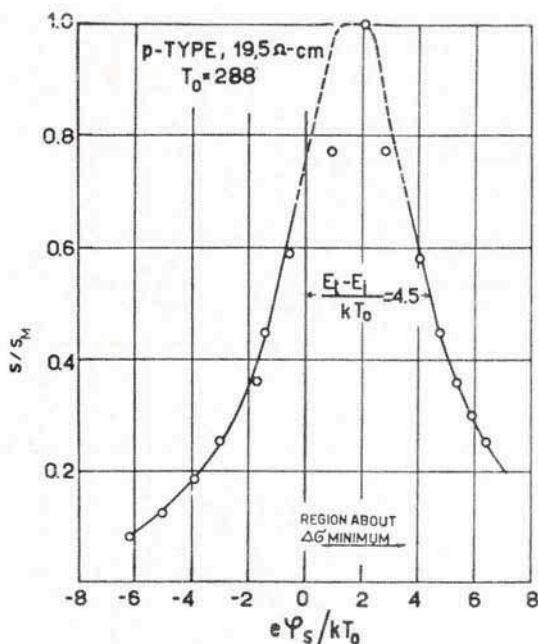


FIG. 9.—Experimental curve of  $s/s_M$  versus  $q\phi_s/kT_0$  for a *p*-type sample.

in Fig. 8. For example, the experimental slopes at  $s/s_M = \frac{1}{2}$  are about  $\pm 0.20$  instead of  $\pm 0.25 (kT_0)^{-1}$ .

Figures 10 and 11 represent measurements which cannot be fitted with the simple model assuming the presence of only one type of significant recombination centers. The two  $s/s_M$  curves in Fig. 10 were taken at two different temperatures  $T_1 = 288^\circ\text{K}$  and  $T_2 = 248^\circ\text{K}$ , and plotted as a function of  $q\phi_0/kT$ , where  $T$  equals  $T_1$  and  $T_2$  respectively. It is clearly seen that the slopes at  $s/s_M = \frac{1}{2}$  are appreciably lower than  $0.25 (kT)^{-1}$ . Moreover, for large and negative  $\phi_s$ ,  $s/s_M$  approaches in both cases a constant value. This is a strong indication of the presence at the surface of another group of significant recombination centers. Indeed, the left branch of the curve corresponding to  $T_1$  can be reduced to the sum of two  $s/s_M$  functions of the type given in Eq. (5), as shown by the dashed curves (a) and (b). In curve (a),  $c_p'c_n = 150$  and  $(E_t - E_i)/kT_1 = 6$ , while the corresponding values in



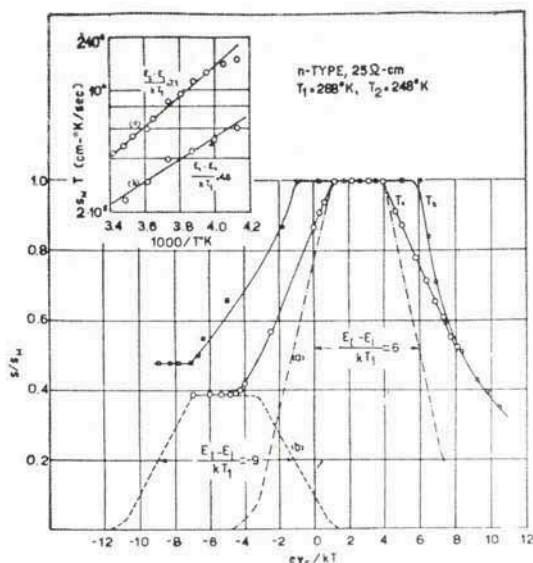


FIG. 10.—Experimental  $s/s_M$  curves for an  $n$ -type sample exhibiting two significant recombination centers, and the temperature dependence of the corresponding  $s$  maxima.

curve (b) are  $4.5 \times 10^{-6}$  and  $-9$ . The centers represented by curve (b) are thus characterized by a much larger cross section for electrons than for holes. Moreover they must be definitely situated below  $E_i$  as the two possible values of  $E_i - E_i$  in this case are both negative. A plot of the temperature dependence of  $s$  maximum for the two centers, also shown in Fig. 10, gives for the respective activation energies 7.1 and 4.6  $kT_1$ , in good agreement with the values deduced from curves (a) and (b). This may serve as an additional confirmation of the above analysis. A similarly simple analysis of the  $s/s_M$  curve for  $T = T_2$  could not be carried out. On the right branches of the curves the data is insufficient to draw any definite conclusions.

In Fig. 11 results are given for a  $p$ -type sample. In the range of  $q\phi_s/kT_0$  values which could be realized,  $s$  does not attain a maximum value. It seems that here, too, two significant centers play an important role in the recombination process, both being characterized by large  $c_p/c_n$  values.

Whereas the above measurements were all carried out in vacuum, Fig. 12 compares the behavior of the same sample in vacuum and in an atmosphere of dry air. The two corresponding  $s/s_M$  curves are in fairly good agreement with Eq. (5), indicating that in each case only one type of centers is dominant in the recombination process over the  $\phi_s$  region examined. It is seen that

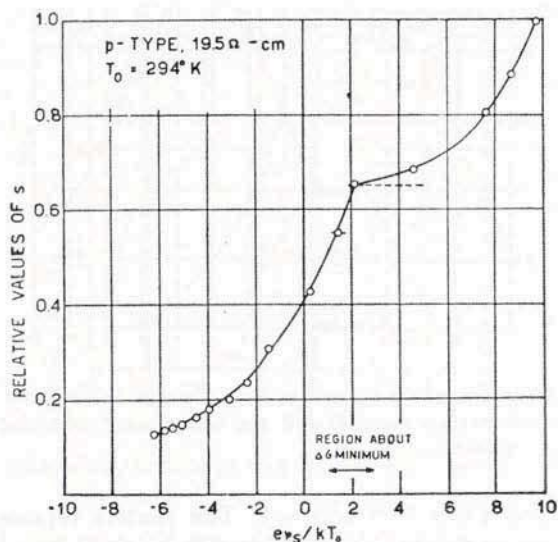


FIG. 11.—Relative values of  $s$  for a  $p$ -type sample, exhibiting complex structure.

in both curves  $\phi_0$  is approximately the same, giving for  $c_p/c_n$  a value of 3. However,  $E_t - E_i$  is appreciably different in vacuum and in air. The respective values of  $s_M$  are 1100 cm/sec and 560 cm/sec. The fact that the characteristics of the centers are ambient dependent is most striking and will be referred to again in the next section.

## VI. DISCUSSION

The first object of the present work was to check the validity of the theory of surface recombination as outlined in Section II. No systematic work was therefore undertaken and filaments were chosen on a non-selective basis from different bulk materials, and

all received the same surface treatment. The results obtained for the various samples show a diversity of behavior. The fact that some of them are in good agreement with Eq. (5) strongly indicates that the basic assumptions of the theory must be considered sound on the whole. The simple model employed in Eq. (5) is, however, found inadequate to account for all the different features of the experimental data. It is therefore necessary to assume in

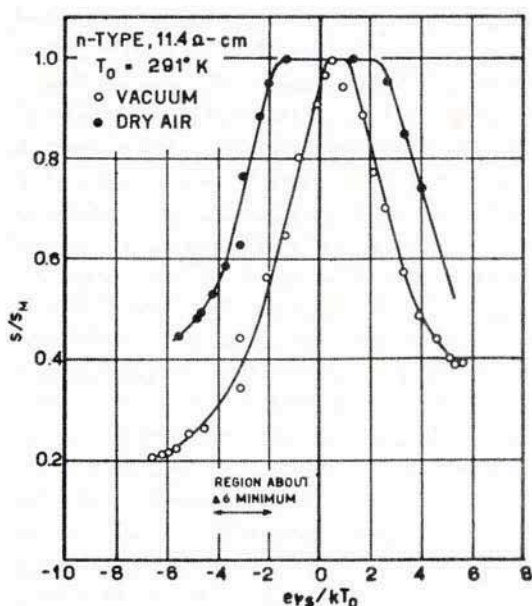


FIG. 12.—Experimental  $s/s_M$  curves obtained for an  $n$ -type sample in vacuum and in dry air.

general a more complicated distribution in energy of the recombination centers. Complex as this distribution may be, the present results indicate that in all cases examined there exists one or two discrete recombination centers having such characteristics and density that they dominate the recombination process.

In all cases where the experimental curves can be analyzed so as to isolate the dominant centers, important information as regards their nature can be obtained. For  $n$ -type as well as  $p$ -type material, irrespective of the bulk conductivity, the most significant



centers are characterized by a larger cross section for holes than for electrons, i.e. they are of the acceptor-like type. In one case (Fig. 10) there is an indication of the existence of donor-like recombination levels. In almost all surfaces studied, for which the figures shown are typical examples, the dominant recombination levels lie above the gap center  $E_1$ .

Another interesting problem on which information can be obtained is whether ambient gases affect directly only the structure and characteristics of the "slow" surface states on the oxide, as has been generally assumed,<sup>9</sup> or whether they have some similar effect on the recombination centers as well. The results in Fig. 12 show that the latter may well be the case. The increase of  $E_t - E_1$ , i.e. the decrease in ionization energy of the centers, in air relative to that in vacuum, is most significant. It has been suggested by Kingston<sup>9</sup> that adsorbed gases might decrease the binding energy of levels on the oxide film. It is possible that a similar explanation may also apply to the recombination levels. The results obtained also indicate that the difference in  $s_M$  in vacuum and in air cannot be accounted for by the difference in  $E_t - E_1$  alone. It thus appears that the possibility of a change in  $N_{tc}$  should also be considered.

The available information is not sufficient to draw definite conclusions about the origin of the significant recombination centers. The fact that their characteristics are similar in  $n$ - and  $p$ -type material of various resistivities seems to indicate that they cannot be related to the concentration of bulk impurities near the surface. On the other hand, as all the samples received the same treatment, within the precautions taken, it is unlikely that the differences in their behavior are due to surface treatment. Some relation to bulk imperfections of some sort cannot, therefore, be ruled out. For further progress in the solution of this problem, a systematic investigation of the dependence of the recombination processes on surface treatment and bulk imperfection is being undertaken along the lines indicated here. To complement the study of the electronic level structure of the germanium surface, it is necessary to ascertain whether the discrete recombination centers discussed above are the only significant "fast" surface states<sup>9</sup> present. There is an indication in the results presented here that this may not be the case, as can be seen from the following

argument. Assuming the validity of Schrieffer's calculations<sup>10</sup> of effective mobility in the space charge layer, the deviations of the experimental  $s/s_M$  curves from Eq. (5) at large values of  $|\phi_s - \phi_0|$  must be ascribed to the presence of centers close to the conduction and valence bands having  $c_p \gg c_n$  and  $c_n \gg c_p$  respectively. According to Eq. (5), levels with such characteristics must have fairly large  $N_t c_p$  or  $N_t c_n$  values in order to increase  $s$  (for large  $|\phi_s - \phi_0|$  values) by the small amount necessary to explain the observed deviations. These surface levels may, on the other hand, be very effective as surface traps. The comparison of the trapped surface charge density versus  $\phi_s$ , as obtained from field effect measurements,<sup>6,7</sup> with the information obtained through recombination data, may be very instructive in this connection.

## DISCUSSION

S. WANG and G. WALLIS (*Sylvania Electric Products, Inc., Woburn, Mass.*): Variation of surface recombination velocity as a function of barrier height has also been investigated at this laboratory. The following quantities were simultaneously measured, (1) surface conductance,  $G_s$ , (2) small-signal ac field-effect conductance,  $(\Delta G_s)_{F.E.}$ , (3) photo current,  $I$ , and (4) change of photo current with the applied ac field,  $(\Delta I)_{F.E.}$ . During the experiment, the surface barrier,  $\phi_s$ , of the sample was altered by changing the gas ambient as in the Brattain and Bardeen cycle. The sample was put in a double-walled tube permitting water to circulate from a constant-temperature bath which also controlled the temperature of the gas. A big block of another sample cut from the same crystal was used as a thermometer, and any conductance change of the test sample due to temperature drifts was corrected.

The first two quantities,  $G_s$  and  $(\Delta G_s)_{F.E.}$ , give us the value for  $\phi_s$ . Around the point of minimum surface conductance, it is very difficult to determine  $\phi_s$  accurately from  $G_s$ . A simultaneous measurement of  $(\Delta G_s)_{F.E.}$  will not only locate the point of minimum surface conductance, but also provide a cross-check on the measurement of  $G_s$ . The quantity,  $I$ , measures the surface recombination velocity,  $V_s$ , while the quantity  $(\Delta I)_{F.E.}$ ,



represents the change of surface recombination velocity due to a small change in barrier height as a result of the applied ac field. In order to get  $(\Delta I)_{F.E.}$ , one subtracts the dark field-effect signal from the field-effect signal in the presence of illumination. Around  $\phi_s = \phi_0$ , i.e.,  $V_s$  is a maximum,  $V_s$  is a very slowly varying function of  $\phi_s$ . However, the quantity,  $(\Delta I)_{F.E.}/I$ , which varies approximately as  $\sinh q(\phi_s - \phi_0)/kT$  around  $\phi_s = \phi_0$ , gives a sharply defined value for  $\phi_0$ . During the experiment, the light intensity was kept low so that change of  $\phi_s$  due to light was negligible. This requirement was checked by reducing the light intensity, and no change in  $\phi_0$  was observed.

Experimental results on a germanium sample (38 ohm-cm, *n*-type, etched in CP-4) yield the following information:  $q\phi_0/kT = 0.8$  and  $|E_t - E_i - q\phi_0|/kT = 2.3$ . These values are considered to be in fair agreement with those obtained by Dr. Many. It is conceivable that crystal orientation as well as surface imperfection might have an effect on the trap energy and the capture cross-sections. Therefore, comparison of the experimental results would be more meaningful if the measurements were made on surfaces of known orientation.

Moreover, before one can attach any significance to the difference in the values of  $\phi_0$  and  $E_t$ , one should realize the experimental uncertainties in determining  $\phi_s$ . First of all, the two surfaces not only may be patchy, but also may not have the same  $\phi_s$ . Secondly, the Schrieffer correction of the space-charge mobility needs experimental confirmation. Besides these, any temperature drift would introduce additional error in  $\phi_s$ . Finally, it should be emphasized that potential probes should be used in measuring the sample conductance. In the Wheatstone-bridge method, the contact resistance between germanium and metal is included in the measurement. It is difficult to estimate how the contact resistance would change due to changing ambient conditions or temperature variations.

A. MANY (*Hebrew University*): We are confident that no serious error did arise from the inhomogeneity in surface potential due to surface "patchiness." The satisfactory fit with theory and, in particular, the consistency in the values of  $E_t$  as derived from both the *s* curve and the temperature dependence of  $s_{max}$  strongly support the above statement. Regarding the comment on the



measurement of sample conductance, it does not seem to be relevant to our case; both ambient and temperature are constant throughout the measurement.

## REFERENCES

1. W. Shockley, *Electrons and Holes in Semiconductors* (D. Van Nostrand Co. Inc., New York, 1950).
2. W. Shockley and W. T. Read, *Phys. Rev.* **87**, 835 (1952).
3. W. H. Brattain and J. Bardeen, *Bell System Tech. J.* **82**, 1 (1953).
4. J. Bardeen, *Phys. Rev.* **71**, 717 (1947).
5. D. T. Stevenson and R. J. Keyes, *Physica* **20**, 1041 (1954).
6. Brown, and Montgomery and Brown, *Phys. Rev.* **98**, 1565 (A) (1955).
7. W. L. Brown, *Phys. Rev.* **100**, 590 (1955).
8. Statz, Davis, and DeMars, *Phys. Rev.* **98**, 540 (1955).
9. R. H. Kingston, *J. Appl. Phys.* **27**, 101 (1956).
10. J. R. Schrieffer, *Phys. Rev.* **97**, 641 (1955).
11. R. H. Kingston, S. F. Neustadter, *J. Appl. Phys.* **26**, 718 (1955).
12. C. G. B. Garrett and W. H. Brattain, *Phys. Rev.* **99**, 376 (1955).
13. R. N. Noyce, Meeting of the Electrochemical Society, Cincinnati, May 1955.
14. D. T. Stevenson, *Phys. Rev.* **98**, 1566 (A) (1955).
15. Y. Kanai, *J. Phys. Soc. (Japan)* **9**, 292 (1954).
16. W. N. Reynolds, *Proc. Phys. Soc.* **B66**, 899 (1953).
17. H. K. Henisch, W. N. Reynolds and P. M. Tipple, *Physica* **20**, 1033 (1954).
18. H. K. Henisch and W. N. Reynolds, *Proc. Phys. Soc.* **B68**, 353 (1955).
19. J. E. Thomas and R. H. Rediker, *Phys. Rev.* **101**, (1956).
20. Many, Margoninski, Harnik and Alexander, *Phys. Rev.* **101**, 1433 (1956).
21. Harnik, Many, Margoninski and Alexander, *Phys. Rev.* **101**, 1434 (1956).
22. In the original figure (Fig. 2 of reference 21), a numerical error has occurred, which is corrected in the present figure.
23. A. Many, *Proc. Phys. Soc.* **B97**, 9 (1954).

SHORT CONTRIBUTION:  
STORAGE OF INJECTED CARRIERS  
AT SURFACES OF GERMANIUM

B. H. SCHULTZ

*Philips Research Laboratories  
N. V. Philips' Gloeilampenfabrieken  
Eindhoven, Netherlands*

Injection of electron-hole pairs in germanium near the surface is accompanied by an increase of the concentrations of the particles in the space charge layer and also of those in the surface states. It is usually assumed that for rapidly changing concentrations, the holes in the "fast acceptor surface states" remain in equilibrium with the holes in the valence band at the surface and also with the holes in the bulk close to the surface, whereas the holes in the "slow surface states," or the "surface ionic charges" do not follow the rapid fluctuations. A similar assumption is made for the electrons. The condition for equilibrium with the particles in the bulk implies Boltzmann factors containing in the exponent the difference  $V_s$  in electrostatic potential between surface and bulk.

We consider injection in  $n$ -type germanium. In the bulk the number of holes may increase by a factor much larger than unity, whereas the number of electrons increases relatively feebly. In an atmosphere containing ozone, the equilibrium number of holes in the fast surface states may be high, and if an inversion layer occurs, here too a high number of holes may be present in equilibrium. If the number of these holes were to increase proportionately with the number of holes in the bulk, then an enormous increase in such numbers would result. Since the corresponding increase in the number of electrons would be relatively feeble, the net result would be a positive charge in the surface region. Actually, there will be a shift in the electrostatic energy, viz. a decrease of  $|V_s|$ , reducing the number of holes and increasing the number of electrons, so that the surface region as a whole remains neutral. The resulting increase in the number of electron-hole pairs in the sur-

face region, i.e., in the surface states and in the space charge layer together, is called surface storage. It comes in addition to the storage in the bulk, which is simply the injected concentration without the "surface excesses," integrated over the volume.

We have made calculations of the surface storage for surfaces such as have been considered by Garrett and Brattain.<sup>1</sup> These calculations are rather laborious and yield numerical results which are given in reference 2. Here the increase of electron-hole pairs per cm<sup>2</sup> of the surface for a given injection concentration  $\Delta$  in  $n$ -type bulk is written in the form  $l(n_0/p_0)r\Delta$ , where  $n_0$  and  $p_0$  are the equilibrium concentrations in the bulk,  $r$  is a reduction factor which is unity for small  $\Delta$ , and the coefficient  $l$  has the dimension of a length and follows from the calculation. For  $p$ -type germanium the surface storage is similarly  $l(p_0/n_0)r\Delta$ . Although  $l$  depends in general on  $n_0$ , on  $V_s$ , and on the densities of the fast surface states, the calculation yields the following result: If a sufficiently strong inversion layer is present,  $l$  is independent of  $V_s$  and of the densities of surface states; its value is then somewhat smaller than the Debye length for the germanium under consideration, i.e.  $(2\kappa\epsilon_0 kT/q^2 n_0)^{1/2}$  for  $n$ -type germanium doped to the concentration  $n_0$ . If  $V_s$  is smaller so that no inversion layer occurs,  $l$  depends on  $V_s$  and on the surface state densities:  $l$  becomes very small for  $\beta V_s \rightarrow 0$  if the densities of the fast donor and acceptor surface states do not exceed  $10^{11}$  cm<sup>-2</sup>. The surface storage is only proportional to  $\Delta$  if  $\Delta$  is smaller than the minority bulk concentration. For larger injections the factor  $r$  decreases.

The total number of injected electron-hole pairs in a thin slab of thickness  $d$  is  $d\Delta + 2l(n_0/p_0)r\Delta$ , and the relaxation time for the recombination becomes

$$\tau_{slab} = [d + 2l(n_0/p_0)r]/[(d/\tau_v) + 2s].$$

The effect of surface storage is usually small, since  $l \leq 10^{-6}$  to  $10^{-5}$  cm; it is large only for thin slabs of low resistivity and for low injection levels. The formula leads to the remarkable prediction that  $\tau_{slab}$  will *increase* with *decreasing* thickness if  $(l/s)(n_0/p_0)r > \tau_v$ . In order to verify this prediction, measurements of  $\tau_{slab}$  have been undertaken using rapidly interrupted light of low intensity. The predicted increase of  $\tau_{slab}$  with decreasing  $d$  was found for  $n$ -type germanium of about 1 ohm-cm



in ozone. Systematic measurements of  $\tau_{slab}$  as a function of  $V_a$  (ambient),  $n_0$  (resistivity) and  $r$  (injection level) are reported in reference 2; the results are qualitatively in agreement with the formula.

A complication in the discussion of these measurements arises from the fact that there are also changes of the surface recombination velocity  $s$  with ambient and injection level, affecting  $\tau_{slab}$ . However, these could easily be separated from changes in  $\tau_{slab}$  due to the surface storage, especially by comparing the results on  $n$ - and  $p$ -type germanium.

This investigation leads to the conclusion that measurements of the relaxation time for the recombination in thin slabs of 1 ohm-cm resistivity or lower are not suitable for the determination of  $s$ , unless one is sure that there is no appreciable effect of surface storage. Thus, results of measurements on photoconduction in different ambients<sup>3</sup> should be interpreted with caution. The same applies to measurements of hole storage at  $p$ - $n$  junctions. On the other hand it follows from what has been said concerning the magnitude of  $l$  that measurement of the surface storage alone does not give useful information concerning the inversion layer or surface states.

#### REFERENCES

1. C. G. B. Garrett and W. H. Brattain, *Phys. Rev.* **99**, 376 (1955).
2. B. H. Schultz, *Philips Res. Rep.* (in preparation).
3. A report of such measurements is given, for instance, by D. T. Stevenson and R. J. Keyes, *Physica* **20**, 1041 (1954).

# FIELD EFFECT AND PHOTO EFFECT EXPERIMENTS ON GERMANIUM SURFACES

## 1. EQUILIBRIUM CONDITIONS WITHIN THE SEMICONDUCTOR

W. L. BROWN, W. H. BRATTAIN, C. G. B. GARRETT,  
and H. C. MONTGOMERY

*Bell Telephone Laboratories  
Murray Hill, New Jersey*

### ABSTRACT

It has been possible to deduce certain aspects of the energy distribution of the fast surface states on etched germanium surfaces from field induced changes in conductivity and surface recombination velocity. The assumptions underlying the interpretation of these experiments are discussed in some detail. Measured changes in surface capacitance are found to substantiate these assumptions over a limited range. The surface state distribution is composed of a density of states the order of  $10^{11} - 10^{12}$  (cm<sup>2</sup> volt)<sup>-1</sup>, slowly varying with energy near the center of the band gap. The results also require higher densities more than 0.1 electron volt both above and below the center.

### I. INTRODUCTION

We are concerned with the properties of germanium surfaces which have been prepared by etching and are subsequently exposed to various gaseous ambients at substantially atmospheric pressure. One would ultimately like to understand the physical and chemical origin of the electronic surface states which appear with this surface preparation. As yet the answer to this question is entirely in the realm of speculation, and the immediate problem is one of describing the properties of the states as they exist. A complete characterization would at least include the energy distribution of the electronic states in the forbidden energy gap at the semiconductor surface and the transition probabilities for electrons between the surface states and the conduction and valence bands and among the surface states themselves. This paper will treat the first of these properties; the paper to follow will be concerned with the second.

## II. THE EXPERIMENT AND ASSUMPTIONS INVOLVED IN ITS INTERPRETATION

Experimentally we have measured the variation in conductance of a germanium sample with application of an ac electric field normal to the sample surface. The sensitivity of the experiment to surface states arises in the following way.<sup>1</sup> The applied electric field induces a net charge  $\Sigma_T$  on the semiconductor.  $\Sigma_T$  is made up partly of changes in electron and hole concentration in a space charge region in the body of the semiconductor but close to the surface; this part will be designated  $\Sigma_{sc}$ . The remainder is present as a change in charge in surface states  $\Sigma_s$ . Thus  $\Sigma_T = \Sigma_{sc} + \Sigma_s$ . The changes in conductance which one measures result almost entirely from  $\Sigma_{sc}$ , the mobility of carriers in the surface states being small compared with the mobility in the space charge region. The presence of surface states is thus experimentally apparent as a reduction in the measured change in conductance below that to be expected if all the induced charge went into the space charge region.

The body of the semiconductor is in equilibrium in these experiments since the applied frequency is low compared with the lifetime of minority carriers. It cannot be said that the whole surface layer, presumably an oxide with various imperfections and impurities, is in equilibrium with the body. Operationally two classes of surface states can be distinguished which differ in this respect. Figure 1 shows the measured change of sample conductance follow-

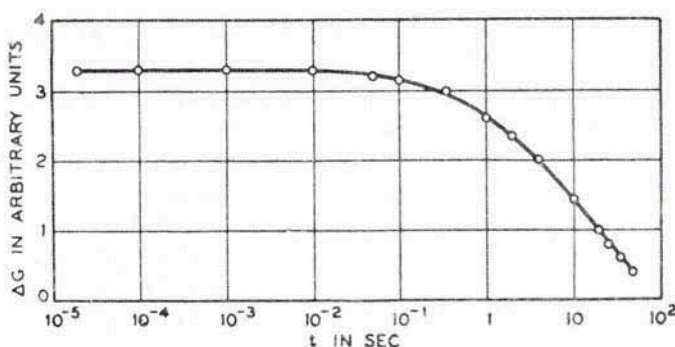


FIG. 1.—Response of sample conductance following an impulse of induced charge.



ing an impulse of induced charge applied at  $t = 0$ . The method is essentially that described by Low.<sup>2</sup> At  $2 \times 10^{-5}$  seconds the conductance change corresponds to a change in the number of mobile carriers which is perhaps 25 percent of the total induced charge. Thus some 75 percent of  $\Sigma_T$  has gone into surface states which are operable in a time at least this short. The conductance is remarkably constant between  $2 \times 10^{-5}$  seconds and about 0.1 seconds, but for still longer times drops off to much lower values. Such a response indicates a second group of surface states which are slow compared with the first. (This long time or low frequency characteristic and its possible implications are discussed by McWhorter, Statz, and Morrison.<sup>3</sup>) Thus one is led to divide the surface states into "slow" and "fast" states with several decades separating the time constants of the two. One thinks of the fast states<sup>4</sup> as being at or very close to the interface between the germanium and its oxide, and hence capable of a rapid interchange of electrons and holes with the body of the semiconductor. One thinks of the slow states as being associated with energy levels spatially more remote from the interface and correspondingly less accessible to carriers from the interior. The measurements which will be discussed in this paper were all made at a frequency the order of a hundred cps (corresponding to times between  $10^{-2}$  and  $10^{-3}$  seconds in Fig. 1) and thus involve changes in the electronic filling of fast states which at this frequency are in equilibrium with the body of the semiconductor. The slow states are incapable of responding to this frequency and appear in the experiment only as a fixed charge which adds a biasing dc field to the interface.

The end product of a measurement of the variation of sample conductance with applied field, or equivalently with  $\Sigma_T$ , is a curve relating the charge in surface states to  $\phi_s$ , the position of the Fermi level at the germanium interface measured with respect to  $E_1$ , the Fermi level in intrinsic material. The method of analysis will be presented here in order to point out some of the assumptions that are made and comment on their importance.

There is a unique relationship between  $\Sigma_{sc}$  and  $\phi_s$ , depending upon the chemical impurity of the body material and the temperature. In deriving this relationship, which involves solution of Poisson's equation in the space charge layer,<sup>5</sup> two basic simplifications are made.

1. The randomly distributed chemical impurity ions (donors and acceptors) in the semiconductor body are replaced with a uniform distribution of charge having the same average value. The average spacing between impurity ions is the same order but somewhat less than the thickness of the space charge region and the Debye length. The waviness of the space charge region that including the actual positions of the ions would introduce will thus not be large and can reasonably be neglected.

2. One assumes that in this system, in which the electrostatic potential near the surface may vary by the order of  $kT$  in an electron wave length, the electron and hole concentrations are related to the electrostatic potential by classical statistics as they would be in less rapidly varying potentials. This sort of problem has been considered by Wigner<sup>6</sup> and others. The complication is most serious at surfaces which are strongly  $n$ - or  $p$ -type. In the vicinity of the minimum in conductance the complication is marginal, and lacking an alternate method of analysis we will ignore it.

Two additional assumptions are made in relating  $\Sigma_{sc}$  to the sample conductance.

1. The mobility of carriers in surface states is assumed to be negligible compared with the mobilities in the space charge region. Measurements at very low temperatures, for example those made by Fritzsche<sup>7</sup> in studying impurity bands, have sometimes given indications of surface conductance which might be occurring in surface states. However, this surface conduction always disappears upon etching the sample. The mobility in surface states on etched surfaces must be very low if their conductivity is not apparent compared with the extremely low body conductivity at helium temperatures. The important surface states in these experiments might conceivably have been completely filled with carriers and thus unable to conduct. However, the conductance is low by so many orders of magnitude at these low temperatures it seems justifiable to neglect the surface state mobility in our experiments.

2. A value for the mobility of carriers in the space charge region must be used. In some cases the carriers in our experiments have a mean free path which is the same order as the depth of the region to which the carriers are constrained at the surface. Schrieffer<sup>8</sup> has considered this point in detail. For small surface potentials, such as are encountered for  $\phi_s$  near zero in high re-



sistivity material, his correction is negligible. At the extremes of surface potential which we have encountered it would introduce a correction the order of 25 percent. It is possible that the surface is not a completely diffuse scatterer of carriers as Schrieffer has assumed, in which case the correction would be even smaller. Thus we have chosen to neglect the correction altogether and have used bulk carrier mobilities in interpreting our data.

Figure 2 shows the dependence of  $G$  on  $\Sigma_{sc}$  calculated with these assumptions for 40 ohm-cm  $p$ -type germanium at room tempera-

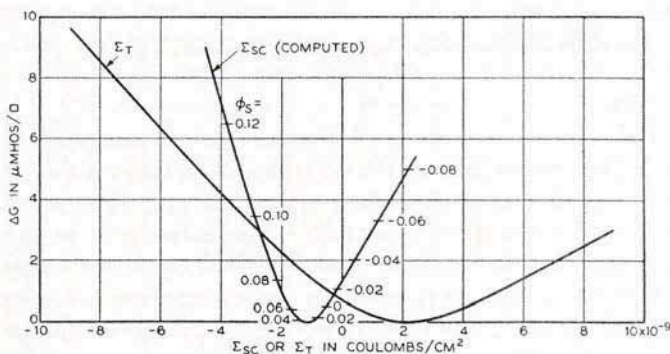


FIG. 2.—Conductance changes (a) computed from changes in space charge  $\Sigma_{sc}$  and (b) measured with changes in total induced charge,  $\Sigma_T$ .

ture. For  $\Sigma_{sc}$  large and positive the space charge layer is dominated by holes (the surface is  $p$ -type) and a positive increment in  $\Sigma_{sc}$  results in an increase in hole concentration and an increase in conductance. For  $\Sigma_{sc}$  large and negative the space charge layer is dominated by electrons (the surface is  $n$ -type) and a positive increment in  $\Sigma_{sc}$  results in a decrease in electron concentration and a decrease in conductance. Between these two extremes there is a minimum in conductance resulting from the competition between addition of holes and removal of electrons. With respect to this minimum, any value of conductance can be related to corresponding values of  $\Sigma_{sc}$  and  $\phi_s$ . In an experiment one measures  $G$  vs  $\Sigma_T$  and such a curve is also shown in Fig. 2. If the minimum in conductance is observed then  $\Sigma_s (= \Sigma_T - \Sigma_{sc})$  and  $\phi_s$  can be determined for all values of  $\Sigma_T$ . In Fig. 2,  $\Sigma_s$  is just the horizontal



difference between the  $\Sigma_{sc}$  and  $\Sigma_T$  curves taken at a constant value of  $G$ . The corresponding value of  $\phi_s$  is read off the  $\Sigma_{sc}$  curve.

From an experimental point of view several additional assumptions have been made which are important in this analysis.

1. The applied electric field is assumed to be uniform over the surface. The actual surface is not flat on a microscopic scale, and the enhancement of the field at protruding points may be considerable. However, the greatest field enhancements go with the smallest point dimensions and these in turn are the least accessible to the current that is flowing for the conductance measurement and hence have least effect on it. With surfaces we have examined, which are shingled to a depth the order of a micron over distances the order of 25 microns this effect would not seem to be very important.

2. The surface conditions of the sample are assumed to be uniform. Non-uniformity may be manifested in large areas having different distributions of surface states. In the absence of an external field these differences might, for example if they were differences in slow surface states only, bias the underlying material in  $n$ - and  $p$ -type surface patches. In the measurement this would amount to displacing the U-shaped  $G$  versus  $\Sigma_T$  curve appropriate to one area by different amounts along the  $\Sigma_T$  axis and taking an average. The result would be a curve with a broad shallow minimum. The  $\Sigma_s$  versus  $\phi_s$  curve derived by taking differences from such a minimum might bear only a very general resemblance to the curve characterizing any part of the surface. The possibility of patchiness is the most serious complication in these experiments.

3. It is assumed that if the surface region is an inversion layer it is not electrically isolated from the conductance measuring current by the  $p$ - $n$  junction existing between the surface and the base material. One calculates that the impedance of the junction formed in this way for the samples we have used is so low compared with the impedance of the inversion layer that this assumption is a very good one.

### III. CAPACITANCE

As an over-all check on the assumptions that are made in deriving the charge in surface states and the position of the Fermi

level at the surface, a measurement of the change in capacitance of the surface region with  $\Sigma_T$  has been made. The capacitance does not involve the mobility of carriers at all. It is the sum of the capacitances of the fast surface states, defined as  $d\Sigma_s/d\phi_s$ , and of the space charge region  $d\Sigma_{sc}/d\phi_s$ , and thus involves quite a different combination of the variables than does the change of conductance which is presumably measuring properties of the space charge region alone. From the conductance measurements, by invoking the assumptions mentioned above, one can deduce the surface capacitance. Figure 3 shows a comparison of such a calculated

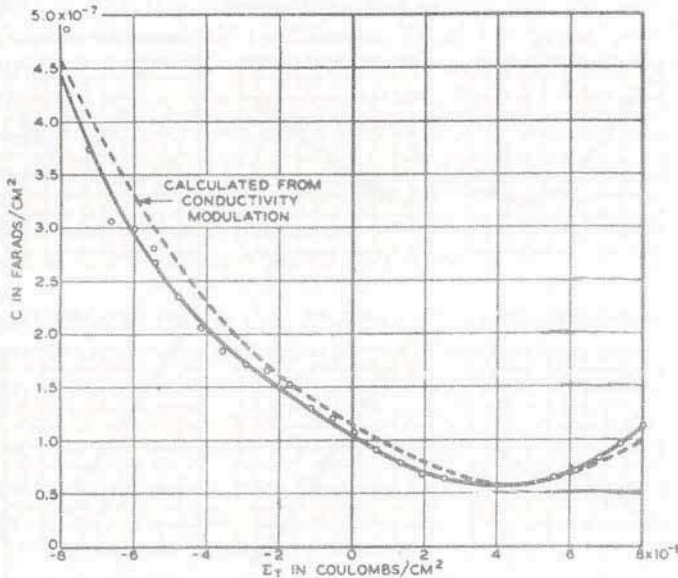


FIG. 3.—Changes in surface capacitance with induced charge (a) calculated for conductivity changes and (b) measured.

curve with the change in capacitance that was experimentally determined. There is one adjustable parameter in this fit, the vertical position of the experimental curve. Choosing this parameter fixes the absolute value of the surface capacitance at one point, chosen in this case to be the minimum. The positions of the minima in  $\Sigma_T$  are in quite good agreement as are also the shapes

of the two curves. Notice that the surface capacitance changes by a factor of about seven over the range of the measurements. Unfortunately the measurements do not involve a sufficiently great range in  $\phi_s$  to make Schrieffer's mobility correction as large as the experimental inaccuracies. Thus the experiment sheds no definite light on this particular matter. However, the two curves of Fig. 3 agree sufficiently well to give one confidence that the numerous assumptions and simplifications discussed in the previous section, including the assumption of a uniform surface, have not introduced any very important error in interpreting the results.

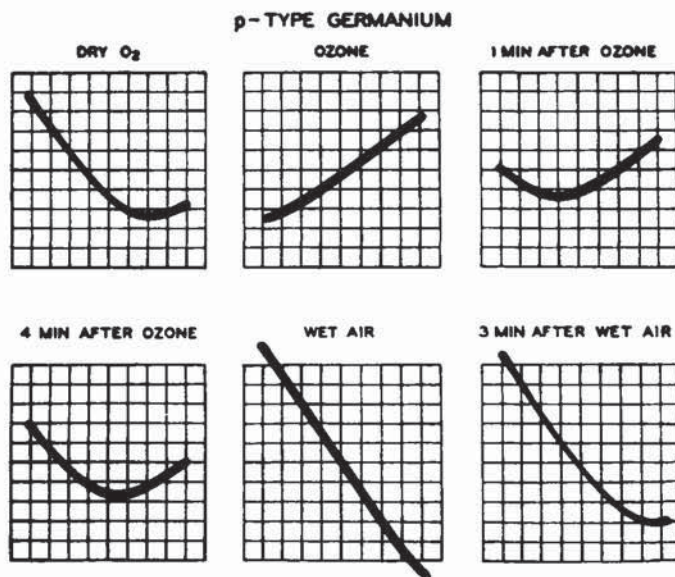


FIG. 4.—Conductance change with induced charge for a series of gaseous ambients.

#### IV. AMBIENT

Measurements have been made of the large signal conductance changes<sup>9</sup> in a series of ambients similar to those used by Brattain and Bardeen.<sup>10</sup> In the original dry oxygen condition the surface has an *n*-type inversion layer on it as indicated by the negative slope of the curve at  $\Sigma_T = 0$ . The most striking feature in this series



of curves is the shift in the position of the minimum in conductance along the  $\Sigma_T$  scale. While the minimum is clearly evident in the dry oxygen condition and in the recovery in oxygen after ozone and water vapor, in the ozone and water vapor extremes the minimum is actually off the curve to the left and right respectively, the surface being strongly *p*-type and *n*-type in these two cases. Since the minimum occurs at a fixed value of  $\Sigma_{sc}$  this shift in the value of  $\Sigma_T$  at the minimum must be associated with a large change in surface state charge. The several curves can be fitted together quite well into a single more extensive curve. This leads one to believe that the gaseous ambients have little effect on the distribution of the fast surface states, for if they did the shapes of the various curves would be different. Thus the change in surface state charge accompanying the change in ambient must occur in slow surface states. One can deduce the values of  $\phi_s$  at  $\Sigma_T = 0$ , zero applied field, for each of the ambient conditions. The changes are of the same sign as those reported by Brattain and Bardeen<sup>10</sup> from their contact potential work but the variations are smaller as one would expect if there were changes in the surface dipole outside of the germanium-germanium oxide interface as well as in  $\phi_s$ .

The charge in fast surface states as a function of  $\phi_s$  has been computed from the composite curve of  $G$  versus  $\Sigma_T$  obtained with the variation in ambients. This computation requires reference to the minimum in conductance as previously discussed. In order to display the character of the dependence more critically the derivative,  $d\Sigma_s/d\phi_s$ , has been plotted as a function of  $\phi_s$  in curve (a) of Fig. 5 rather than  $\Sigma_s$  itself. Dividing by  $e$  gives a scale which has the dimensions of a density of surface states ( $\text{cm}^2 \text{ volt}^{-1}$ ).

As long as the fast surface state distribution is at least approximately unchanged by ambient the fast surface state charge can be obtained by other methods which keep track of the minimum of conductance as one changes the ambient without using the large signal features of conductance modulation that were essential to the preceding paragraphs. Morrison,<sup>4</sup> for example, through careful temperature control, measures the dc sample conductance relative to the minimum. Small signal conductance modulation then provides the equivalent of the slope of the large signal curve at each point along it.

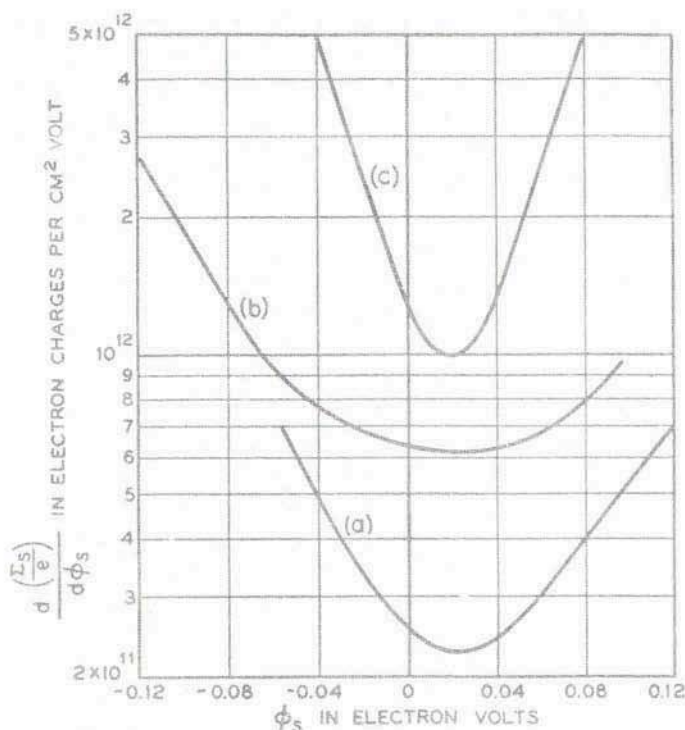


FIG. 5.  $d\Sigma_s/d\phi_s$  vs  $\phi_s$  (a) deduced from a superposition of curves such as those of Fig. 4, (b) deduced from changes of  $s$  and  $ds/d\Sigma_T$  with ambient, and (c) calculated assuming two discrete surface states outside the limits of  $\phi_s$  shown.

It has been found possible<sup>11</sup> to maintain a knowledge of the position of the minimum throughout a gas cycle by measuring the variations in surface recombination velocity. (The non-equilibrium aspects of this work will be discussed in the following paper.) The trick that is used depends upon the variation of  $s$  with ambient, and upon  $ds/d\Sigma_T$ , the small signal variation of  $s$  with induced charge. Choosing some reference ambient with a corresponding  $s_0$ , one can compute the equivalent value of  $\Sigma_T$  which would be required at the reference ambient to achieve the value of  $s$  appropriate to any other ambient in the gas cycle.

$$\Sigma_T = \int_{s_0}^s (d\Sigma_T/ds) ds$$

This is just a way of exchanging the effect of ambient on  $\phi_s$  for the effect of induced charge on the same quantity, assuming that the fast surface states are independent of ambient. Then from  $dG/d\Sigma_T$ , a small signal measurement, and  $s$  one can construct a complete curve of  $G$  versus  $\Sigma_T$ . From this curve  $\Sigma_s(\phi_s)$  can be derived as before. The derivative  $d\Sigma_s/d\phi_s$  obtained with this method appears as curve (b) in Fig. 5. The sample in this case was 22 ohm-cm  $n$ -type germanium etched heavily in CP-4. The sample of curve (a) was 40 ohm-cm  $p$ -type etched in sodium hydroxide and superoxol. While the consistency of the results obtained with  $n$ - and  $p$ -type material has been checked using the variation of  $s$ , the large signal field effect has unfortunately not been checked against this method using the same surface preparation. There are found to be substantial differences in the variation of  $s$  through a gas cycle depending on the surface treatment, so we believe that the differences between (a) and (b) of Fig. 5 result from real differences in the fast surface state distribution and not from inconsistencies in the methods.

The curves of Fig. 5 represent the starting point in an attempt to determine the equilibrium energy distribution of the fast surface states. If one had the energy distribution he could uniquely determine  $\Sigma_s(\phi_s)$ . P. A. Wolff<sup>12</sup> has shown that the inverse operation of deducing the state distribution from  $\Sigma_s(\phi_s)$  is not unique unless one has data over an infinite range in  $\phi_s$ . With less extensive data one can, however, approximately determine the distribution over the range in energy actually explored by the Fermi level at the surface in these measurements and can conclude less specific things about the distribution which exists outside the range of exploration.

Several general conclusions can be drawn from both curves (a) and (b) of Fig. 5.

1. The minimum in these curves indicates there must be surface states both above and below the position of the Fermi level at the surface for this point. The minimum occurs at very nearly the same  $\phi_s$  for the two cases. The approximate symmetry around this point suggests an approximately symmetrical distribution of states.
2. There is no evidence of a decrease in  $d\Sigma_s/d\phi_s$  or its derivative toward the extremes of  $\phi_s$  that would be expected if most of the surface states lay inside the range of measurement or even close to the limits.



3.  $d\Sigma_s/d\phi_s$  changes too slowly with  $\phi_s$  to be consistent with two energy levels, one on either side of the minimum and outside the range of measurement. Curve (c) is a plot of this case. In fact, no combination of states wholly outside the range of measurement will fit the experimental observations.

Two pairs of discrete levels, one inside the limits of measurement in  $\phi_s$  and one outside, are sufficient to fit the curves. One may equally well choose a smooth distribution rather than discrete states to represent the data. At room temperature  $kT$  is a sufficiently large fraction of the total range of measurement that the distinction between discrete and distributed states is a meager one. A smooth distribution has the advantage of analytical simplicity.

It is found that functions of the form

$$N(\Delta) = A \cosh [B(e\Delta/kT + C)]$$

will also give a good empirical fit to the data.  $N$  is the state density at an energy  $\Delta$  measured relative to  $E_i$  and  $A$ ,  $B$  and  $C$  are constants. For curve (a) this becomes

$$N(\Delta) = 1.3 \times 10^{11} \cosh [0.50(e\Delta/kT - 0.9)] \text{ (cm}^2 \text{ volt)}^{-1}$$

and for curve (b)

$$N(\Delta) = 4.5 \times 10^{11} \cosh [0.36(e\Delta/kT - 0.8)] \text{ (cm}^2 \text{ volt)}^{-1}$$

Curve (c) which has been constructed from two remote states, fits this same form but with  $B$  equal to unity.

It can be said from these measurements that there is a density of fast surface states the order of  $10^{11}$  to  $10^{12}/\text{cm}^2 \text{ volt}$  located near the middle of the band, and an even larger density of states located more than 0.1 electron volt away from the middle in both directions.

## V. TEMPERATURE MEASUREMENTS

Clearly to get more information about the fast surface state distribution one needs to extend the range of measurement in  $\phi_s$ . The limitation in this respect is set by the maximum induced charge one can practically obtain in a given ambient, or by the range afforded by the ambients used. Going to a different gas cycle leaves one in the position of having to verify the independence of

the fast surface state distribution on ambient, so that ultimately a large signal conductance measurement is desired. The practical limit in  $\Sigma_T$  has not been reached in the measurements described here, but the additional range in  $\phi_s$  that can be achieved at room temperature by going to higher electric fields is not very great simply because  $\Sigma_{sc}$  increases so rapidly as  $\phi_s$  departs by more than a few  $kT$  from 0. This limitation can be reduced by lowering the temperature with a gain roughly in proportion to the inverse temperature.

A series of large signal conductivity modulation measurements<sup>12</sup> from room temperature to 170°K have been analyzed for the 40 ohm-cm *p*-type sample for which the ambient results were given in Figs. 4 and 5.  $\Sigma_s(\phi_s)$  has been extracted in the way described in Section II and is shown in Fig. 6. The same ambient data

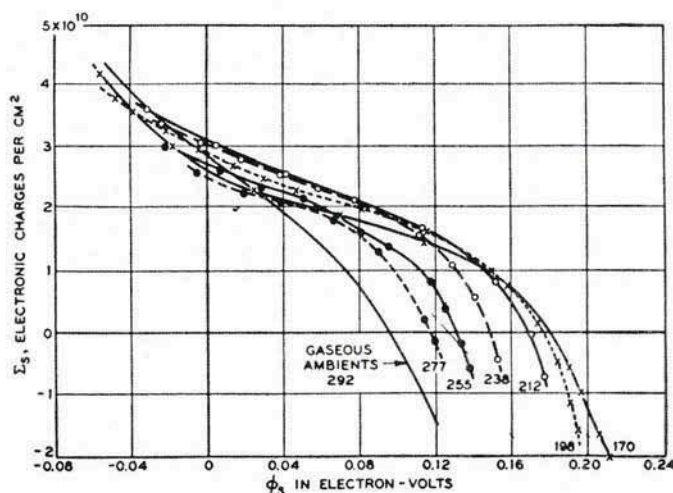


FIG. 6.  $\Sigma_s$  vs  $\phi_s$  from large signal conductance measurements between room temperature and 170°K. The data of curve (a) of Fig. 5 is shown as the ambient curve at 292°K.

which appeared in (a) of Fig. 5 as  $d\Sigma_s/d\phi_s$  are shown here before differentiation. The question as to whether the surface state distribution itself is changing with temperature cannot really be answered from these measurements. However, similarity of the slopes of the family of curves around  $\phi_s = 0$  shows that the state

density in the vicinity of  $\Delta = 0$  is not changing very much. There is a smooth progression through the family, the almost linear part of the curve extending to larger values of  $\phi_s$  for lower temperatures and then breaking into a steeper slope. This is qualitatively what one would expect if there were a slowly varying surface state distribution around  $\Delta = 0$  with a much higher density of states beyond the limits of the curves toward the conduction band. The steeper slopes occur at larger  $\phi_s$  since the Fermi level must come closer to the high density states at lower temperatures before there is a significant change in the electronic population of these states. Even for the lowest temperature curve there is no indication of a turning over in  $\Sigma_s$  toward large positive  $\phi_s$ . Apparently the high state density in the upper half of the band must be more than 0.2 electron volts above the middle. In the low temperature curves there is no appearance of fine structure in the broad region of almost uniform  $d\Sigma_s/d\phi_s$  such as one might expect to see if the distribution in this region were really composed of several discrete states. This is at least a point in favor of a continuum of surface states, but not a very strong one. Qualitatively these temperature results express the same rising density of states as one departs from  $\Delta = 0$  as found in the ambient measurements. However, the analytic function for  $N$  in the preceding section does not satisfy this series of measurements and a compatible form has not yet been determined.

## VI. CONCLUSIONS

It has been found that for germanium surfaces prepared by normal etching techniques and examined in several simple ambients the distribution of fast surface states is a slowly varying function of energy around the middle of the band with a density between  $10^{11}$  and  $10^{12}$  (cm<sup>2</sup> volt)<sup>-1</sup>. There must also be higher densities in regions of the band gap more than 0.1 electron volt away from the middle at room temperature and more than 0.2 electron volt above the middle at about -100°C. The distribution is at least approximately unaffected by changes in the gaseous ambient.

One can scarcely overemphasize the importance of experiments which depend on the surface properties in some different way



than the measurement of conductance does. The experiment of change in capacitance is in this class, but it needs to be extended over more and different situations than has been possible so far, in order to give one an even greater level of confidence in the analysis of the conductance measurements than it gives over its limited range. Measurements of magneto-resistance and perhaps Hall effect may be made to contribute significantly on this problem.

## REFERENCES

1. W. Shockley and G. L. Pearson, *Phys. Rev.* **74**, 232 (1948). W. L. Brown, *Phys. Rev.* **100**, 590 (1955).
2. G. G. E. Low, *Proc. Phys. Soc. (London)* **B68**, 10 (1955).
3. A. L. McWhorter, *Phys. Rev.* **98**, 1191 (1955); Stutz, deMars, Davis and Adams, *Phys. Rev.* **101**, 1272 (1956). S. R. Morrison, *Phys. Rev.* **102**, 1297 (1956).
4. J. Bardeen and J. R. Morrison, *Physica* **20**, 873 (1954).
5. R. H. Kingston and S. F. Neustadter, *J. Appl. Phys.* **26**, 718 (1955). C. G. B. Garrett and W. H. Brattain, *Phys. Rev.* **99**, 376 (1955).
6. E. Wigner, *Phys. Rev.* **40**, 749 (1932); J. G. Kirkwood, *Phys. Rev.* **44**, 31 (1933).
7. H. Fritzsche, *Phys. Rev.* **99**, 406 (1955).
8. J. R. Schrieffer, *Phys. Rev.* **97**, 641 (1955).
9. H. C. Montgomery and W. L. Brown (in press).
10. W. H. Brattain and J. Bardeen, *Bell System Tech. J.* **32**, 1 (1953).
11. W. H. Brattain and C. G. B. Garrett (in press).
12. P. A. Wolff, private communication.

# FIELD EFFECT AND PHOTO EFFECT EXPERIMENTS ON GERMANIUM SURFACES

## 2. NON-EQUILIBRIUM CONDITIONS WITHIN THE SEMICONDUCTOR

C. G. B. GARRETT, W. H. BRATTAIN, W. L. BROWN,  
and H. C. MONTGOMERY

*Bell Telephone Laboratories  
Murray Hill, New Jersey*

### ABSTRACT

By measurement of such non-equilibrium phenomena as (i) change of contact potential with light, (ii) surface recombination as deduced from photo conductivity and its exponential decay, throughout a Brattain-Bardeen cycle, along with measurements of change of conductivity due to a transverse field, one concludes that the fast surface traps near the center of the forbidden energy band are primarily acceptor-type. The estimated cross-sections for trapping of holes and electrons in these fast traps are  $\sigma_p \sim 6 \times 10^{-18} \text{ cm}^2$  and  $\sigma_n \sim 4 \times 10^{-17} \text{ cm}^2$  respectively. If the field effect experiment is performed at high enough frequency the germanium cannot stay in equilibrium with the field because of the time constants of body recombination and of surface trapping. One can estimate from the cross-sections that the surface trapping relaxation times must be very short. This conclusion is consistent with the high frequency field effect data, i.e., no dispersion from this cause up to frequencies of the order of 5 megacycles/second.

### I. INTRODUCTION

The preceding paper contains a discussion of measurements of field effect on germanium surfaces under conditions in which there is a thermodynamic equilibrium within the semiconductor. This paper is concerned with various experiments on germanium surfaces for which the thermodynamic equilibrium between holes and electrons in the semiconductor has been upset. For the purposes of these papers "equilibrium inside the semiconductor" means that the product  $np$  of the electron and hole density is everywhere equal to the equilibrium value  $n_i^2$ . Evidently this condition is well satisfied in experiments on the modulation of surface conductivity and surface capacity by external electric

field within the frequency range discussed in the preceding paper. The experiments and analysis on which this paper is based are reported in detail elsewhere.<sup>1</sup>

One way in which the equilibrium within the semiconductor may be upset is by illumination of the surface. Light of quantum energy large enough to excite electrons across the energy gap will create excess hole-electron pairs at a certain rate which, in the steady state, will be equal to the rate at which the excess carriers disappear by recombination in the semiconductor and at the surface. One effect of illuminating the surface is to change the work function or contact potential of the semiconductor surface. Measurements of this change, taken together with field effect measurements, provide information on the distribution of charge near the semiconductor surface. These experiments, together with measurements of surface recombination velocity, enable one to determine the transition probabilities between the conduction and valence bands of the semiconductor and localized states on the surface.

Another way in which the hole-electron equilibrium within the semiconductor may be upset is by the injection or extraction of minority carriers across a surface of the semiconductor. Such injection or extraction may take place, for example, by transition from the various kinds of surface states into the body of the semiconductor. The application of an electric field normal to the surface may itself stimulate such processes. This means that, in the appropriate frequency range, the field effect measurements themselves may involve injection or extraction of minority carriers.

In the succeeding sections, we shall present the results of both types of experiment, and the conclusions that can be made from them about the nature of the semiconductor surface.

## II. PHOTO EFFECTS: SURFACE PHOTO VOLTAGE

Measurements have been made of the surface photo voltage, that is, the change of contact potential with light, as a function of the barrier height, measured by the field effect technique. The barrier height is described by quoting the quantity  $Y$ , which is defined as the difference, measured in units  $kT/e$ , between the



electrostatic potential at the surface and the electrostatic potential deep in the interior. The Brattain-Bardeen cycle<sup>2</sup> was used to vary  $Y$  over as large a range as possible. To compare values of  $Y$  for different samples, one may quote the results in terms of the quantity  $(Y - \ln \lambda)$ , where  $\lambda = (p_0/n_i)$ . This quantity is the difference measured in units of  $kT$ , between the Fermi level at the surface and the Fermi level for intrinsic material.

Figure 1 shows the results of measurements of the surface photo voltage for two germanium samples, one  $n$ -type (22.4 ohm-cm)

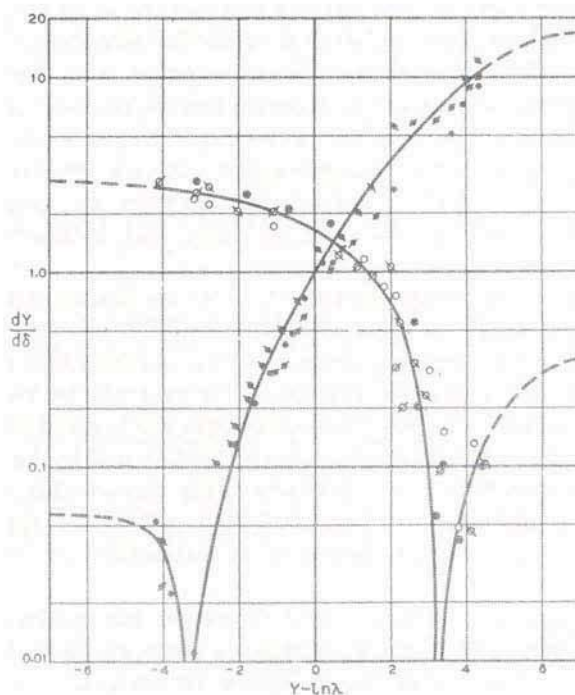


FIG. 1.  $d\phi/d\delta$  vs  $Y - \ln \lambda$ .

and one  $p$ -type (8.1 ohm-cm). The surfaces were etched in CP-4. The vertical axis shows the ratio of the change in contact potential to the change in the quantity  $\delta$ , defined as the ratio of the added carrier density  $\Delta p$  to the intrinsic carrier density  $n_i$ . The physical interpretation of the surface photo voltage experiment is as follows. When the surface is illuminated, the densities of holes and

electrons in the interior are changed. The surface has then to re-adjust itself to the changed availability of holes and electrons. This is done by rearrangement of charge in the space-charge region, and in the population of such states as are in equilibrium with the interior of the semiconductor. In the case that the surface charge consists entirely of holes and of charge in acceptor-like fast states, one expects the barrier to be lowered by an amount equal to the lowering of the quasi Fermi level for holes in the interior. This entails a value for the quantity  $d\phi/d\delta$  of  $+\lambda^{-1}$ . In the contrary case of an electron-rich surface the value of  $d\phi/d\delta$  equals  $-\lambda$ .

The data shown in Fig. 1 have been analyzed as follows. The space-charge region contains a (positive or negative) surface excess of holes  $\Gamma_p$  and of electrons  $\Gamma_n$ . The  $\Gamma$ 's are functions of both  $Y$  and  $\delta$ , and their values at a given  $Y$  may be calculated from standard space-charge theory. The charge in fast states  $\Sigma_s$  is taken to be also a function of  $Y$  and  $\delta$ :

$$\Sigma_s = \Sigma_s(Y, \delta) \quad (1)$$

The dependence of  $\Sigma_s$  on  $Y$  has been determined by the field-effect experiment. Now it may be shown that the surface photo voltage depends on all four of the partial derivatives:

$$\begin{aligned} [\partial(\Gamma_p - \Gamma_n)/\partial Y]_{\delta=0}, \quad [\partial(\Gamma_p - \Gamma_n)/\partial \delta]_Y, \\ [\partial \Sigma_s/\partial Y]_{\delta=0} \quad \text{and} \quad [\partial \Sigma_s/\partial \delta]_Y. \end{aligned}$$

Since the first two of these may be calculated,<sup>3</sup> and the third is known from the field effect experiment, the surface photo voltage experiments lead to a measurement of the fourth quantity.

The function  $(\partial \Sigma_s/\partial Y)_{\delta=0}$  depends only on the distribution of the fast states in the energy gap, the function  $(\partial \Sigma_s/\partial \delta)_Y$  depends both on the distribution of fast states and on the ratio of the capture cross-sections. The further interpretation of the experimental results consists of an attempt to deduce both the distribution function and the ratio of capture cross-sections from measurements of these two quantities. The measurements are consistent with a rather uniform distribution of fast states near the center of the gap, as has been discussed in detail in the previous paper. The measurements of  $(\partial \Sigma_s/\partial \delta)_Y$  have been interpreted from the assumption that all states have the same ratio of capture cross-sections.

One may then show that the zeros of  $(\partial \Sigma_s / \partial \delta)_Y$  are given by the equation

$$Y_0 = \ln \lambda + \frac{1}{2} \ln (\sigma_p / \sigma_n) + F(\lambda) \quad (2)$$

where  $\sigma_p$  and  $\sigma_n$  are the cross-sections for transitions to the valence and conduction band respectively, and  $F(\lambda)$  is a known function of  $\lambda$ . From the experimental results shown in Fig. 1 one finds

$$\sigma_p / \sigma_n \sim 150. \quad (3)$$

Since  $\sigma_p$  is found to be considerably greater than  $\sigma_n$ , it is clear that the two conditions of a fast state are negative and neutral rather than neutral and positive, i.e., the surface states are acceptor-like.

Another way of presenting these results is to calculate  $(\partial \Sigma_s / \partial \delta)_Y$  from the experimental data and to plot the derived quantity

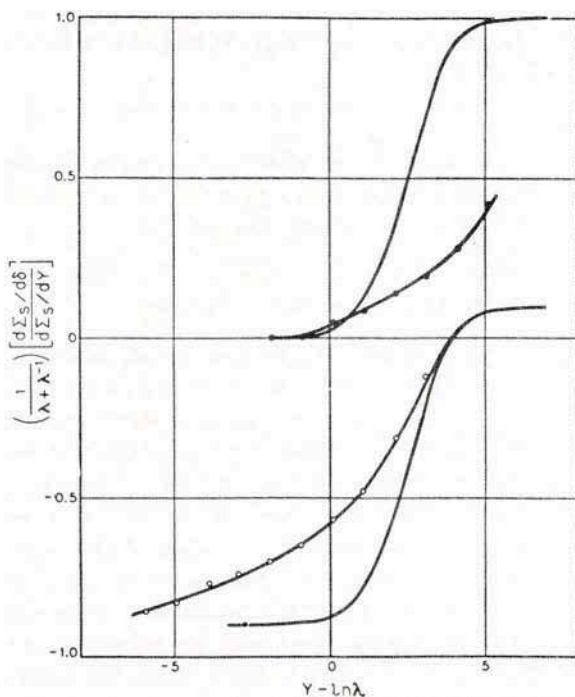


FIG. 2.—Ratio  $(\partial \Sigma_s / \partial \delta)$  to  $(\partial \Sigma_s / \partial Y)$  divided by  $(\lambda + \lambda^{-1})$  vs  $Y - \ln \lambda$ . Solid lines theory, circles and dots with smooth curves through the points are the experimental results for the *n*- and *p*-type samples respectively.



$[(\partial \Sigma_s / \partial \delta) / (\partial \Sigma_s / \partial Y)] / (\lambda + \lambda^{-1})$  vs  $(Y - \ln \lambda)$ , (Fig. 2). The limiting values of this quantity should be  $\lambda / (\lambda + \lambda^{-1})$  and  $-\lambda^{-1} / (\lambda + \lambda^{-1})$  so that the vertical distance between limiting values should be one, independent of  $\lambda$ . The theoretical curves have been drawn to give the best fit between theory and experiment at the points where the ordinates change sign giving the above ratio of  $\sigma_p / \sigma_n$ . The fit between theory and experiment is not quite as good as could be expected in that the magnitude of the experimentally deduced values does not increase with  $Y$  as fast as theory would predict. We shall see later a similar result for the case of surface recombination. Considering the probable accuracy of these results it does not seem appropriate to try to improve the fit by additional theoretical assumptions. The disagreement might be due to non-uniformities in surface potential and with such an assumption one would have enough parameters to fit anything.

The above statements as to the distribution of states must be restricted to the energy range  $\pm 0.1$  volts from the center of the gap. This is because the field effect and surface photo voltage experiments are generally sensitive only to the states lying rather close to the Fermi level under the conditions of the experiment. Figure 3 shows the extremes of surface potential which were accessible in the experiments described above. One does not exclude the possibility of the existence of discrete fast state levels

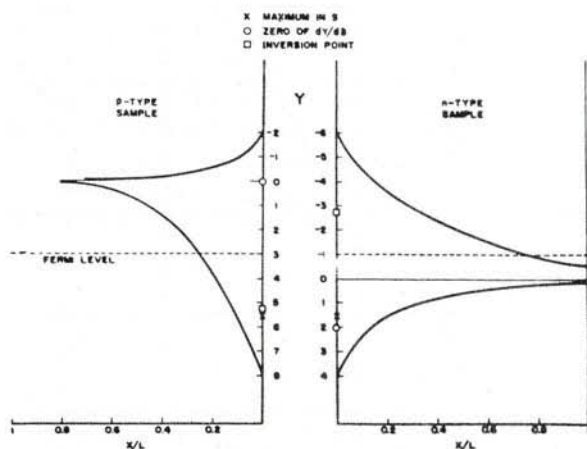


FIG. 3.—Electron energy vs depth for  $n$ - and  $p$ -type samples.

near the conduction or valence band edges, although one can set an upper limit to the density of such states. It is clear, however, from these results and those presented in the previous paper that the measurements in the vicinity of  $Y = 0$  cannot be understood without the postulation of a more or less continuous distribution of fast states near the center of the gap, unless there is considerable surface inhomogeneity.

### III. PHOTO EFFECT: PHOTO CONDUCTIVITY

Measurements have been made of the photo conductivity in thin slices of germanium under the conditions of the experiments reported in the previous paragraph. Measurements have been made of (1) low frequency photo conductivity; (2) the decay time constant in photo conductivity; (3) the modulation of photo conductivity by the application of field. From these measurements, and from simultaneous field effect experiments, it is possible to construct graphs showing the surface recombination velocity  $s$  as a function of  $(Y - \ln \lambda)$  (Fig. 4). The measurements are quoted

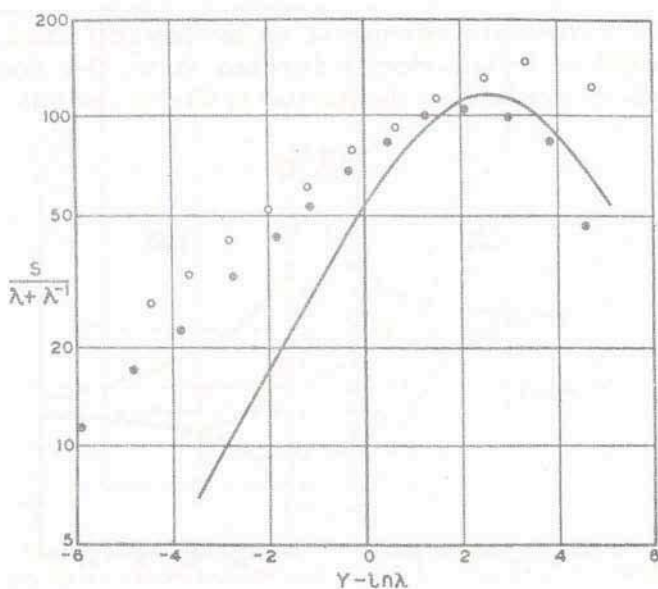


FIG. 4.  $s/(\lambda + \lambda^{-1})$  vs  $Y - \ln \lambda$ .

in terms of the quantity  $s/(\lambda + \lambda^{-1})$ , since it is this quantity, rather than  $s$  itself, which should be the same for all  $\lambda$ , so long as the distribution of surface recombination centers is itself independent of  $\lambda$ . It must be emphasized that Fig. 4 refers to one specific treatment (CP-4 etch) of the surface. Other treatments which have been tried have been found to give rise to quite different variations of  $s$  with  $Y$ , or even no variation at all. The results shown here agree qualitatively with those reported by Many.<sup>4</sup>

The measurements shown in Fig. 4 have been interpreted on the assumption that the surface recombinations centers are identical to the fast states studied in the work of previous sections. One may show that the surface recombination velocity depends on the distribution of fast states, the ratio  $(\sigma_p/\sigma_n)$ , and also on the geometric mean cross-section  $(\sigma_p\sigma_n)^{1/2}$ . Using the distribution of states deduced from the field effect work, and the value of  $(\sigma_p/\sigma_n)$  deduced from the surface photo voltage, one may calculate the geometric mean cross-section, provided one assumes that this quantity is constant for all traps. In this way it is possible to get quite a good fit to the results, as shown in Fig. 4, and to deduce the following values for the cross-sections  $\sigma_p$  and  $\sigma_n$ .

$$\begin{aligned}\sigma_p &\sim 6 \times 10^{-16} \text{ cm}^2 \\ \sigma_n &\sim 4 \times 10^{-17} \text{ cm}^2\end{aligned}\tag{4}$$

The fit, as will be seen from Fig. 4, is not perfect; the maximum in  $s$  comes about where it should, but the experimental values for  $s$  seem to vary more slowly with  $Y$  than one would expect. There are various possible reasons for this discrepancy, such as patchiness of the surface, and under the circumstances the agreement is not too bad. The inherent reasonableness of the estimates of the capture cross-sections lends support to the assumption that the surface recombination centers are indeed the fast states.

#### IV. INJECTION-EXTRACTION EFFECTS

There will be dispersion phenomena in the field effect experiment at any frequency at which the time lag in the transfer of charge between some surface state and the interior is comparable with the reciprocal frequency. The field effect experiment is



usually carried out at a frequency chosen to minimize such dispersion effects; but it is found that these come in at both higher and lower frequencies. Similarly there are dispersion effects in surface photo voltage and photo conductivity experiments. At frequencies lower than those customarily used the dispersion arises from the transfer of the charge into and out from the slow states on the surface. At higher frequencies there are effects arising from the time for minority carriers to recombine; at still higher frequencies one would hope to find time constants specifically associated with the emptying and filling of the fast states.

Other workers<sup>5</sup> have reported that at sufficiently low frequencies the effective mobility measured in the field effect experiment becomes less than at the frequencies customarily used, and have studied the decay of the field-induced conductivity in response to a step change of field. In the present work it has been found that if measurements are made with an ac field, and a dc field is superimposed at a given instant, the range of surface potential covered shifts in the expected direction, but gradually returns over a time of the order of seconds. Removal of the dc field causes an overshoot to occur, followed by a drift back to the original state. Similar effects have been observed in the surface photo voltage experiment in response to a step change in light intensity. It has also been found that application of a sufficiently large ac field may itself shift the surface potential at the point corresponding to zero field. A further study of these processes, in particular relation to the nature of the chemical material on the surface, is clearly of the highest importance in trying to understand the nature and properties of the so-called slow states.

A study has been made of the behavior of the field effect experiment at higher frequencies.<sup>6</sup> Generally it is found that the dispersion effects are small under the conditions that the surface is rich in carriers of the same sign as the majority carrier in the interior. At the opposite extreme of surface potential, dispersion effects are found at frequencies of the order of the reciprocal of the minority carrier lifetime. At low frequencies the effective mobility has a sign corresponding to the minority carrier and a magnitude that is less than that of the minority carrier by an amount governed by the density and distribution of fast states. As the frequency is increased the effective mobility is found to change sign, and

eventually, at sufficiently high frequencies, may reach a value that is even larger than the bulk mobility of the majority carrier. Typical results are shown in Fig. 5. Clearly what is happening is that there is not time, within one cycle, for the charge induced by the applied field to be supplied by minority carriers. The fact that the effective mobility at high frequencies may be larger than the bulk value is at first sight surprising. This behavior is, however, predicted by a quantitative analysis, which may be understood as follows. Consider what would happen if there were

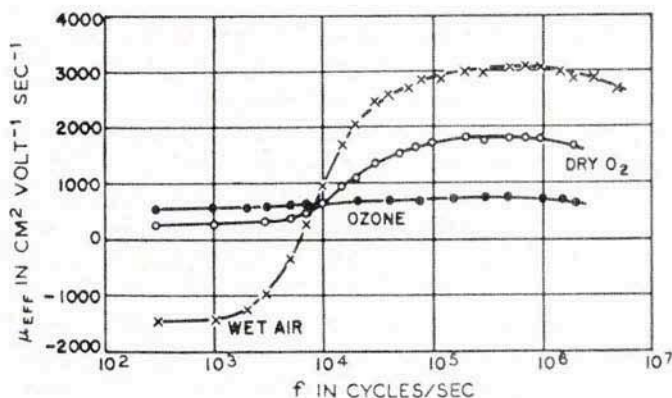


FIG. 5.  $\mu_{eff}$  vs frequency.

no fast surface states. Suppose that we have a  $p$ -type sample, with an  $n$ -type inversion layer. Now apply a field of such a sign and magnitude as to cause removal of one negative charge per unit area of surface. At sufficiently low frequencies, this can take place by the removal of one electron per unit area from the surface inversion region into the interior, followed by recombination of the electron with a hole that has flowed in through the contacts. At the frequencies in question however there is not time for this recombination to occur. Instead therefore of the conductance of the slice having been decreased to the extent of one electron per unit area, we still have the electron, and one extra hole per unit area as well. The effective mobility has therefore changed from  $-\mu_n$  to  $+\mu_p$ . In the case that there are fast states the same thing can happen, with the additional consideration that the electron in question may have come, not from the inversion region, but



from a fast state. If the electron has come from a fast state, the conductance of the sample has increased to the extent of both an extra hole and an extra electron, so that the change in conductance will correspond to an effective mobility of  $(\mu_p + \mu_n)$ .

It is interesting to compare the field effects and photo effects experiments under these conditions. Sudden illumination of the surface causes a change of the barrier height, the quasi Fermi level for minority carriers (electrons) changing by an equal amount. Sudden application of a field also changes the barrier height, but changes the quasi Fermi level for minority carriers by a very much smaller amount: just enough, in fact, to describe the situation in which enough majority carriers have flowed in through the contacts to account for the induced charge.

From the point of view of information as to the fast states, the high frequency field effect experiment is important mainly in that it shows that the time constants for filling and emptying the fast states are shorter than the reciprocal of the highest frequency used. This result is in agreement with the conclusions which may be drawn from the results as to the distribution and cross-sections of the fast states presented in the previous sections. From these one can show that the longest time constant, even under the most critical conditions, should be of the order of  $10^{-6}$  seconds, and that most of the time constants should be very much shorter than this. The interpretation of the field effect experiments at still higher frequencies may be exceedingly complicated, because, in addition to the possible effect of these short trapping constants, one must begin to consider the time required for transfer of charge across distances that are not long in comparison with the thickness of the space charge region.

## V. QUESTIONS, ANSWERED AND UNANSWERED

The experiments reported in this and the preceding paper evidently offer a rather powerful tool for the quantitative investigation of properties of the so-called fast state on semiconductor surfaces. Using these techniques, one obtains a rather complete description of the fast states existing in that part of the gap which is accessible to measurement. Of course we do not know what the fast states are. The fact that, on the surface studied, the fast



states appear to be acceptor type suggests that they may be associated with dislocations, corners, etc. The fact that they are unchanged in the Brattain-Bardeen cycle<sup>2</sup> of gases suggests that they are not associated with easily desorbable atoms. One knows that mechanical damage of the surface increases the density of the fast states, but that there appears to be a perfectly definite lower limit on the density that can be obtained by careful etching techniques.

The information on the slow states is much less clearcut. One knows qualitatively that an oxidizing environment tends to promote a *p*-type surface, the smallest value of  $(Y - \ln \lambda)$  accessible being about  $-5$ . One knows also that a wet environment, particularly in the absence of oxygen, tends to promote an *n*-type surface, with  $(Y - \ln \lambda)$  as large as  $+5$ . Beyond this, nothing is known. One would like to be able to characterize the distribution and cross-section of the slow states in the same way that we have done for the fast states. But one does not even know whether it is sensible to talk about a fixed density of slow states. When one is experimenting on a sample of germanium that is maintained in a gas ambient, there is always the possibility of upsetting the adsorption equilibrium with a gas. Morrison<sup>7</sup> has in fact shown that it is possible to account for the observed spectrum of time constants of the slow states by appealing to the Elowitch adsorption equation. Clearly one would like to have better control of the adsorption chemistry. With this end in view, experiments of the type described in these papers have been started in cooperation with J. T. Law on surfaces cleaned by the Farnsworth technique<sup>8</sup> and maintained in very high vacuum.<sup>9</sup> When such results are obtained, it should be possible to build up a quantitative picture of the effect of various "impurity" materials on the physical properties on the surface, and, through use of the field-effect and photo effect techniques, to arrive at a quantitative description of the "slow states" as well.

#### REFERENCES

1. H. C. Montgomery and W. L. Brown, *Phys. Rev.* (in press). W. H. Brattain and C. G. B. Garrett, *Bell System Tech. J.* (in press). C. G. B. Garrett and W. H. Brattain, *Bell System Tech. J.* (in press).

2. W. H. Brattain and J. Bardeen, *Bell System Tech. J.* **32**, 1 (1953).
3. C. G. B. Garrett and W. H. Brattain, *Phys. Rev.* **99**, 376 (1955).
4. Many, Margoninski, Harnik and Alexander, *Phys. Rev.*, **101**, 1433 and 1434, (1956).
5. G. G. E. Low, *Proc. Phys. Soc. (London)* **B68**, 10 (1955); R. H. Kingston and A. L. McWhorter, *Phys. Rev.* **98**, 1191 (1955); Statz, de Mars, Davis, and Adams, *Phys. Rev.* **101**, 1272 (1956).
6. H. C. Montgomery and B. A. McLeod, *Bull. Am. Phys. Soc.*, **1**, 53 (1956).
7. S. R. Morrison, *J. Phys. Chem.* **57**, 860 (1953).
8. Farnsworth, Schlier, George, and Burger, *J. Appl. Phys.* **26**, 252 (1955).
9. J. T. Law and C. G. B. Garrett, *J. Appl. Phys.* **27**, 656 (1956).

# MEASUREMENTS OF INVERSION LAYERS ON SILICON AND GERMANIUM AND THEIR INTERPRETATION

H. STATZ, G. A. DE MARS, L. DAVIS, JR.,  
and A. ADAMS, JR.

*Research Division  
Raytheon Manufacturing Company  
Waltham, Massachusetts*

## ABSTRACT

Steady-state and nonsteady-state inversion layer conductance on silicon and germanium can be understood in terms of two types of surface states. One type of state is located at the interface of the semiconductor and semiconductor oxide film and is believed to be responsible for the surface recombination of electrons and holes. The other type of state is located at the surface of the oxide with perhaps some states in the oxide film. These states result mainly from adsorbed gas molecules. Depending on the surrounding ambient gas, they are either predominantly of acceptor or donor type and it is principally these states which determine the direction in which the bands at the surface are bent. From steady-state conductance measurements, the thickness of the oxide film on silicon is estimated to be about 10 Å thick. It is possible to determine the number and energy interface states from nonsteady-state inversion layer conductance measurements. For the surface treatments used, the following results were obtained: In silicon, there are states with a density of approximately  $10^{12}$  states/cm<sup>2</sup> about 0.45 v below the middle of the gap and another set of states with a density between  $10^{11}$  to  $10^{12}$  states/cm<sup>2</sup> varying in position between 0.42 to 0.48 v above the middle of the gap. For germanium, only the states in the lower half of the gap have been measured. There is one set of states with a density of approximately  $10^{11}$  states/cm<sup>2</sup> about 0.14 v below the middle of the gap. It is found that high fields across the oxide film can influence the density of those states in silicon lying above the middle of the gap. Anomalies in inversion layer conductance are found when vapors of certain liquids are adsorbed. A possible explanation is discussed.

## I. INTRODUCTION

Inversion layers are thin layers ( $10^{-4}$  to  $10^{-6}$  cm) of semiconductor material just below the surface which have a different conductivity type than the bulk of the material. Thus, a thin *p*-type layer on *n*-type material or a thin *n*-type layer on *p*-type



material will be called an inversion layer. The inversion layers which will be considered in this article result not from a different doping of a thin surface layer but rather from a net electric charge on the surface. Obviously, a net negative charge on an  $n$ -type semiconductor or a net positive charge on a  $p$ -type semiconductor can result in an inversion layer. For example, the negative charge on the surface will repel the free electrons in the conduction band and attract holes in the valence band. A positive charge on  $n$ -type material or a negative charge on  $p$ -type material will only attract more electrons or holes to the surface, respectively; but it will not produce a  $p$ - $n$  junction (Fig. 1). In order to produce an

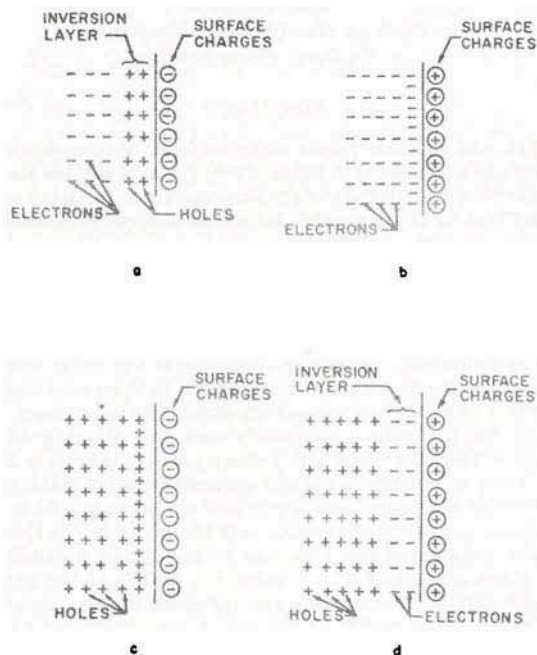


FIG. 1.—Effects of positive and negative surface charges on  $n$ - and  $p$ -type semiconductors.

inversion layer, the charge must exceed a minimum amount which, in general, will depend on the concentration of the doping material.

This net negative or positive charge usually results from electrons or holes bound in localized quantum states at the surface

of the material (so-called surface states). However, it is also possible to produce inversion layers by bringing a charged condenser plate near the surface (field effect). Due to a slow change in the occupancy of the surface states, the effect of this charged plate is slowly screened out and the inversion layer disappears in time (of the order of a fraction of a second to one hour). In this paper, field-induced inversion layers will not be discussed. The existence of an inversion layer is, therefore, determined by the densities of acceptor and donor type surface states and their energy levels. From measurements of the conductance of inversion layers, information can be obtained about the various types of surface states. The results obtained by this method are summarized.

In the bulk of germanium and silicon, a great number of localized energy states have been found which were due to various doping elements and lattice defects. A great variety of levels should be found at the surface, probably even more than in the bulk.

Germanium and silicon are usually covered by an oxide film unless special precautions are taken. Thus, there is a true surface on the oxide and an interface between the bulk material and the oxide. First, consider the interface where the semiconductor and semiconductor oxide lattice join. At present, it is not known whether the oxide crystallizes in its own configuration or in a lattice imposed by the underlying material. If there were an ideal joining of the two lattices, both having the same lattice constant, then it would be possible in principle for Tamm-like states to exist.<sup>1,2</sup> In quantum mechanics, these states correspond to wave functions exponentially damped into the semiconductor and into the oxide film. The existence of such waves depends critically on the potential in both lattices and at the interface. No general prediction of the states can be made. However, because of the two-dimensional periodicity in the plane of the interface, it can be concluded, as in the case of a two-dimensional metal, that there are as many independent wave functions for each spin as there are unit cells at the interface. Thus, there should be a density of interface states in silicon and germanium of the order of  $10^{15}/\text{cm}^2$ . As yet, no such states have been observed. If the two lattices do not join continuously, there may be lattice defects located at the interface which result in localized states. If the oxidation theory of Cabrera and Mott<sup>3</sup> applies, then there should be vacancies,

i.e., missing atoms, in the surface layer of the semiconductor which are the result of atoms pulled into the oxide film under the action of an electric field. The electric field is due to negative oxygen atoms on the surface of the oxide. In experiments in this laboratory, evidence has been found for such a mechanism. Some of the results will be given below. In the interface, there may be atoms from the etching solution which have been trapped by the growing oxide film. At the present time, it seems that some of the interface states can be explained by the latter mechanism. It should be mentioned that interface states will be important in the recombination processes of electrons and holes because of their physical proximity to the semiconductor.

The oxide film may be imperfect and have interstitial semiconductor atoms.<sup>3</sup> These interstitial atoms should be mobile and their number and position should depend on the electric field strength across the film. Effects ascribable to such a mechanism have been observed.

The surface of the oxide film could also give rise to Tamm-like states. However, from the experimental results, it appears that the amount and the sign of the charge depend critically on the surrounding ambient gas. This indicates that these surface states are induced by adsorbed gas atoms and that there are no Tamm-like states. Adsorbed gas atoms on the surface<sup>3,4</sup> act quantum mechanically much like impurity atoms in the interior of the crystal and will, in general, give rise to localized electronic states. If there is a complete monomolecular layer of adsorbed gas atoms, then there will be interactions between neighboring atoms, and surface energy bands will be formed as in a two-dimensional metal. These surface energy bands belong to electrons moving in the layer of adsorbed material. As long as the energy of these states is in forbidden zones of the underlying semiconductor, the wave functions will be damped exponentially into the semiconductor. If these surface energy bands are only partly filled, surface conduction can be expected. It now appears that this type of conduction is present if the layer of adsorbed material is coherent and sufficiently thick, as in the case of several adsorbed liquids, especially water.<sup>5</sup> Adsorption measurements for water vapor<sup>6,7,8</sup> indicate that at 100 percent humidity, there are many layers of adsorbed water on either silicon or germanium.



In order to create an inversion layer, the surface must have a net charge. The only surface states that are readily influenced are those due to adsorbed surface atoms. In Table I, materials are listed which are known to give surface charges.<sup>5,9,10,11</sup>

TABLE I  
SOME MATERIALS WHICH GIVE SURFACE CHARGES  
UPON ADSORPTION

POSITIVE CHARGES	NEGATIVE CHARGES
Ammonia <sup>6,10,11</sup>	Boron Trifluoride <sup>9</sup>
Acetone Vapor <sup>6</sup>	Ozone
Water Vapor	Oxygen
Dioxane Vapor <sup>6</sup>	Chlorine <sup>11</sup>
Pyridine Vapor <sup>6</sup>	
Methyl Alcohol Vapor	

The molecules giving positive charges must introduce energy levels in the vicinity of but not too far below the normal position of the Fermi level (Fig. 2a) which are filled in the neutral atom. The condition corresponding to an atom adsorbed on the surface, which tends to become negatively charged, is shown in Fig. 2b. In this case, the molecule must introduce a level in the vicinity of the normal position of the Fermi level at the surface. This level is slightly above the Fermi level and is empty in the neutral molecule.

## II. EXPERIMENTAL PROCEDURES

Channel conductance has been studied and inversion layers across base regions of *n-p-n* or *p-n-p* structures have been investigated.<sup>10,12-16</sup> Measurements by Brown<sup>12</sup> were made with an impedance bridge. However, a direct reading set-up (Fig. 3) first used by Kingston<sup>13,14</sup> is preferable, especially for transient measurements.<sup>10,15,16</sup>

In the measurements by Brown,<sup>12</sup> the *n-p-n* germanium grown junction transistors were encapsulated in plastic. The inversion layers on these units are due to water vapor adsorbed on the surface. Kingston<sup>13,14</sup> made his studies on bare *n-p-n* germanium junction transistors which were etched in hydrofluoric acid and after washing, exposed to a cycle of wet oxygen and wet nitrogen.

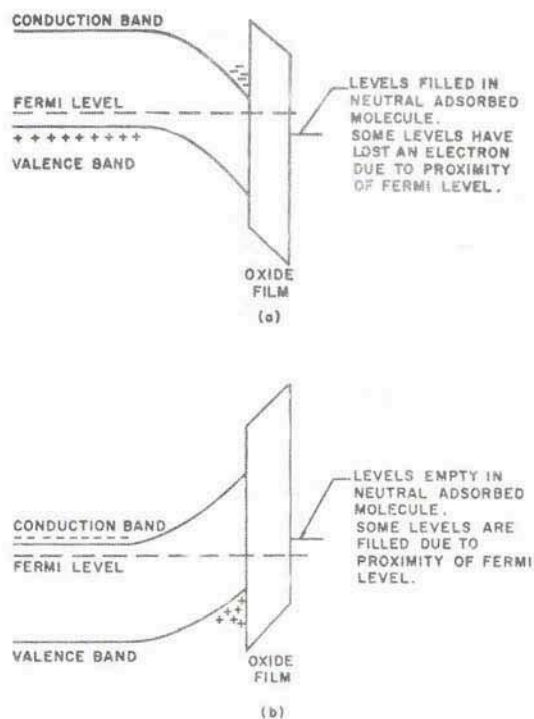


FIG. 2.—Energy bands at surface with adsorbed molecules giving (a) donor type surface states, and (b) acceptor type surface states.

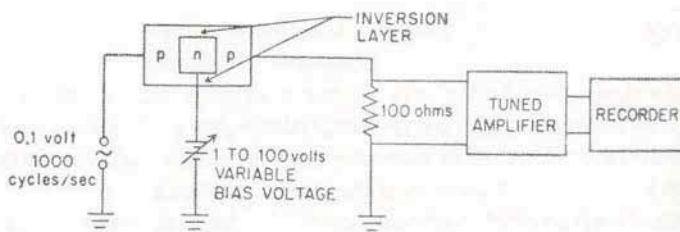


FIG. 3.—Diagram of circuit used to measure conductance of inversion layers as a function of bias voltage.

After stabilization of the inversion layer, conductance measurements were made in either nitrogen or oxygen at various relative humidities. In this laboratory, both germanium  $p$ - $n$ - $p$  and silicon  $n$ - $p$ - $n$  and  $p$ - $n$ - $p$  bars were etched in CP-4 and carefully washed. To produce an inversion layer on the base region of either germanium or silicon  $p$ - $n$ - $p$  bars, the units were oxidized in a mixture of wet oxygen and ozone and then exposed to dry oxygen or ozone. In order to produce an inversion layer on the base region of an  $n$ - $p$ - $n$  silicon bar, the samples were exposed to dry ammonia either immediately after washing or after oxidation in wet oxygen and ozone. Water vapor can also be used to create an inversion layer; however, side effects are present.<sup>5-8</sup>

### III. FORMULAS FOR INTERPRETATION OF INVERSION LAYER MEASUREMENTS

Brown<sup>12</sup> has shown that it is possible to calculate from the conductance of the inversion layer, the total charge in the surface states and the position of the quasi Fermi level. In the following, formulas are given which apply to inversion layers on  $n$ -type material;<sup>10</sup> however, by a suitable change in the subscripts they also hold for inversion layers on  $p$ -type material.

The energy bands near the surface are shown in Fig. 4. A voltage  $V_a$  is applied between the  $p$ -type inversion layer and the underlying  $n$ -type semiconductor; no single Fermi level exists and the semiconductor is described by two quasi Fermi levels  $-q\phi_n$  and  $-q\phi_p$ .  $\phi_n$  is approximately constant in the  $n$ -type region and  $\phi_p$  is constant in the inversion layer region.

The conductance  $g$  of a square of the inversion layer is given by

$$g = q\mu_p p, \quad (1)$$

where  $q$  is the electronic charge,  $\mu_p$  is the average mobility of the holes in the inversion layer, and  $p$  is the number of holes per  $\text{cm}^2$  of  $p$ -type skin. The mobility depends on the width of the inversion layer because the mean free path of holes is of the order of the thickness of this layer and a large amount of scattering occurs at the surface.  $\mu_p$  has been calculated by Schrieffer<sup>17</sup> under the assumption of diffuse scattering at the surface,  $\mu_p$  is a function of



the applied voltage  $V_a$ , the position of the quasi Fermi level  $\phi_s$  (Fig. 4) with respect to the middle of the band, and the charge density  $\rho_d$  arising from ionized donor atoms. The quantity  $p$  can be shown<sup>10</sup> to lie between the following limits

$$\begin{aligned}
 & (\epsilon/2\pi)^{\frac{1}{2}}(1/q)\{\rho_d(|V_a| + |\psi_n| + |\phi_s| - kT/q) \\
 & \quad + (kT/q)q n_i \exp(q|\phi_s|/kT)\}^{\frac{1}{2}} \\
 & - (\epsilon/2\pi)^{\frac{1}{2}}(1/q)\{\rho_d(|V_a| + |\psi_n| + |\phi_s| - kT/q) + (kT/q)q n_i\}^{\frac{1}{2}} < p < \\
 & (\epsilon/2\pi)^{\frac{1}{2}}(1/q)\{\rho_d(|V_a| + |\psi_n| - kT/q) \\
 & \quad + (kT/q)q n_i \exp(q|\phi_s|/kT)\}^{\frac{1}{2}} \\
 & - (\epsilon/2\pi)^{\frac{1}{2}}(1/q)\{\rho_d(|V_a| + |\psi_n| - kT/q) + (kT/q)q n_i\}^{\frac{1}{2}}. \quad (2)
 \end{aligned}$$

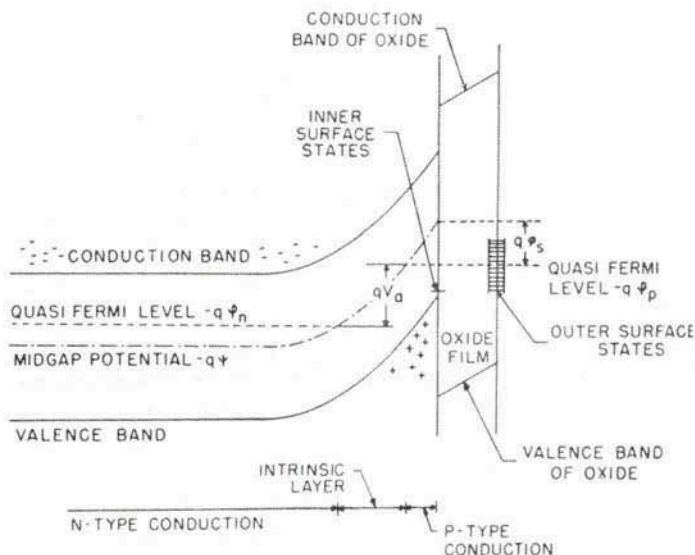


FIG. 4.—Energy band and surface state structure at semiconductor surface.

In the following,  $p$  can be represented by either limit since they are so close together.  $\epsilon$  is the dielectric constant,  $k$  is Boltzmann's constant,  $T$  is the absolute temperature,  $n_i$  is the intrinsic density of electrons or holes, and  $\psi_n$  is defined by

$$\rho_d = q n_i \exp(q|\psi_n|/kT). \quad (3)$$

The absolute magnitude signs have been introduced so that the formula can be used without checking whether the various quantities are positive or negative in their definitions.

From Schrieffer's work and Eq. (2) it can be seen that  $g$  is a function of  $\rho_d$ ,  $V_a$ , and  $\phi_s$ . Thus, for a given crystal, i.e., for a given  $\rho_d$ ,  $g$  depends only on  $V_a$  and  $\phi_s$ . For practical applications, it has been found useful to plot  $g$  as a function of  $\phi_s$  for a series of  $V_a$  values. For a measured conductance value, the corresponding value of  $\phi_s$  can be obtained from these graphs. The total charge in the surface states is given by

$$Q = -(\epsilon/2\pi)^{\frac{1}{2}} \{ \rho_d (|V_a| + |\psi_n| + |\phi_s| - kT/q) + qn_i(kT/q) \exp(q|\phi_s|/kT) \}^{\frac{1}{2}}. \quad (4)$$

For  $n$ -type inversion layers on  $p$ -type material,  $Q$  is positive. It is useful to plot  $Q$  as a function of  $\phi_s$  for the same set of bias voltages used above. By this method, a large number of experimental curves can be evaluated.

#### IV. STEADY-STATE INVERSION LAYER CONDUCTANCE

The first measurements on inversion layers were carried out by Brown.<sup>12</sup> Most of his experiments were made at dry-ice temperatures. Brown observed that the conductance goes to zero at a certain voltage, i.e., the inversion layer pinches off. It is now believed that this pinch-off is not present in steady-state conductance measurements. At low temperatures, the time necessary to reach an equilibrium value of conductance may have been long compared with the time required to measure the conductance of the inversion layer as a function of bias voltage. Steady-state inversion layer conductance measurements have been reported by Kingston.<sup>13,14</sup> For inversion layers which have a relatively low conductance, Kingston finds that their conductance varies approximately as  $1/V_a$ . Kingston interprets this result by assuming  $\phi_s$  to be constant and independent of the applied voltage. Measurements in this laboratory<sup>10,15,16</sup> have shown that such a result is obtained quite generally. In Figs. 5, 6, and 7, results are shown for  $p$ -type inversion layers on  $n$ -type (8 ohm-cm) germanium.

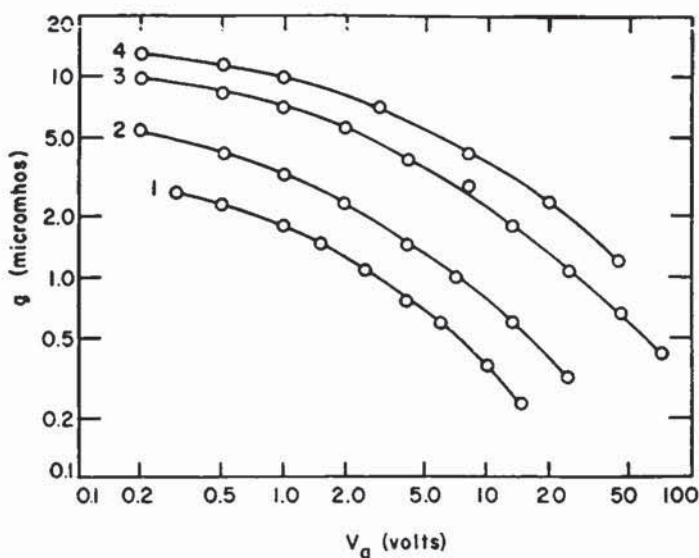


FIG. 5.—Steady-state conductance of  $p$ -type inversion layers on  $n$ -type germanium versus bias voltage.

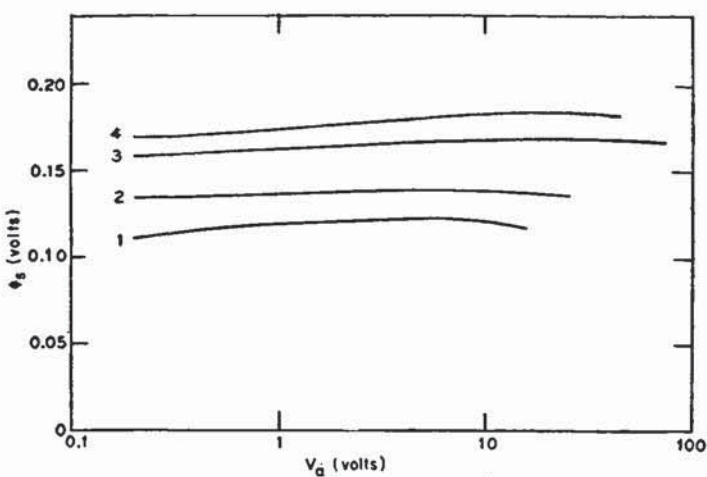


FIG. 6.—Position of quasi Fermi level versus bias voltage for the steady-state conductance measurements of Fig. 5.



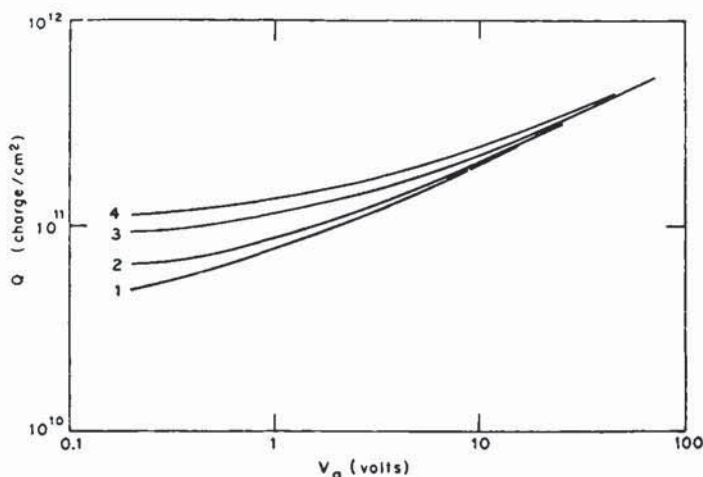
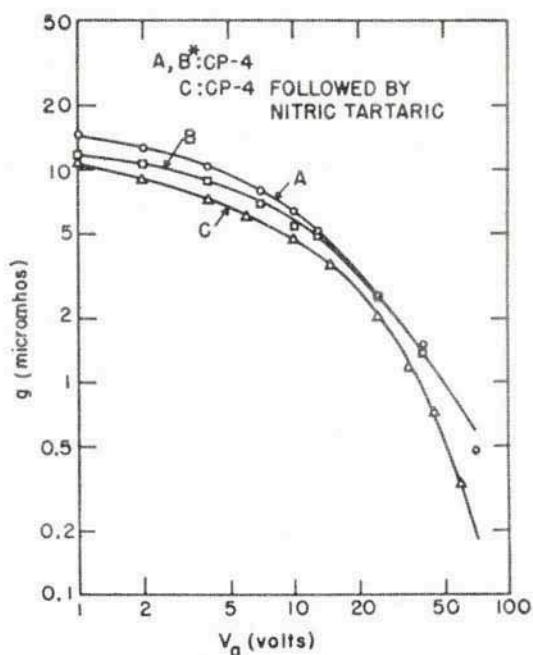


FIG. 7.—Total charge in surface states versus bias voltage for the steady-state conductance measurements of Fig. 5.

Figure 5 shows steady-state conductance curves for four different inversion layers. In general, the inversion layer conducts better for a longer exposure to wet oxygen and ozone in the surface treatment. The position of the quasi Fermi level with respect to the middle of the band, i.e.,  $\phi_s$ , as a function of bias voltage is shown in Fig. 6. In Fig. 7, the total charge as a function of the bias voltage is given. It can be seen that  $\phi_s$  is approximately constant and independent of the bias voltage and that the charge in the surface states increases considerably as the bias voltage increases. Thus, the quasi Fermi level for holes  $-q\phi_p$  must determine the occupancy of the surface states and the total density of all the surface states is high. The small deviations of  $\phi_s$  from a constant value are probably within experimental error or within the accuracy expected from the theoretical calculations of the mobility.<sup>17</sup>

In Figs. 8, 9, and 10, corresponding results are shown for a *p*-type inversion layer on *n*-type (1.1 ohm-cm) silicon. The results are very similar to those found for *p*-type inversion layers on *n*-type germanium. It is seen that the deviations of  $\phi_s$  from a constant are somewhat larger.

No explanation can be given for the small increase in  $\phi_s$  at low



\* Temperature for B 5°C above room temperature.

FIG. 8.—Steady-state conductance of *p*-type inversion layers on *n*-type silicon versus bias voltage.

voltages which may result from the above-mentioned assumptions in the theory of mobility in space-charge regions. The decrease of  $\phi_s$  with  $V_g$  can be explained. For a finite density of surface states,  $\phi_s$  decreases with increasing charge in the surface states. As will be shown later, the relatively large density of states arises mainly from states at the surface of the oxide. Consider, for example,  $N$  levels of the same energy located  $\Delta$  (volts) above the middle of the gap such that the levels are far from the quasi Fermi level. Suppose that there is no net charge arising from these states when they are empty; then, the charge per unit area becomes

$$Q = -qN \exp(-q(\Delta + \phi_s)/kT). \quad (5)$$

In order to increase the total charge by a factor  $e$ , the quantity  $\phi_s$  must decrease by  $kT/q$  ( $\approx 1/10$  volt). From Figs. 9 and 10, the

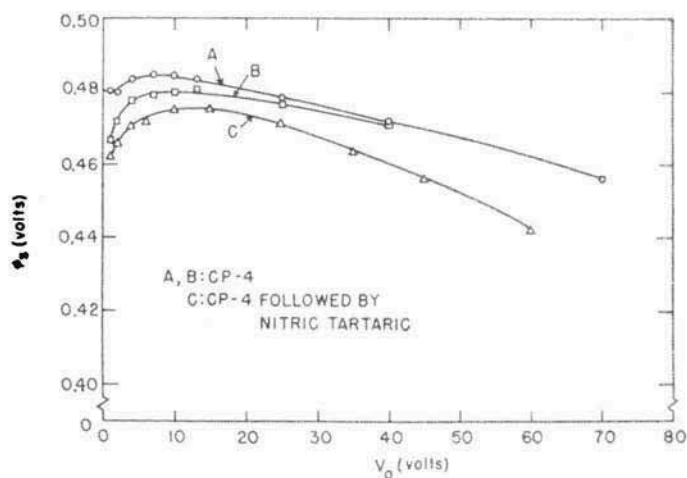


FIG. 9.—Position of quasi Fermi level at surface versus bias voltage for the steady-state conductance measurements of Fig. 8.

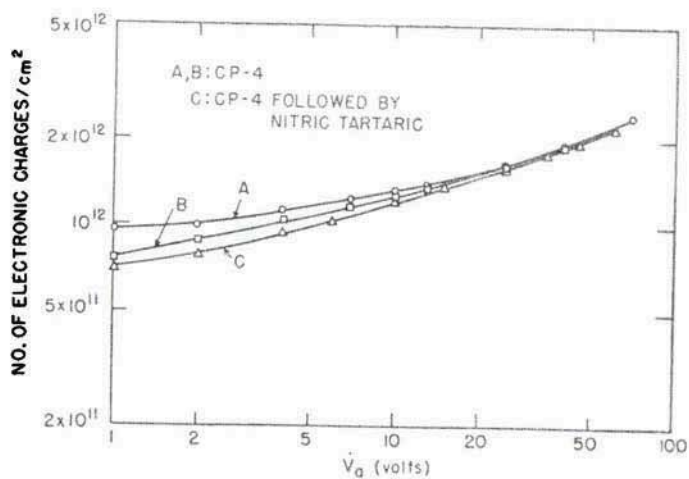


FIG. 10.—Total charge in surface states versus bias voltage for the steady-state conductance measurements of Fig. 8.



changes in charge over the measured bias range are the order of  $e$  and the changes in  $\phi_s$  are the order of  $kT/q$ . In spite of the apparent agreement, the situation is probably not quite that simple. It is very likely that there is not just one type of level and that the Fermi level is fixed in a given position more tightly than indicated by Eq. (5), i.e., the net charge changes much more than by a factor  $e$  for a change in  $\phi_s$  of  $kT/q$ . This is indicated by the following consideration. The large density of states is at the surface of the oxide. As the charge in these outer surface states changes, the electric field strength in the oxide film and the potential drop across the oxide film also change. As can be seen from Fig. 11, if the Fermi level is fixed with respect to the outer surface

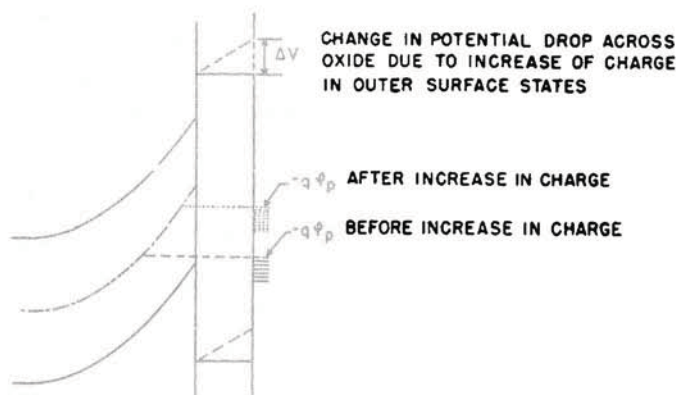


FIG. 11.—Diagram of change in potential drop across oxide film resulting from change in charge in outer surface states.

states,  $\phi_s$  must decrease when the charge increases. This latter effect is added to that arising from a finite density of states of the oxide surface. Thus, an upper limit for the thickness of the oxide film can be obtained by attributing all the decrease in  $\phi_s$  to a potential drop across the oxide film. In Fig. 12, the potential drop  $\Delta V$  across the oxide is added to  $\phi_s$ . As can be seen from Fig. 11, a constant value for  $\phi_s$  is expected. To obtain Fig. 12, an oxide film of 10 Å thickness and a dielectric constant of 3.78 (fused quartz) has been assumed.

Some of the change in total charge occurs in states located at the interface because the position of the Fermi level has been

shifted slightly. In determining this contribution and correcting for it, use is made of the knowledge of the interface states described below. The potential drop is arbitrarily set equal to zero at the right-hand edge of the  $\phi_s$  curve (Fig. 12). Since 10 Å is a reasonable figure for the thickness of the oxide film, there should be only a negligible contribution to the decrease of  $\phi_s$  resulting from a finite density of states. The sample shown as curve C in

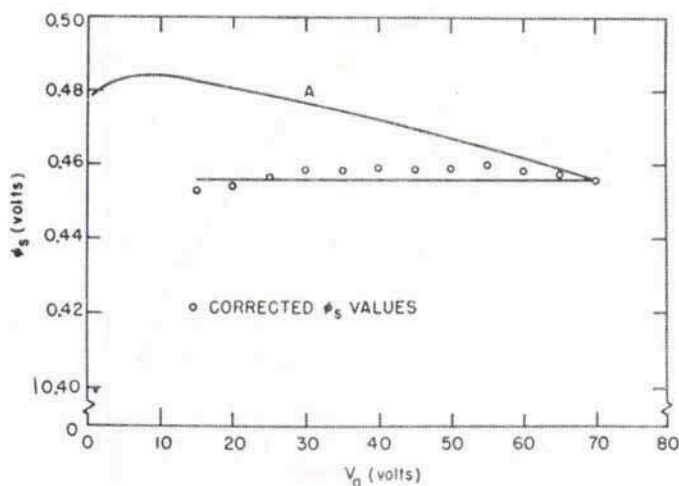


FIG. 12.—Quasi Fermi level for silicon (run A, Fig. 9) corrected for potential drop in oxide film.

Fig. 9 has been further oxidized in nitric and tartaric acids and the upper limit for the thickness of the oxide film is larger than 10 Å.

In Figs. 13 to 15, the corresponding results for conductance measurements on an *n*-type inversion layer on *p*-type (11 ohm-cm) silicon are shown. In the present notation,  $\phi_s$  is always assumed positive since no confusion can arise as to which direction the bands are bent. The same general conclusions can be drawn for the measurements on *n-p-n* silicon bars as for the corresponding structures discussed above. In curve B of Fig. 14,  $\phi_s$  was corrected by again assuming an oxide film of 10 Å. The surface was first oxidized in wet oxygen and ozone and then exposed to

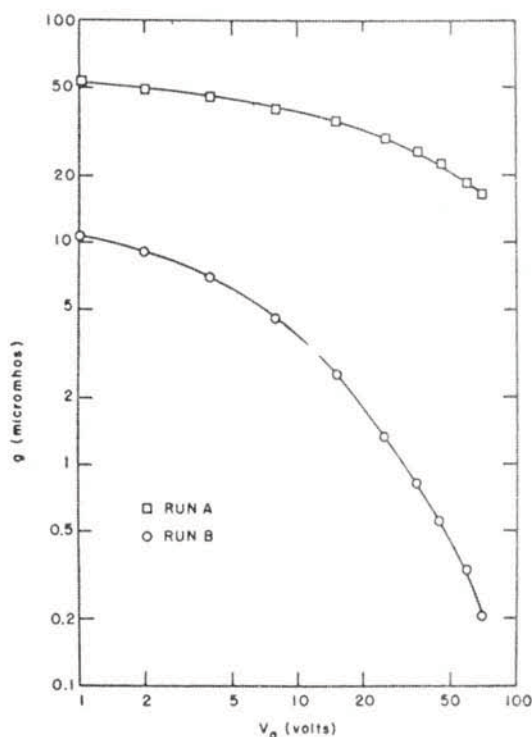


FIG. 13.—Steady-state conductance of  $n$ -type inversion layers on  $p$ -type silicon versus bias voltage.

dry ammonia. Thus, the oxide film thickness is expected to be similar to that for inversion layers on  $n$ -type silicon. For curve *A* of Fig. 14, the surface was etched and then immediately exposed to dry ammonia. No correction for the thickness of the oxide film has been made for curve *A*, but it is evident that the upper limit for the thickness of the oxide film for curve *A* must be smaller than for curve *B*.

#### V. NONSTEADY-STATE INVERSION LAYER CONDUCTANCE

For all inversion layer measurements, transients were observed when the bias voltage was switched from one value to another. This is shown schematically in Fig. 16. In Fig. 17, the total charge  $Q$  in the surface states is shown as a function of time.



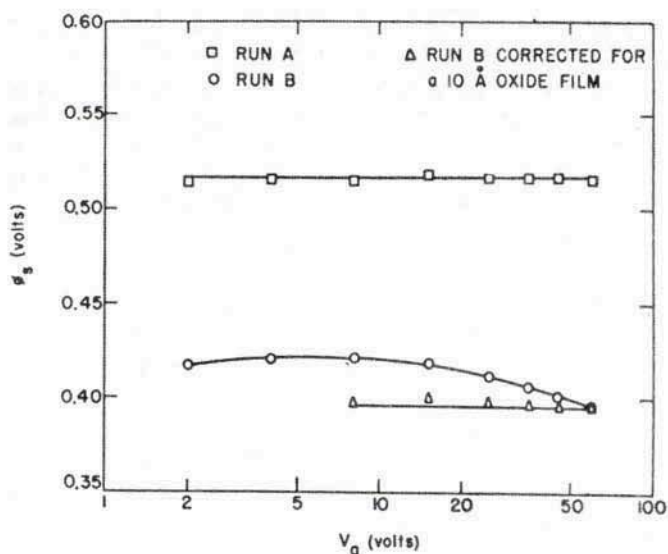


FIG. 14.—Position of quasi Fermi level versus bias voltage for the steady-state conductance measurements of Fig. 13.

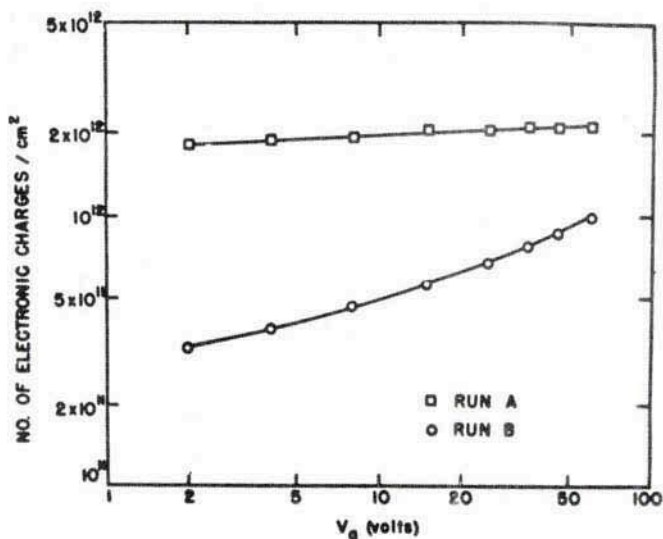


FIG. 15.—Total charge in surface states versus bias voltage for the steady-state conductance measurements of Fig. 13.

The first sharp rise or drop could not be measured with the present equipment but appeared to be of the order of the lifetime of minority carriers in the sample. The relatively long time in which the new conductance or charge value was approached was found

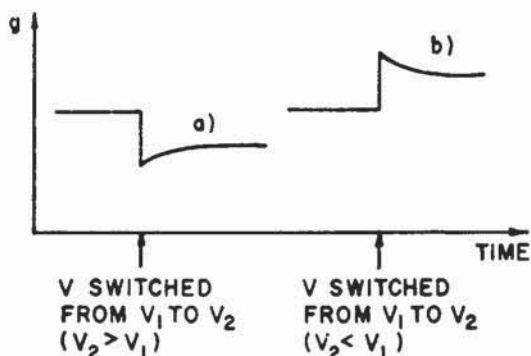


FIG. 16.—Conductance of inversion layer versus time.

to be a function of the surface treatment. In general, oxidation made this period of time longer. For well oxidized surfaces in dry atmospheres, the time constants were of the order of seconds to minutes for germanium and seconds to one hour for silicon. For the longer transients, the curves for conductance and charge

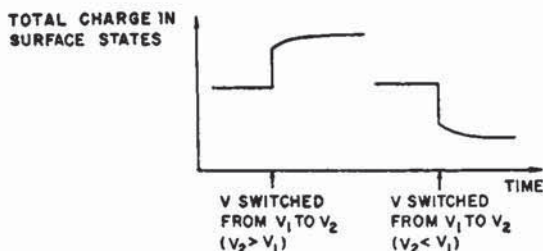


FIG. 17.—Total charge in surface states versus time.

as a function of time apparently have a single time constant; however, for very thin oxide films and wet samples there appears to be a distribution of time constants.<sup>18</sup> For the short transient, there seems to be no appreciable variation in the time constants with temperature;<sup>18</sup> however, for the longer transients, a time constant of the form  $\exp(u/kT)$  was observed.<sup>10</sup> As will be shown

below, the type of the transient is determined by the mechanism of charge transfer through the oxide film. This mechanism is not clearly understood and more work must be done on it.

The curves of Figs. 16 and 17 are interpreted in terms of two types of surface states; the "fast" states are located at the interface of the semiconductor and the semiconductor oxide and the "slow" states at the surface of the oxide and possibly in the oxide film. The "fast" states are responsible for the surface recombination.

Due to the difference in the time constants of the two types of states, it is possible to investigate the "fast" states separately. For this purpose, the conductivity as a function of bias voltage was recorded in a short enough period of time that the charge in the "slow" states was constant but in a long enough period of time so that the "fast" states were in equilibrium with the bulk of the material. For silicon with the long time constant, measurements were made on an x-y recorder and a curve traced in about 10 seconds (conductance as a function of bias voltage). For silicon with the shorter time constant and for germanium, the measurements were taken point by point. For example, from a steady-state conductance value with a bias voltage of 3 volts, the voltage was switched to 5 volts and the conductance recorded immediately after switching; equilibrium was restored at 3 volts, and then the voltage was switched to 7 volts, etc. Curves obtained for *p*-type inversion layers on *n*-type germanium are shown in Fig. 18. The charge in the outer surface states is assumed to be constant along such curves.

For the nonsteady-state curves, "pinch-off" is reached at some voltage. At this point, the quasi Fermi level  $-q\phi_p$  can be considered to be close to the middle of the gap. (An exact description of pinch-off will not be considered here.) It was found that the quasi Fermi level describes the occupancy of the interface states as has been predicted theoretically.<sup>19</sup> From the curves of Fig. 18, it is possible to obtain the total charge in the surface states as a function of  $\phi_s$ . To eliminate the constant charge in the outer surface states, the charge in all surface states at pinch-off is subtracted from the charge obtained at an arbitrary  $\phi_s$  value. If there are no interface states in the vicinity of the middle of the gap, then by this procedure it is possible to obtain for *p-n-p* type



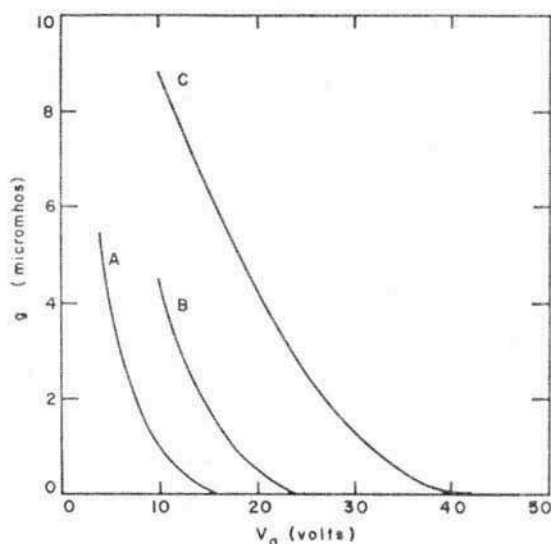


FIG. 18.—Conductance of *p*-type inversion layers on *n*-type germanium when bias voltage is varied from low to high values in a short time.

structures the charge arising from holes in states in the lower half of the gap and for *n-p-n* type structures the charge arising from electrons in states in the upper half of the gap. In Fig. 19, the

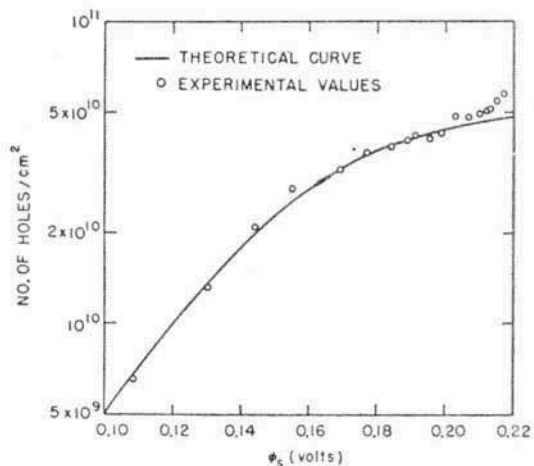


FIG. 19.—Number of holes in inner surface states in lower half of gap versus the position of the quasi Fermi level for germanium.

number of holes in the interface states of germanium in the lower half of the gap is plotted as a function of  $\phi_s$  as calculated from curve C of Fig. 18. The theoretical curves of Fig. 18 are for one level at 0.138 v below the middle of the gap. (More accurately, by the middle of the band we mean that position at which the Fermi level would lie if the semiconductor were intrinsic.) For the effective masses and energy gap as quoted by Herman,<sup>20</sup> an energy of 0.175 v above the valence band is obtained. The number of holes  $p_{is}$  in these interface states as a function of  $\phi_s$  is assumed to be

$$p_{is} = N_s / [1 + 2 \exp \{q(|\phi_L| - |\phi_s|)/kT\}]. \quad (6)$$

Here,  $N_s$  is the number of states and  $\phi_L$  is the position of the state with respect to the middle of the gap. The factor of 2 is a result of the assumption that each level can only be occupied by one electron of either plus or minus spin but not by two electrons with plus and minus spin. For the curves in Fig. 19,  $N_s$  ranges from  $5 \times 10^{10}$  to about  $10^{11}$  states/cm<sup>2</sup>.

From similar experiments with *p-n-p* type silicon bars curves of the type shown in Fig. 20 were obtained. Again a single level

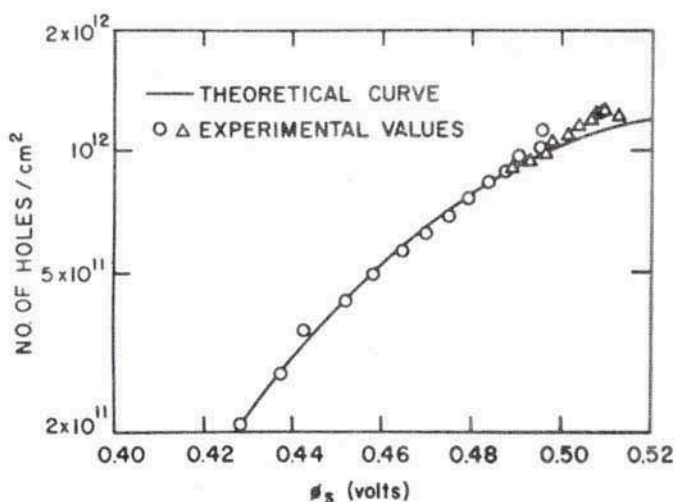


FIG. 20.—Number of holes in inner surface states in lower half of gap versus the position of the quasi Fermi level for silicon.

describes the observed behavior satisfactorily. The energy level lies about 0.455 v below the middle of the gap or 0.117 v above the valence band for the parameters quoted by Herman<sup>20</sup> but using a band gap of 1.17 v.<sup>21</sup>  $N_s$  is  $1.4 \times 10^{12}$  states/cm<sup>2</sup>.

In Fig. 21, the number of electrons in interface states in the upper half of the gap of silicon is shown as deduced from inversion

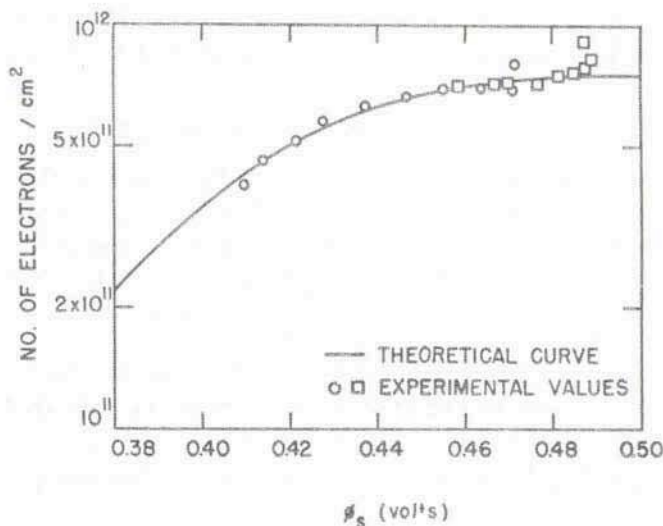


FIG. 21.—Number of electrons in interface states in upper half of gap versus the position of the quasi Fermi level for silicon.

layer measurements on  $n$ - $p$ - $n$  bars. The solid line shows the Fermi distribution function

$$n_{is} = N_s / \{1 + \frac{1}{2} \exp [q(|\phi_L| - |\phi_s|)/kT]\}. \quad (7)$$

Here,  $n_{is}$  is the number of electrons/cm<sup>2</sup> in the interface states,  $|\phi_s|$  is the distance by which the quasi-Fermi level lies above the middle of the gap, and  $|\phi_L|$  is the position of the interface states in the upper half of the gap with respect to the middle of the gap. The factor  $\frac{1}{2}$  in Eq. (7) is due to the assumption that the interface levels can be occupied by one electron with plus or minus spin but not by two electrons. In Fig. 21,  $N_s = 7.8 \times 10^{11}$  states/cm<sup>2</sup> and  $\phi_L = 0.42$  v, i.e., a level 0.178 v below the conduction band. In



Fig. 21, the surface treatment consisted of etching the sample and exposing it immediately after washing to dry ammonia. In Fig. 22, the surface was oxidized in wet oxygen and ozone before being exposed to dry ammonia. In Fig. 22,  $N_s = 1.4 \times 10^{12}$  states/cm<sup>2</sup> and  $\phi_L = 0.48$  v (0.118 v from conduction band). In this sample, oxidation seemed to increase the density of interface

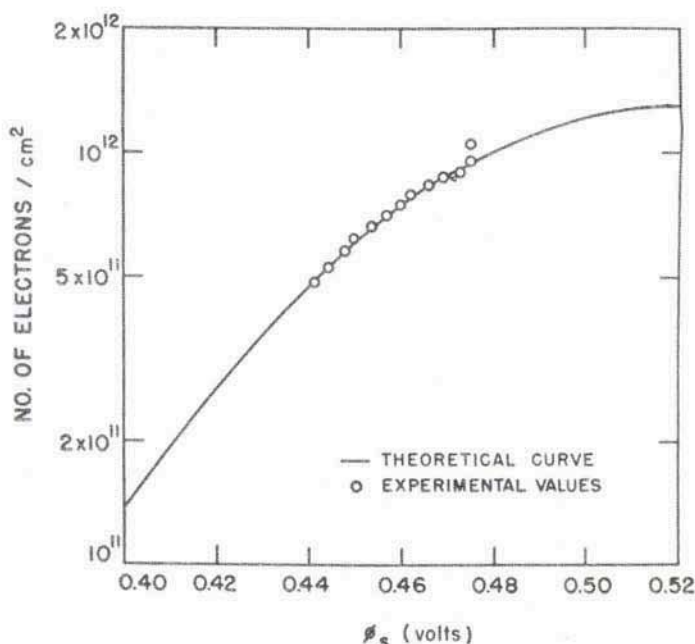


FIG. 22.—Number of electrons in the interface states in upper half of gap versus the position of the quasi-Fermi level for silicon, after oxidation.

states and also shifted the energy of the levels toward the conduction band. Figures 21 and 22 were computed from conductance curves which had the same equilibrium conductance. The "pulsed" conductance curves covered the same range in conductance values and also had the same starting point. Therefore the difference is real, provided the surface was homogeneous. A second sample was investigated in which the density and the energy of the states varied somewhat, depending upon equilibrium conductance of the inversion layer. The energy level before oxidation was found

to be about  $\phi_L \approx 0.42$  v with  $N_s \approx 2 \times 10^{11}$  states/cm<sup>2</sup>. Upon oxidation, little change in energy and density was found. However, from other experiments to be described below, it is evident that changes pertaining to these levels occur during oxidation and also when high fields exist across the oxide film.

## VI. SOME ADDITIONAL EXPERIMENTS AND THE PHYSICAL ORIGIN OF THE RECOMBINATION STATES

The steady-state charge on the oxide surface increases as the bias voltage is increased (Figs. 7, 10, 15). It is thus possible to make the field strength across the oxide film very large. For  $2 \times 10^{12}$  electronic charges/cm<sup>2</sup> on the surface of the silicon oxide, the field strength across the oxide film is approximately  $10^6$  volts/cm. Experimentally, it was observed that changes occur in the oxide film and in the surface energy level structure.<sup>22</sup> So far, such changes have only been observed when the surface was oxidized for some time in wet oxygen and ozone. No effects from the field were observed when the surface was exposed to dry ammonia immediately after etching. First consider a *p-n-p* type structure which has been treated to produce an inversion layer over the base region. In these experiments, when the voltage was raised to 70 to 100 volts for silicon (11 ohm-cm base region), the conductivity of the inversion layer decayed—fast for the higher voltages and slower for the lower voltages. However, the entire charge did not disappear because if the bias voltage was decreased to some low value there was still a measurable conductance. After the “breakdown,” there was no measurable change in the density and the energy parameter of the states in the lower half of the gap. Inhomogeneities in the channel after such a treatment have been observed; thus it was difficult to establish such small changes.

The results for *n*-type inversion layers on *p*-type silicon, i.e., *n-p-n* structures, were different. A decay of the conductance at high bias voltages was also found; however, there was a large change in the density of the interface states in the upper half of the gap. The states in the upper half of the gap seemed to have disappeared completely. Experimental runs before and after application of a high field are shown in Fig. 23. If the voltage was

kept at a low value, the density of the states slowly built up again from minutes to hours. The very low densities seen immediately after the application of the high field are obtained by subtracting two large quantities and the errors are therefore very large. Apparently there are inhomogeneities in the channel because the conductance curves are unusually erratic even for the larger

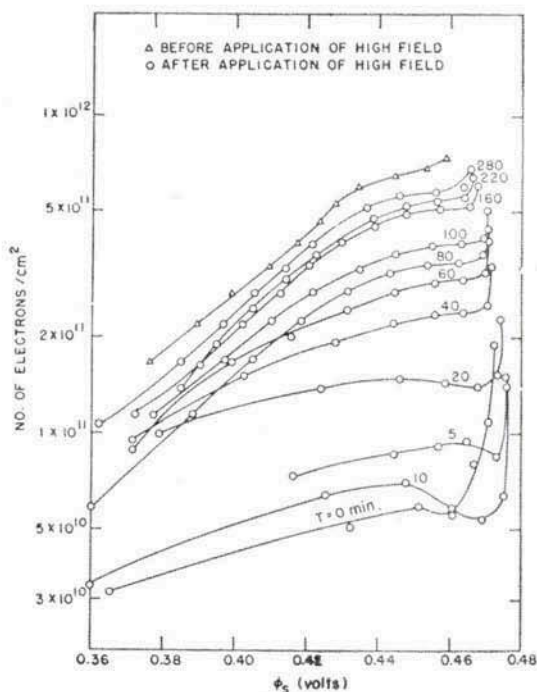


FIG. 23.—Runs of  $Q$  vs  $\phi_s$  for silicon before and after application of high field.

densities. Figure 24 shows the density of interface states as a function of time after application of a high field as deduced from Fig. 23.

More experiments must be carried out in order to determine the internal mechanism leading to the observations described above. If it is assumed that the oxidation theory of Cabrera and Mott<sup>3</sup> applies, the following tentative explanation can be given: When the negative charge on the outside of the oxide becomes



very large, positive  $\text{Ge}^{++++}$  ions or  $\text{Si}^{++++}$  ions are drawn from the semiconductor lattice into the oxide film and to the surface of the oxide film. A space charge in the oxide is formed which neutralizes some of the negative charge on the surface of the oxide, and the conductance of the inversion layer decays to a lower value. When a large positive charge is located on the surface of the oxide, the interstitial  $\text{Ge}^{++++}$  or  $\text{Si}^{++++}$  ions return to the interface, join the lattice, and lose their charge again. Thus, the conductance decays. In addition, it must be assumed that atoms

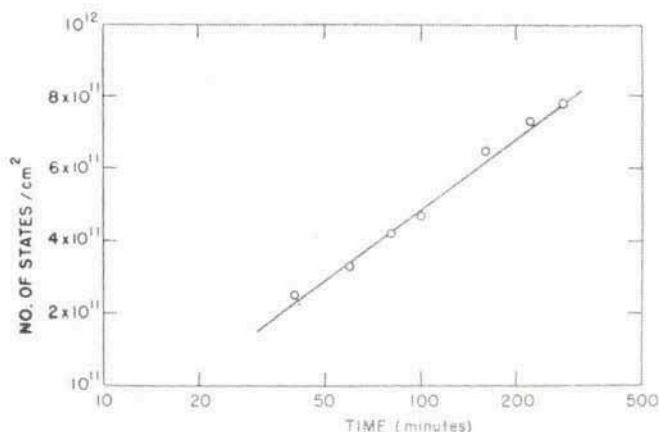


FIG. 24.—Density of interface states versus time for silicon after application of high field.

drawn from the semiconductor leave additional lattice defects in the surface which result in interface states in the upper half of the gap. When the atoms return to the interface, these interface states would be canceled. The lack of observable changes when the surface has not been oxidized in wet oxygen and ozone would indicate that under those conditions a large number of interstitial semiconductor atoms is not present in the oxide film. Further experiments should corroborate this mechanism of oxidation.

All the above experiments have been made in dry atmospheres. It was found that in the presence of water vapor, effects were observed which may be explained in terms of changes in the oxide film. These latter changes were found to take place even at lower bias voltages, i.e., smaller electric fields across the oxide film. It

is felt that a detailed investigation of induced changes in the structure and density of interface states will eventually reveal their physical origin.

## VII. THE EFFECT OF ADSORBED LIQUIDS

When vapors of certain liquids were present, the conductance of an inversion layer as a function of bias voltage may no longer be described by a constant value of  $\phi_s$ . It appears that there is another conduction path across the base region in addition to the inversion layer. It has been postulated<sup>6-8</sup> from observations on excess currents in diodes that there is some form of ionic conduction in adsorbed water films. Experiments in this laboratory<sup>6</sup> have shown that there is no measurable evolution of oxygen or hydrogen and no observable mass transport. It also appears that besides water, other liquids such as methyl alcohol, pyridine, dioxane, acetone, etc., give the same type of excess conduction. In Fig. 25, the steady-state conductance of water vapor and

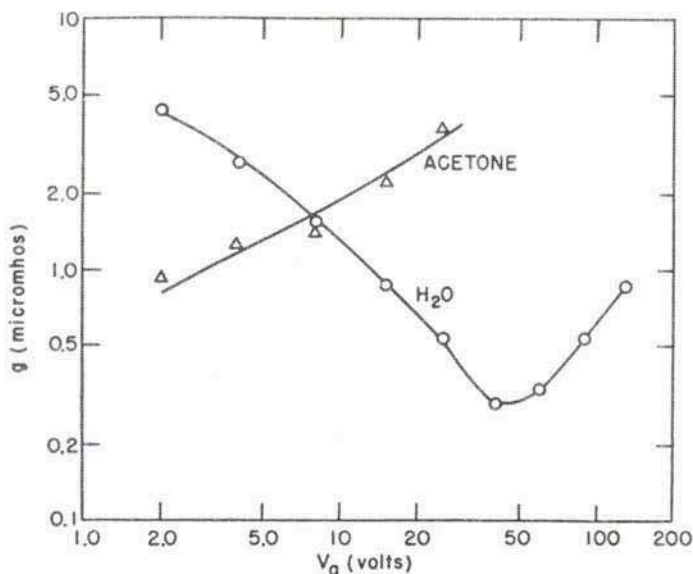


FIG. 25.—Steady-state conductance of water vapor and acetone vapor induced inversion layers on germanium versus bias voltage.

acetone vapor induced inversion layer on *p*-type germanium is shown. The water vapor induced inversion layer behaves normally in the lower bias range; at higher bias voltages the conductance increases with increasing bias voltage which is not observed in conventional inversion layers. The acetone induced inversion layer shows a conductance which increases with increasing bias voltage over the whole bias range. At present no quantitative theory of this conduction mechanism exists; however, it is believed that there is a true hole conduction in the adsorbed liquid film much like in a molten semiconductor. In Fig. 26, a surface of *p*-type

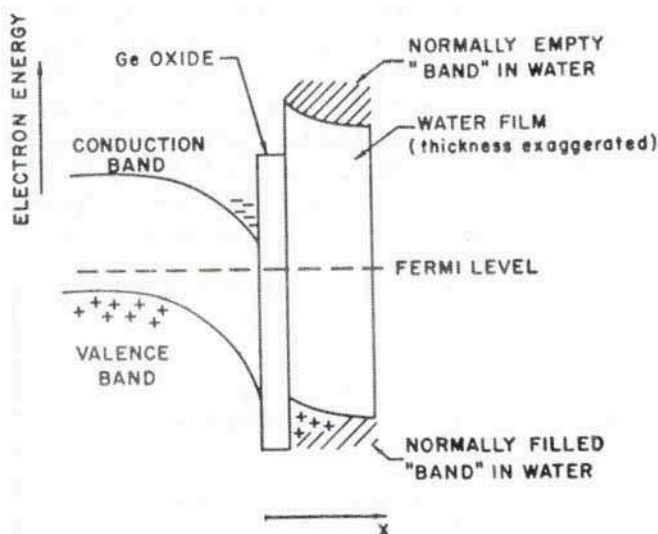


FIG. 26.—Energy diagram showing germanium surface with thick adsorbed water film.

germanium with an adsorbed liquid film is shown. The fact that an inversion layer was formed indicates that the filled levels of the water molecule must lie close to the Fermi level of the underlying semiconductor. Figure 26 shows schematically the contact of *p*-type germanium with a thick water film. If the liquid film is thick and coherent, there is no physical reason why there should not be any hole conduction in the water film. The mobility of holes in liquids has not yet been measured. However, to be consistent with the observations, such a mobility would have to lie in the



range from 1 to 100 cm<sup>2</sup>/volt sec or greater. Acetone is an example of a substance with an especially large excess conduction. For a quantitative understanding of this excess conduction it is necessary to first study the role of the oxide film. It is not clear how large an electrical resistance the oxide film represents to carriers flowing from the semiconductor body to the liquid film. If the inversion layer is induced by adsorbed gases, this type of conduction is not observed. Gases probably adsorb to a much lesser extent and the adsorbed film may not be coherent enough for this type of conduction. Ammonia is an exception in that some of this excess conduction is observed on ammonia induced inversion layers on *p*-type germanium, but not on silicon.

#### ACKNOWLEDGMENTS

The authors wish to thank Miss J. Sullivan and Miss J. Haynes for carrying out the computations and Mrs. M. Sturm for help in the preparation of the manuscript.

#### DISCUSSION

C. G. B. GARRETT (*Bell Telephone Laboratories*): The authors' suggestion of the existence of an electronic (rather than ionic) current within the polarization layer in the electrolyte adjacent to the semiconductor surface is very interesting. I wonder whether the authors have come across the work of O'Connor and his co-workers in Australia,<sup>23</sup> which seems relevant to this idea. These workers have made a careful study of both streaming currents and zeta potential for various systems involving the flow of electrolytes over solids, including silica. In this way, one may compare the total amount of ionic charge in the diffuse layer (from the zeta potential and Poisson's equation) with the observed streaming current, and see whether there is any discrepancy. For some solids—ferric oxide was one, I believe—there was indeed an additional current component, which the authors ascribe to electronic current *within* the solid. For silica, however, there was no discrepancy, and the experimental results seem to allow little room for the existence of any electronic current, whether inside or outside the solid.

H. STATZ (*Raytheon Manufacturing Company*): There is ample evidence in the electrochemical literature (see for example *Colloid Science*, Vol. 1, H. R. Kruyt, Editor, Elsevier Publishing Company, New York, 1952, p. 236) that there are additional currents arising from surfaces in contact with electrolytes. It is felt that no conclusion can be drawn from measurements of this nature whether these extra currents are within or exterior to the solid. We agree with O'Connor in that water films on the silicon oxide layer have so little charge, they hardly produce an inversion layer in underlying *p*-type silicon. Thus, in this case, practically no excess current is to be expected.

## REFERENCES

1. I. Tamm, *Physik. Z. Sowjetunion* **1**, 733 (1932).
2. H. M. James, *Phys. Rev.* **76**, 1611 (1949).
3. N. Cabrera and N. F. Mott, *Repts. Progr. in Phys.* **12**, 163 (1949).
4. N. F. Mott, *Proc. Inst. Elect. Engrs.* **96**, Pt. I, 253 (1949).
5. Eriksen, Statz, and deMars (to be published).
6. J. T. Law, *Proc. Inst. Radio Engrs.* **42**, 1367 (1954).
7. J. T. Law, *J. Phys. Chem.* **59**, 67 (1955).
8. J. T. Law and P. S. Meigs, *J. Appl. Phys.* **26**, 1265 (1955).
9. H. Letaw, private communication.
10. Statz, deMars, Davis, and Adams, *Phys. Rev.* **101**, 1272 (1956).
11. R. H. Kingston, *J. Appl. Phys.* **27**, 101 (1956).
12. W. L. Brown, *Phys. Rev.* **91**, 518 (1953).
13. R. H. Kingston, *Phys. Rev.* **93**, 346 (1954).
14. R. H. Kingston, *Phys. Rev.* **98**, 1766 (1955).
15. deMars, Statz, and Davis, *Phys. Rev.* **98**, 539 (1955).
16. Statz, Davis, and deMars, *Phys. Rev.* **98**, 540 (1955).
17. J. R. Schrieffer, *Phys. Rev.* **97**, 641 (1955).
18. R. H. Kingston and A. L. McWhorter (to be published). We wish to thank the authors for a preprint of this article.
19. W. H. Brattain and J. Bardeen, *Bell System Tech. J.* **32**, 1 (1953).
20. F. Herman, *Proc. Inst. Radio Engrs.* **43**, 1703 (1955).
21. R. O. Carlson, C. B. Collins and C. J. Gallagher, *Bull. Amer. Phys. Soc.* **1**, 128 (1956).
22. To be published.
23. O'Connor, Street and Buchanan, *Austr. Journ. Chem.* **7**, 245 (1954).